

INSTITUTO NACIONAL DE PESQUISAS DA AMAZÔNIA – INPA  
UNIVERSIDADE DO ESTADO DO AMAZONAS - UEA  
Programa Integrado de Pós-Graduação - Clima e Ambiente – PPG-CLIAMB

**Estudo da advecção horizontal de CO<sub>2</sub> em florestas na Amazônia e sua  
influência no balanço de Carbono**

JULIO TÓTA

Manaus, Amazonas  
Outubro 2009

INSTITUTO NACIONAL DE PESQUISAS DA AMAZÔNIA – INPA  
UNIVERSIDADE DO ESTADO DO AMAZONAS - UEA  
Programa Integrado de Pós-Graduação - Clima e Ambiente – PPG-CLIAMB

**Estudo da advecção horizontal de CO<sub>2</sub> em florestas na Amazônia e sua  
influência no balanço de Carbono**

JULIO TÓTA

Orientador: Dra. MARIA ASSUNÇÃO FAUS DA SILVA DIAS

Co-Orientador: Dr. DAVID ROY FITZJARRALD

Tese de doutorado apresentada ao PPG-  
CLIAMB como parte dos requisitos  
para obtenção do título de Doutor em  
Clima e Ambiente, área de  
concentração: Geociências.

Manaus, Amazonas

Outubro 2009.

C586e Silva, Julio Tóta da

Estudo da advecção horizontal de CO<sub>2</sub> em florestas na Amazônia e sua influência no balanço de carbono / Julio Tóta da Silva. -- Manaus : [s.n.], 2009.

xviii, 93 f. : il. (algumas color.)

Tese (doutorado em Clima e Ambiente)--INPA/UEA, Manaus, 2009.

Orientadora: Maria Assunção Faus da Silva Dias

Co-orientador: David Roy Fitzjarrald

Área de concentração: Interações Clima-Biosfera na Amazônia

1.Advecção-Carbono 2.Florestas tropicais-Amazônia 3.Vórtices turbulentos I.Título

CDD 19<sup>a</sup> ed. 551.5112

**Sinopse:**

Este estudo apresenta observações da dinâmica do escoamento do vento dentro e acima em área de Floresta Tropical na Amazônia, verificando sua relação com o transporte horizontal de CO<sub>2</sub> sobre terrenos de topografia complexa e avaliando seu impacto no balanço de carbono com o uso do sistema de correlações de vórtices turbulentos (Eddy Correlation System).

**Palavras-chaves:** Advecção Horizontal de CO<sub>2</sub>, Floresta Tropical, Amazônia, Escoamento de drenagem; Sistema de Correlações de Vórtices Turbulentos, CO<sub>2</sub>.

***Dedico***

*Aos meus pais Antonio Tota e Severina  
Soares, e aos meus filhos Luny Tota e Luan Tota*

## **Agradecimentos**

A Deus,

Ao Instituto Nacional de Pesquisas da Amazônia (INPA), pela oportunidade de formação,

À Fundação de Amparo a Pesquisa do Estado do Amazonas (FAPEAM) pela bolsa de estudos,

Agradeço ao Conselho Nacional de Desenvolvimento Científico e Tecnológico – CNPq,

Eu sou especialmente grato aos meus orientadores Dra. Maria Assunção e Dr. David Fitzjarrald, pela paciência, orientação e apoio constante e pela amizade,

Agradeço aos membros da banca pelas sugestões e revisão do texto da tese,

Expresso minha gratidão ao Dr. Manzi, Coordenador do Programa de Pós-Graduação em Clima e Ambiente (CLIAMB-INPA/UEA), pelo constante encorajamento, a atenção e pela amizade desses muito anos,

Agradeço a todos os amigos que me ajudaram nesse caminho: Hermes, Amaury, Juliana, Julio, Galúcio, Madruga, Alessandro, Celso, Betânia, Veber, e muitos... Todos os funcionários do LBA Manaus, eu sou grato por todo o apoio logístico,

Especial obrigado para Claudia Vitel e Edwin Keiser pela amizade e apoio,

Aos professores do Programa CLIAMB-INPA/UEA e aos colegas de classe,

## RESUMO

Fluxos horizontais e verticais de CO<sub>2</sub> foram feitos na floresta tropical na Amazônia dentro da Reserva de Floresta Nacional do Tapajós (FLONA-Tapajós - 54°58'W, 2°51'S). Duas campanhas de medidas observacionais foram conduzidas em 2003 e 2004 para descrever o escoamento abaixo do dossel, determinar sua relação com o vento acima da floresta, e estimar como este escoamento transporta CO<sub>2</sub> horizontalmente. Atualmente já está reconhecido que o transporte horizontal de CO<sub>2</sub> respirado abaixo da floresta não está representado pelo balanço obtido somente em um ponto de medida nas torres de fluxos (Eddy Covariance - EC), com erros mais significativos sob condições de noites calmas. Neste trabalho testamos a hipótese de que o transporte horizontal médio, anteriormente não medido em florestas tropicais, possa representar a quantidade de CO<sub>2</sub> respirado destas condições. Foi instalada uma rede de sensores de vento e CO<sub>2</sub> abaixo da vegetação. Um significativo transporte horizontal de CO<sub>2</sub> foi observado nos primeiros 10 metros da floresta. Os resultados indicaram que a advecção de CO<sub>2</sub>, para todas as noites calmas estudadas, representou 73 e 71% do déficit noturno, definido pela diferença entre a respiração total do ecossistema (medida ecológica) e o fluxo medido pelo sistema EC na torre de fluxo, durante as estações seca e chuvosa, respectivamente. Foi também encontrado que a advecção horizontal de CO<sub>2</sub> noturna é igualmente importante, tanto para condições de baixos níveis de turbulência como para aquelas com altos valores de velocidade de fricção (nível de turbulência), sendo estes limiares comumente usados para correções dos fluxos noturnos (correção por  $u_*$ ). Sobre uma área de terreno complexa coberta por floresta tropical densa (Reserva Biológica do Cuieiras – ZF2 - 02°36'17.1"S, 60°12'24.5"W) foram medidos gradientes horizontais e verticais de temperatura do ar, concentrações de CO<sub>2</sub> e o campo de vento durante as estações seca e chuvosa de 2006. Foi testada a hipótese de que escoamento de drenagem horizontal sobre a área de estudo é significativa e pode afetar a interpretação das altas taxas de absorção de carbono reportadas por trabalhos anteriores. Um experimento de campo similar ao desenvolvido por Tóta et al. (2008) foi usado, incluindo uma rede de sensores de vento, temperatura do ar e concentração de CO<sub>2</sub>, acima e abaixo da floresta. Foi observado um padrão de escoamento abaixo da floresta, persistente e sistemático, sobre uma área de encosta de moderada inclinação (~12%), subindo durante a noite (associada com flutuabilidade positiva) e descendo durante o dia (flutuabilidade negativa). Acima da floresta (38m) sobre a mesma área de encosta foi também observado um movimento vertical descendente indicando convergência vertical e correspondente divergência horizontal em direção ao centro do vale próximo a torre de

medida. Foi observado que as micro-circulações acima da floresta foram dirigidas pelo balanço entre as forças gradiente de pressão e de flutuabilidade (buoyancy), e abaixo da floresta também foram dirigidas pelo mesmo mecanismo físico. Os resultados também indicaram que os gradientes horizontais e verticais de CO<sub>2</sub> foram modulados pelas micro-circulações acima e abaixo da vegetação, sugerindo que as estimativas da advecção usando a estratégia experimental anterior não são apropriadas devido a natureza tri-dimensional do transporte horizontal e vertical do local.

## SUMMARY

Horizontal and vertical CO<sub>2</sub> fluxes and gradients were obtained in an Amazon tropical rain forest, the Tapajós National Forest Reserve (FLONA-Tapajós - 54°58'W, 2°51'S). Two observational campaigns in 2003 and 2004 were conducted to describe subcanopy flows, clarify their relationship to winds above the forest, and estimate how they may transport CO<sub>2</sub> horizontally. It is now recognized that subcanopy transport of respired CO<sub>2</sub> is missed by budgets that rely only on single point Eddy Covariance measurements, with the error being most important under nocturnal calm conditions. We tested the hypothesis that horizontal mean transport, not previously measured in tropical forests, may account for the missing CO<sub>2</sub> in such conditions. A subcanopy network of wind and CO<sub>2</sub> sensors was installed. Significant horizontal transport of CO<sub>2</sub> was observed in the lowest 10m of the canopy. Results indicate that CO<sub>2</sub> advection accounted for 73% and 71%, respectively of the carbon budget deficit (difference between total ecosystem respiration and respective eddy flux tower measured) for all calm nights evaluated during dry and wet periods. We found that horizontal advection was significant to the canopy CO<sub>2</sub> budget even for conditions with the above-canopy friction velocity higher than commonly used thresholds ( $u_*$  correction). On the moderate complex terrain cover by dense tropical Amazon rainforest (Reserva Biológica do Cuieiras – ZF2 - 02°36'17.1"S, 60°12'24.5"W) subcanopy horizontal and vertical gradients of the air temperature, CO<sub>2</sub> concentration and wind field were measured for dry and wet periods in 2006. We tested the hypothesis that horizontal drainage flow over this study area is significant and it can affect the interpretation of the high carbon uptake reported by previous works. A similar experimental design to the one by *Tota et al.* (2008) was used with subcanopy network of wind, air temperature and CO<sub>2</sub> sensors above and below the forest canopy. It was observed a persistent and systematic subcanopy nighttime upsloping (positive buoyancy) and daytime downsloping (negative buoyancy) flow pattern on the moderate slope (~12%) area. Above canopy (38 m) on the slope area was also observed a downward motion indicating vertical convergence and correspondent horizontal divergence into the valley area direction. It was observed that the micro-circulations above canopy were driven mainly by the balancing pressure and buoyancy forces and that in subcanopy was driven similar physical mechanisms. The results also indicated that the horizontal and vertical scalar gradients (e.g. CO<sub>2</sub>) were modulated by these micro-circulations above and below canopy, suggesting that advection estimates using the previous experimental approach is not appropriate due to the tri-dimensional nature of the vertical and horizontal transport locally.



## LISTA DE FIGURAS

**Capítulo I:** Amazon rain Forest subcanopy flow and the carbon budget: Santarém LBA-ECO Site.

- Figura 1.** Site Location in the vegetation cover image and high resolution (30m grid space) tower-base local topography as determined by the Shuttle Radar Topography Mission (SRTM). The arrows shows the modal wind direction at 57.8 m (red, from East) and in the subcanopy (magenta, from southeast)..... 22
- Figure 2.** Main tower and Draino deployed instruments systems.....23
- Figure 3.** The autocorrelation coefficient for total wind speed (left panel) and CO<sub>2</sub> concentration (center panel) as a function of distance between sampling points 1.8m above ground in the subcanopy. (3-minute averages data from “Draino” Phase 1 (DOY 198-238/2003). “C” represents the calibration period. The right panel shows the temporal autocorrelation, the solid line represents the median, and the thinner lines the upper and lower quartiles. Mean wind speed in the subcanopy was 0.13 m/s. ....27
- Figure 4.** Typical nighttime normalized median profiles of CO<sub>2</sub>, wind speed and their product (uc) horizontal transport (left panel); and the diurnal cycle of the shape factor for horizontal advection (right panel). ....30
- Figure 5.** Night time composite of averaged subcanopy CO<sub>2</sub> concentration field and wind vectors for Phase 1 and Phase 2 campaigns. The units are in ppm and ms<sup>-1</sup>, respectively. (Largest arrow is 0.15 m s<sup>-1</sup>).....32
- Figure 6.** Vertical profiles of concentration of CO<sub>2</sub>, wind speed, temperature, and water vapor, for both Phases (dry and wet) .....33
- Figure 7.** Frequency distribution histogram of friction velocity ( $u^*$ ) at 57.8 m, for Phase 1 and Phase 2 measurements, separate day and night periods. ....34
- Figure 8.** Nighttime distribution of the wind rose and its magnitude (m s<sup>-1</sup>) for the Draino sonic anemometer network and at top of main tower (57.8 m), including its localization see Figure 2). ....37
- Figure 9.** Diurnal cycle of buoyancy term forcing fractions relative to stress divergence term for Phase 1 (top panel) and Phase 2 (middle panel) observations, and (bottom panel) the buoyancy forcing term vs. subcanopy wind direction. ....38

<b>Figure 10a.</b> Hourly-averaged summary of results for the Phase 1 and all the terms except eddy flux are average values for 0 to 57.8 m control volume. Top panel: vertical eddy flux at 57.8 m; 2nd panel: storage; 3th panel: east-west advection; and 4th panel: south-north advection, terms. ....	39
<b>Figure 10b.</b> Hourly-averaged summary of results for the Phase 2 and all the terms except eddy flux are average values for 0 to 57.8 m control volume. Top panel: vertical eddy flux at 57.8 m; 2nd panel: storage; 3rd panel: vertical advection; 4th panel: east-west advection; and 5th panel: and south-north advection, terms. ....	40
<b>Figure 11a.</b> Top panel: Hourly-averaged vertical eddy flux at 57.8 m; 2nd panel: storage term; 3rd panel: east-west advection term; and 4th panel: and south-north advection, terms. Note the change in vertical scale between the phases. ....	41
<b>Figure 11b.</b> Top panel: Hourly-averaged vertical eddy flux at 57.8 m; 2nd panel: storage term; 3rd panel: vertical advection term; 4th panel: east-west advection term; and 5th panel: and south-north advection terms. Note the change in vertical scale between the phases....	42
<b>Figure 12a.</b> Mean nocturnal variation of the NEE (Eddy covariance flux + storage), ecosystem respiration, horizontal advection and NEE plus advection, for Phase 1 (Dry period). ....	43
<b>Figure 12b.</b> Same Figure 12a, for Phase 2 (Wet period). ....	44
<b>Figure 13.</b> Mean nocturnal variation of the advection term as a function of the friction velocity rank, for Phase 1 (left panel) and Phase 2 (right panel) datasets. Solid line with dots indicates binned average values (0.1 intervals)). Error-bar also is plot with standard deviation, respectively. ....	45

## **Capítulo II:** Amazon rain Forest subcanopy flow and the carbon budget: Manaus LBA Site - a complex terrain condition.

<b>Figure 1.</b> Detailed measurements towers's view in the ZF-2 Açu catchment (East-West valley orientation) from SRTM-DEM datasets. Large view in the above panel and below panel the points of measurements (B34 – Valley, K34 – Plateau, and subcanopy Draino system measurements over slopes in south and north faces (red square points).....	51
<b>Figure 2.</b> (a) Açu Cachment with level terrain cotes and vegetation cover from IKONOS's image and (b) vegetation structure measured from Lidar sensor over yellow transect (a). From (a) the blue color is valley and vegetation transition to plateau areas (red colors)....	52

<b>Figure 3.</b> Draino measurement system used in Manaus LBA (South Face, see also Figure 4).....	54
<b>Figure 4.</b> Draino measurement system (South and North Slope face) implemented at Manaus LBA Site, including topographic view and instrumentation deployed.....	55
<b>Figure 5.</b> 10 days time series of the CO <sub>2</sub> concentration, air temperature (DRAINO System) and total precipitation (plateau tower).....	57
<b>Figure 6.</b> Boxplot of the virtual potential temperature vertical profile for dry (a, b) and wet periods (c,d) of the 2006 during night (b,d) and daytime (a,c), on the plateau K34 tower..	59
<b>Figure 7.</b> Daily course of the vertical deviation of the virtual potential temperature for dry (a) and wet (b) periods of the 2006, on the plateau K34 tower.....	60
<b>Figure 8.</b> Boxplot of the virtual potential temperature vertical profile for dry (a, b) and wet periods (c, d) of the 2006 during night (b, d) and daytime (a, c), on the slope area DRAINO System tower (south face, see Figure 2).....	61
<b>Figure 9.</b> Daily course of the vertical deviation of the virtual potential temperature for dry (a) and wet (b) periods of the 2006, and virtual potential temperature vertical gradient (c), on the slope area DRAINO System tower.....	62
<b>Figure 10.</b> Frequency distribution of the wind speed and direction. For dry (a, b) and wet (c, d) periods from 2006 during day (a, c) and nighttime (b, d), on the plateau K34 tower.....	64
<b>Figure 11.</b> Frequency distribution of the wind speed and direction above canopy (38 m above ground level – a.g.l). For dry (a, b) and wet (c, d) periods from 2006 during day (a, c) and nighttime (b, d), on the slope area at DRAINO system tower.....	65
<b>Figure 12.</b> Frequency distribution of the wind speed and direction in the subcanopy array (2 m above ground level – a.g.l) on the microbasin south face slope area at DRAINO horizontal array system (see Figure 4). For dry (a-f) and wet (g-l) periods from 2006, during day (a, b, c, g, h, i) and nighttime (d, e, f, j, k, l).....	67
<b>Figure 13.</b> Frequency distribution of the subcanopy wind direction (a) upsloping (from north quadrant) and (b) downsloping (from south quadrant) on the south face slope area at DRAINO horizontal array system (see Figure 4).....	69
<b>Figure 14.</b> Mean vertical velocity raw and correct vertical velocity (a) for DRAINO system slope tower (38 m), and hourly mean vertical velocity (b) for: plateau K34 tower (55 m), DRAINO system slope tower (above canopy - 38 m and subcanopy - 3 m) and for valley B34 (43 m) towers (see Figure 4, for details).....	70
<b>Figure 15.</b> Schematic local circulations in the site studied, valley and slopes flow (a), 2D view from suggested below and above canopy airflow (b).....	72

- Figure 16.** Example at midnight (local time) of the horizontal CO<sub>2</sub> concentration over the DRAINNO System south face domain including an interpolated horizontal wind field (10 m grid), note the geographic orientation and the red arrow indicating slope inclination (see Figure 4).....74
- Figure 17.** Hourly average of the subcanopy (2 m) CO<sub>2</sub> concentration and horizontal wind speed over DRAINNO System south face area during dry period of the 2006, note the geographic orientation and the red arrow indicating slope inclination (see Figure 4). The axis represents distances from center of the main tower.....75
- Figure 18.** Hourly average of the subcanopy (2 m) CO<sub>2</sub> concentration on the DRAINNO System north face area during dry period of the 2006, note the geographic orientation (see Figure 4). The axis represents distances from center of the main tower.....76

## SUMÁRIO

INTRODUÇÃO GERAL.....	14
OBJETIVO GERAL.....	16
OBJETIVOS ESPECÍFICOS.....	16
<b>Capítulo I:</b> Amazon rain forest subcanopy flow and the carbon budget: Santarém LBA-ECO .....	18
Abstract .....	18
1. Introduction .....	19
2. Material and Methods .....	21
2.1 Site description .....	21
2.2. Instrumentation and observation .....	23
2.3. Preinstallation intercomparison .....	26
2.4. CO <sub>2</sub> conservation equations .....	28
2.5. Vertical integration of the horizontal advection terms .....	30
3 – Results and Discussion .....	32
3.1. CO <sub>2</sub> concentration field .....	32
3.2. Subcanopy horizontal wind field .....	36
3.3. Subcanopy flow forcing terms .....	37
3.4. Estimates of Advection Terms .....	39
3.5. CO <sub>2</sub> budget .....	43
3.6. Correlation between advection components and friction velocity .....	44
4. Summary and Conclusions .....	45
<b>Capítulo II:</b> Amazon rain Forest subcanopy flow and the carbon budget: Manaus LBA Site - a complex terrain condition .....	48
Abstract .....	48
1. Introduction .....	49
2. Material and Methods .....	50
2.1 Site description .....	50
2.2. Measurements and instrumentation .....	53

3 – Results and Discussion .....	57
3.1. Air Temperature field .....	58
3.1.1 - Plateau K34 tower .....	58
3.1.2 – DRAINNO System Slope tower .....	60
3.2. Wind field .....	63
3.2.1 – Horizontal wind regime - above canopy.....	63
3.2.1.1 - Plateau K34 tower .....	63
3.2.1.2 - DRAINNO System slope tower .....	64
3.2.2 – Horizontal wind regime – Subcanopy array measurements (2 m a.g.l) .....	65
3.2.3 – Mean Vertical wind velocity – subcanopy and above canopy .....	69
3.3. Phenomenology of the local circulations: Summary .....	72
3.4. CO <sub>2</sub> concentration and subcanopy horizontal wind field .....	73
4. Summary and Conclusions .....	77
CONCLUSÃO GERAL.....	79
REFERÊNCIAS.....	82

## INTRODUÇÃO GERAL

Nas últimas décadas há um crescente interesse da comunidade científica em quantificar as trocas líquidas de dióxido de carbono ( $\text{CO}_2$ ) entre ecossistemas florestais e a atmosfera, devido ao nível de incerteza das estimativas das fontes e sumidouros desses ecossistemas no balanço global de carbono. Enquanto as estimativas do crescente nível de aumento de  $\text{CO}_2$  atmosférico e os sumidouros de  $\text{CO}_2$  pelos oceanos são bem conhecidas, as fontes e sumidouros da biosfera ainda não são estimados precisamente (IPCC 2007). Reduzir as incertezas das fontes e sumidouros de dióxido de carbono da biosfera tem sido um grande desafio da comunidade científica atualmente visando melhor entender o balanço global de carbono e o papel dos biomas terrestres no assim chamado “aquecimento global”.

Os biomas florestais exercem um papel importante no balanço global de carbono, pois representam 80% de biomassa aérea e 40% de biomassa de raízes e serrapilheira do carbono orgânico global (Dixon et al., 1994). Dentre estes ecossistemas, as florestas tropicais da Amazônia são uma importante componente para o balanço global de carbono, em função da sua grande quantidade de biomassa armazenada e de seu rápido ciclo de carbono através dos processos de fotossíntese e respiração. As florestas da Amazônia representam 10% da produtividade primária terrestre e do carbono armazenado nos ecossistemas terrestres (Melillo et al., 1993; Malhi et al., 1998). Portanto, para melhor quantificar o balanço global de carbono é preciso também determinar o balanço regional de carbono na Amazônia e sua variabilidade em resposta as mudanças do meio ambiente. Para isso, torna-se crítico entender os processos de respiração e fotossíntese do ecossistema Amazônico detalhadamente.

Atualmente não há um consenso da comunidade científica se as florestas tropicais na Amazônia atuam como fontes ou sumidouros de  $\text{CO}_2$  atmosférico. Estimativas com base em medidas biométricas, sugerem tanto um papel de sumidouro (Phillips et al., 1998; Baker et al., 2004), como uma fonte de  $\text{CO}_2$  atmosférico (Rice et al., 1998; Miller et al., 2004). Por outro lado, estimativas com base em medidas pelo método das covariâncias de vórtices turbulentos (EC – “Eddy covariance System”), sugerem que o ecossistema de floresta tropical na Amazônia atua como sumidouro (Grace et al., 1995; Malhi et al., 1998; Araújo et al., 2002), uma pequena fonte (Saleska et al., 2003; Huttyra et al., 2007), ou em equilíbrio (Miller et al., 2004), com relação às trocas líquidas de  $\text{CO}_2$  atmosférico.

Portanto, existe uma urgente necessidade em melhor entender e quantificar as incertezas dessas estimativas em ecossistemas terrestres, em especial na Amazônia.

As estimativas realizadas por EC na escala espacial das torres micrometeorológicas, são uma importante ferramenta para quantificar as trocas líquidas entre a superfície e a atmosfera e amplamente utilizada desde seu desenvolvimento (Montgomery, 1948; Swinbank, 1951) para estimativas das trocas de energia (Antonia et al., 1979; Fitzjarrald et al., 1988; Bergstrom and Hogstrom, 1989; Gao et al., 1989; Shuttleworth, 1989) e gases traços, como CO<sub>2</sub> (Fan et al., 1990; Lee et al., 1992; Wofsy et al., 1993; Grace et al., 1995; Black et al., 1996; Moncrieff et al., 1997; Malhi et al., 1998; Baldocchi et al., 2001; Araújo et al., 2002). A metodologia de EC tem a vantagem de obter medidas diretas e de longo prazo dos fluxos de CO<sub>2</sub> na interface floresta-atmosfera (Wofsy et al., 1993; Goulden et al., 1996; Urbanski et al., 2007).

Entretanto, teoricamente este método assume que as áreas representativas das medidas sejam horizontalmente homogêneas e planas para uma melhor estimativa dos fluxos turbulentos obtidos pelas torres. Dessa forma, considera que a mistura turbulenta atmosférica seja suficientemente efetiva para eliminar o efeito da variabilidade da cobertura da superfície em pequena escala (tipo de vegetação e terreno) e represente o fluxo turbulento médio da área obtido nas torres de fluxos.

Em termos de balanço de energia ou de gases, isto significa que os termos de transportes horizontais (advecção) são desprezados ou não significativos, predominando apenas os fluxos verticais turbulentos. Isto tem um efeito significativo nas trocas líquidas entre o ecossistema e a atmosfera (NEE – “Net Ecosystem Exchange”), a qual é obtida, neste caso, somente pela soma dos fluxos verticais turbulentos e o termo de armazenamento (Storage) abaixo do nível da medida ( $NEE = \text{Eddy Flux} + \text{Storage}$ ). O termo de armazenamento, por exemplo, na Amazônia, tem sido obtido raramente de maneira contínua, dada as dificuldades específicas de cada sítio e das condições ambientais adversas, gerando uma barreira para as estimativas de NEE (Iwata et al., 2005).

Sob certas condições de baixo nível de turbulência atmosférica (geralmente nos períodos noturnos) e certo grau de complexidade topográfica, circulações secundárias e escoamento horizontal sobre as encostas do terreno, o chamado escoamento de drenagem (“Drainage Flow”), podem se desenvolver (Yoshino et al., 1984). Isto tem sido evidenciado por vários estudos em diversas localidades, os quais indicam a importância da advecção de CO<sub>2</sub> no balanço de carbono (Aubinet et al., 2003; Staebler and Fitzjarrald, 2004, 2005; Marcolla et al., 2005; Feigenwinter et al., 2008; Leuning et al., 2008). Porém, os estudos de



advecção de CO<sub>2</sub> foram realizados sobre regiões montanhosas de latitude média e não em regiões de florestas tropicais, passando a ser uma motivação e um desafio, investigar a existência e quantificar a importância da advecção de CO<sub>2</sub> no balanço de carbono das áreas de floresta tropicais na Amazônia.

Com o objetivo de quantificar e melhor entender as fontes e sumidouros de CO<sub>2</sub> na região de floresta tropical na Amazônia, o Projeto de Grande Escala da Biosfera-Atmosfera na Amazônia (LBA - “Large Scale Biosphere-Atmosphere experiment in Amazonia”) estabeleceu uma rede de torres micrometeorológicas com o sistema EC em vários pontos na região (Keller et al., 2004).

Esta tese visa investigar os processos de transporte não turbulentos, os quais são os termos advectivos componentes da equação de balanço de carbono, e os mecanismos físicos que os dirigem, nos sítios experimentais do Projeto LBA de Santarém (PA) e de Manaus (AM). Para isso, foi concebido um sistema de medida direta e detalhada das principais variáveis (velocidade do vento, temperatura do ar e concentração de CO<sub>2</sub>) usadas para caracterizar a dinâmica do escoamento acima e abaixo da floresta, e calcular os termos advectivos de transporte de CO<sub>2</sub> sobre as áreas representativas das torres micrometeorológicas do projeto LBA.

## OBJETIVO GERAL

Esta tese tem como objetivo geral investigar e quantificar através de medidas observacionais os mecanismos físicos que dirigem os termos não turbulentos das equações de balanço de carbono associados com o transporte lateral de CO<sub>2</sub> em dois sítios de floresta tropical do projeto LBA na Amazônia.

## OBJETIVOS ESPECÍFICOS

- 1) Implementar um sistema de medidas observacional para investigar a dinâmica do escoamento acima e abaixo da floresta tropical na Amazônia sobre terrenos complexos, capaz de medir baixos limiares de velocidade do vento e gradientes horizontais de CO<sub>2</sub> abaixo da copa da floresta;

- 2) Determinar e quantificar os gradientes horizontais e verticais de concentrações de CO<sub>2</sub> importantes para os transportes horizontais de CO<sub>2</sub>, (advecção horizontal – Capítulo I – Sítio do LBA em Santarém - PA);
- 3) Avaliar e/ou determinar a existência do escoamento horizontal abaixo da copa da floresta, bem como, sua persistência e sistemática em produzir transporte horizontal de CO<sub>2</sub> para fora da área de representatividade do sistema EC das torres micrometeorológicas do projeto LBA e determinar sua validade;
- 4) Determinar os mecanismos físicos da dinâmica do escoamento responsáveis pela advecção horizontal de CO<sub>2</sub>;
- 5) Quantificar os termos de transportes horizontais e/ou advecção horizontal de CO<sub>2</sub>, que contribuem para o balanço de carbono na escala das torres micrometeorológicas do LBA;

**Capítulo I - Amazon rain forest subcanopy flow and the carbon budget:  
Part I – Santarém LBA-ECO <sup>1</sup>**

**Abstract**

Horizontal and vertical CO<sub>2</sub> fluxes and gradients were obtained in an Amazon tropical rain forest, the Tapajós National Forest Reserve (FLONA-Tapajós - 54°58'W, 2°51'S). Two observational campaigns in 2003 and 2004 were conducted to describe subcanopy flows, clarify their relationship to winds above the forest, and estimate how they may transport CO<sub>2</sub> horizontally. It is now recognized that subcanopy transport of respired CO<sub>2</sub> is missed by budgets that rely only on single point Eddy Covariance measurements, with the error being most important under nocturnal calm conditions. We tested the hypothesis that horizontal mean transport, not previously measured in tropical forests, may account for the missing CO<sub>2</sub> in such conditions. A subcanopy network of wind and CO<sub>2</sub> sensors was installed. Significant horizontal transport of CO<sub>2</sub> was observed in the lowest 10 m of the canopy. Results indicate that CO<sub>2</sub> advection accounted for 73% and 71%, respectively of the carbon budget *deficits* for all calm nights evaluated during dry and wet periods. We found that horizontal advection was significant and important to the canopy CO<sub>2</sub> budget, during environmental conditions with lower above-canopy friction velocity values and also during higher values commonly used thresholds to the u\* corrections approach.

**Key words:** Amazon Rainforest; Advection, Drainage Flow, Eddy Covariance, Subcanopy.

---

<sup>1</sup> Tóta, J., Fitzjarrald, D.R., Staebler, R.M., Sakai, R.K., Moraes, O.M.M., Acevedo, O.C., Wofsy, S.C., Manzi, A.O., 2008. Amazon rain forest subcanopy flow and the carbon budget: Part I – Santarém LBA-ECO Site. *Journal of Geophysical Research – Biogeosciences*, 113, 1-15.

## 1. Introduction

In the last decade tower-based eddy-covariance (EC) observations have been established worldwide to monitor net ecosystem exchange (NEE) of carbon dioxide [Goulden *et al.*, 1996; Black *et al.*, 1996; Baldocchi *et al.*, 2001]. This micrometeorological method is considered the most accurate when applied at nearly flat sites that have long homogeneous upwind fetches. Its application has spawned global scale flux-measuring networks [Baldocchi *et al.*, 1988; Aubinet *et al.*, 2000] whose justification has been to estimate long-term carbon exchange. Two related issues complicate this ambition. First, proper estimates of nocturnal respiratory fluxes are essential, but weak turbulent mixing at night is common. This issue of underreporting of nocturnal CO<sub>2</sub> fluxes has been addressed using the approach advocated by Goulden *et al.* [1996], formalized by the FLUXNET committee [Baldocchi *et al.*, 2001]. Data on very calm nights (often an appreciable fraction of all nights) is simply discarded and replaced with the result of an ecosystem respiration rate found on windy nights that are otherwise similar [Miller *et al.*, 2004; Gu *et al.*, 2005]. A second issue is that many flux-observing sites lie in complex terrain [Lee, 1998; Paw U *et al.*, 2000; Aubinet *et al.*, 2003; Feigenwinter *et al.*, 2004; Staebler and Fitzjarrald, 2004, 2005]. On the very calm nights for which flux underestimates occur, subcanopy drainage flows are most common [Yoshino *et al.*, 1984; Sun *et al.*, 2007]. Whether or not subcanopy drainage flows also advect sufficient CO<sub>2</sub> laterally out of the budget “box” to account for the ‘missing flux’ on calm nights is site specific, and must be determined observationally [Lee, 1998; Feigenwinter *et al.*, 2004; Staebler and Fitzjarrald, 2004; Aubinet *et al.*, 2005]. Previous studies show that, under light wind and very stable conditions over the canopy, the importance of advection on the carbon balance can be as large as, or even larger than, the magnitude of NEE, observed by the EC approach when there are drainage flows [Staebler, 2003; Staebler and Fitzjarrald, 2004,

2005; *Sun et al.*, 2007]. To assess the importance of subcanopy flows one must present a plausible physical mechanism to account for this underestimation as past studies asserted [*Kruijt et al.*, 2004; *Araújo et al.*, 2002]. Even on gentle slopes, it is risky to assume that there is no lateral motion or divergence that can advect CO<sub>2</sub> (e.g., *Acevedo and Fitzjarrald*, 2003) and applying the ideal site criteria to more typical situations is questionable [*Baldocchi et al.*, 2000; *Staebler and Fitzjarrald*, 2004, 2005].

Most studies of subcanopy advection to date have been done at midlatitude sites. We are not aware of similar studies in the tropical rain forest. The forests in the Amazon region account for 10% of the world's terrestrial primary productivity and about the same fraction of carbon stored in land ecosystems [*Malhi et al.*, 1998]. In the last decade reports have suggested that this region has such a positive sink of CO<sub>2</sub>, which, when scaled for the entire Amazon region, could account for a significant fraction of the carbon budget, the so called residual terrestrials sink (IPCC, 2007). Since results from the Large Scale Biosphere-Atmosphere experiment in Amazonia (LBA, *Keller et al.*, 2004) will likely be used to represent the Amazon in its entirety in global change models, it is important to identify systematic observation problems. In this paper we describe a detailed subcanopy CO<sub>2</sub> and wind system sensors deployed for the first time in the Amazon tropical rainforest combined with EC tower flux and respiration measurements and analyze the results with the aim to better understand the local carbon budget. Formally, we test the hypotheses that EC measurements underestimate the CO<sub>2</sub> flux on calm nights because of lateral air flow out of the control volume at the km67 Santarém LBA site. We seek to demonstrate that observed subcanopy horizontal CO<sub>2</sub> gradients and wind transport processes yield significant mean net transport of CO<sub>2</sub> into or out of the control volume. Following *Staebler and Fitzjarrald* [2004, 2005], we examine the importance of subcanopy advection in the following steps:

(1) We must show that systematic subcanopy flows exist and are measurable; and

(2) Observed subcanopy flows must be related to a physical driving mechanism (e.g. drainage forcing) that ensures that they are sufficiently systematic so that long-term budgets are affected.

## 2. Material and Methods

### 2.1. Site description

The study site (54° 58'W, 2° 51'S) is part of the ecological component of the Large Scale Biosphere-Atmosphere experiment in Amazonia (LBA-ECO), which aims to achieve better understanding of the regional carbon balance. It is located in the Tapajós National Forest reserve (FLONA Tapajós), near km 67 of the Santarém-Cuiabá highway (BR-163). The average temperature, humidity, and rainfall are 25.8°C, 85%, and about 1800 mm per year, respectively [Parotta *et al.*, 1995]. This area contains predominantly nutrient-poor clay oxisols with some sandy utisols [Silver *et al.*, 2000], each of which has low organic content and cation exchange capacity.

Vegetation consists of occasional 55 m height emergent trees with a closed canopy at 40m and below [Parker *et al.*, 2004]. Trees include *Manilkara huberi* (Ducke) Chev., *Hymenaea courbaril* L., *Betholletia excelsa* Humb. and Bonpl., and *Tachigalia spp* species, and epiphytes. There is overall an uneven age distribution, but the forest can be considered to be primary or old growth [Clark, 1996; Goulden *et al.*, 2004].

Local topographic features include a steep nearby river escarpment sloping to the Tapajós River to the west, but with a weak eastward-facing slope into the basin of the Curua-Una watershed. Except near the escarpment, drainage flows would be expected to move opposing the easterly prevailing wind field (red arrow in the Figure 1).

Several studies have demonstrated a significant seasonal variations in solar radiation, net radiation, air temperature, and vapor pressure deficit, all of which increase substantially with the seasonal decline in precipitation, while surface litter and soil moistures also decline [da Rocha *et al.*, 2004].

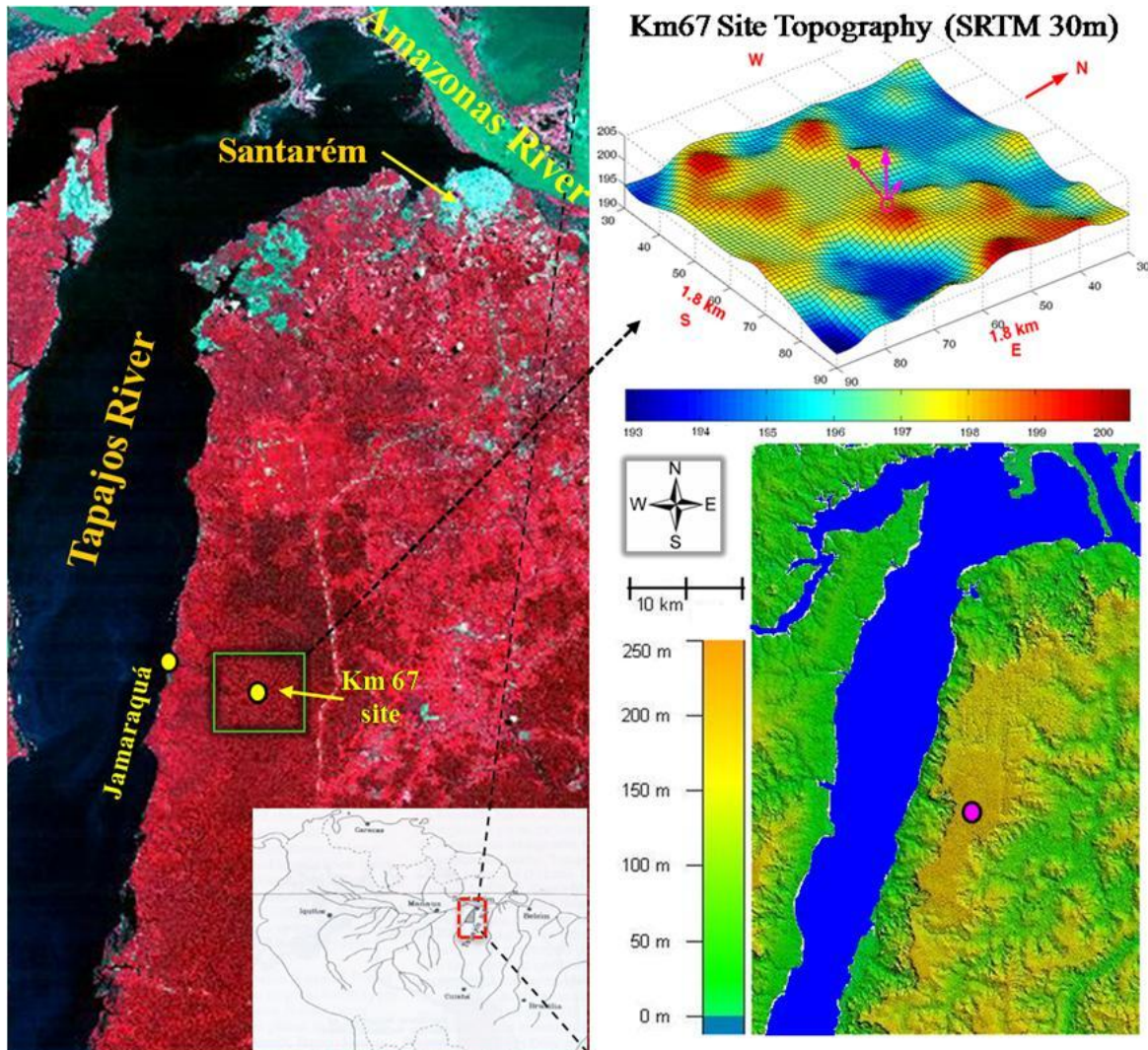


**Figure 1.** Site Location in the vegetation cover image and high resolution (30m grid space) tower-base local topography as determined by the Shuttle Radar Topography Mission (SRTM). The arrows shows the modal wind direction at 57.8 m (red, from East) and in the subcanopy (magenta, from southeast).

## 2.2. Instrumentation and observation

The field measurements at the old growth forest site at km67 in the LBA study area included several meteorological and EC measurements from 2001 to 2006, focusing on the dynamics of primary forest ecosystems. Several LBA groups have made observations of meteorological quantities, such as EC fluxes of  $\text{H}_2\text{O}$ ,  $\text{CO}_2$ , temperature, and wind fields. We share datasets obtained by the LBA Project groups CD03 and CD10 (CD – Carbon Dynamics).

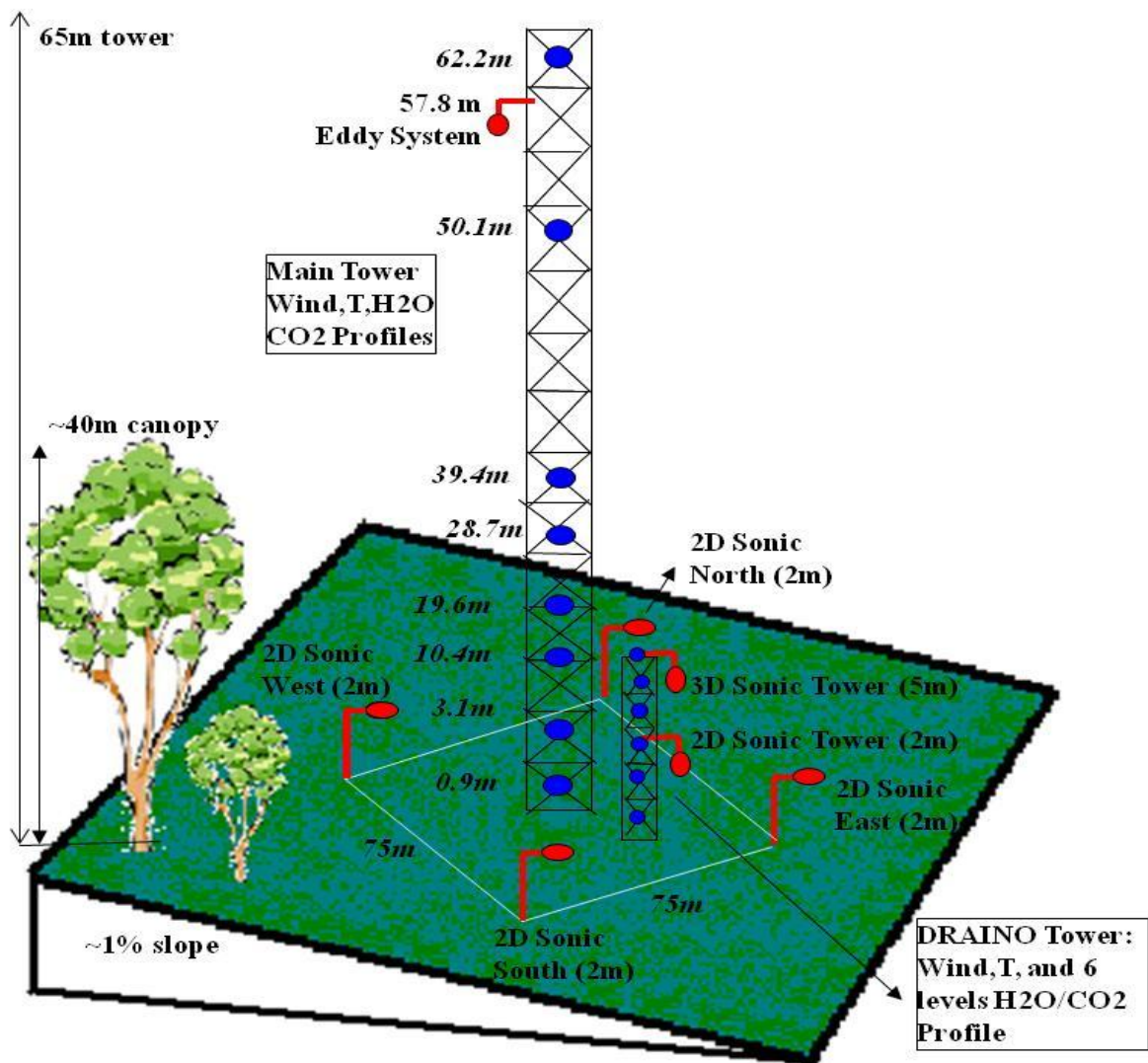


**Figure 2.** Main tower and Draino deployed instruments systems.



The CD10 tower systems include EC and meteorological wind, CO<sub>2</sub>, temperature and water vapor profiles collected between 2001 and 2006 (Table 1 and Figure 2). The instrumentation descriptions and quality control procedures for the basic datasets obtained at the main km67 tower site are given in *Saleska et al.* [2003] or at the online web page <http://www-as.harvard.edu/data/lbadata.html>. A weather station was deployed in Jamaraguá at the base of the Tapajós escarpment to help in identifying topographical effects. A high resolution STRM map was made, based on a 90m grid, interpolated to 30 meters, to describe the gentle topography around the tower site (Figure 1).

**Table 1. LBA – Old Growth (KM67) Site Sensors**

Level (m)	Parameter	Instrument
64.1,52,38.2,30.7 57.8	Wind speed u' v' w' T', CO <sub>2</sub> , H <sub>2</sub> O	Cup anemometers CSAT 3D sonic anemometers LI-7000 CO <sub>2</sub> /H <sub>2</sub> O analyzers
5 1.8	U' v' w' T' CO <sub>2</sub> , U, V, T (horizontal array)	ATI 3D sonic anemometer CATI/2 2D sonic anemometers, LI-7000
62.2,50.1,39.4,28.7 19.6,10.4,3.1,0.9	CO <sub>2</sub> , H <sub>2</sub> O Profile	LI-7000 CO <sub>2</sub> /H <sub>2</sub> O analyzer
61.9,49.8,39.1,28.4 18.3,10.1,2.8,0.6	Temperature	Aspirated thermocouples

Subcanopy network observations are available for two campaigns in 2003 (Phase 1, DOY 198-238) and 2004/2005 (Phase 2, DOY 250-366 and 01-32). The subcanopy data complement observations that were made around the central 65-meter tower. The observation and acquisition approach was developed at Atmospheric Sciences Research Center, ASRC (*Staebler and Fitzjarrald, 2005*) and includes a PC operating in Linux, an outboard Cyclades multiple serial port (CYCLOM-16YeP/DB25) collecting and merging serial data streams from all instruments in real time, with the data archived into 12-hour ASCII files.

Observations include CO<sub>2</sub>, temperature, H<sub>2</sub>O and wind field measurements at 1 Hz (Figure 2), this sufficient to cover advection and storage fluxes (non turbulent fluxes). The

system included a LI-7000 Infrared Gas Analyzer (LI-COR inc., Lincoln, Nebraska, USA), a multi-position valve (Vici Valco Instrument Co., Inc.) controlled by a CR23x Micrologger (Campbell Scientific, Inc., Logan, Utah, USA), which also monitored flow rates. The instrument network array (Figure 2 and Table 1) consisted of 6 subcanopy sonic anemometers: a Gill HS (Gill Instruments Ltd., Lymington, UK) 3-component sonic anemometer at 5 m elevation in the center of the grid and 5 SPAS/2Y (Applied Technologies Inc., CO, USA) 2-component anemometers (1 sonic at center and 4 sonic along the periphery), with a resolution of  $0.01 \text{ m s}^{-1}$ . The horizontal gradients of  $\text{CO}_2/\text{H}_2\text{O}$  were measured in the array at 2 m above ground, by sampling sequentially from 4 horizontal points surrounding the main tower location at distances of 70-80m, and from points at 6 levels on the small Draino tower, performing a 3 minute cycle. Air was pumped continuously through 0.9 mm Dekoron tube (Synflex 1300, Saint-Gobain Performance Plastics, Wayne, NJ, USA) tubes from meshed inlets to a manifold in a centralized box.

A baseline air flow of 4 LPM from the inlets to a central manifold was maintained in all lines at all times to ensure relatively “fresh” air was being sampled. The air was pumped for 20 seconds from each inlet, across filters to limit moisture effects. The delay time for sampling was five seconds and the first ten seconds of data were discarded. At the manifold, one line at a time was then sampled using an infrared gas analyzer (LI-7000, Licor, Inc.). The 6-level  $\text{CO}_2$  profile on the 5 m tower was determined in a similar, sequential manner, using a LI-7000 gas analyzer sampling pumped air from all 10 points (6 vertical, 4 horizontal) in the measurement array. Flow rates at the inlets were checked regularly to ensure proper flow and to detect potential leaks.

### 2.3. Preinstallation intercomparison

Following *Staebler and Fitzjarrald* [2004] an initial instrument intercomparison was made to identify the performance of the integrated subcanopy observation system. The CO<sub>2</sub> sensor (Licor 7000 sensor) and the sonic anemometers (CATI/2 and SPAS/2Y, Applied Technologies, Inc. sensors) were co-located on the small tower for a calibration period (5 days) before being deployed at 1.8 meters above the ground (Figure 2). We anticipated that the horizontal transport product  $uc$  would be near its largest value at this height, a finding later confirmed at this site (see Figure 4 below). We had insufficient instrumentation to construct a network of towers to measure the CO<sub>2</sub> concentration up to canopy top, and this led us to continue our earlier practice of asserting a profile similarity hypothesis, where one hypothesizes spatial similarity between vertical CO<sub>2</sub> and wind profiles and their product (the horizontal transport). Using a single gas analyzer with a common path multi-position valve for the horizontal and vertical profiles minimizes the potential for systematic concentration errors. A field calibration was performed by co-locating sensors and gas inlets at the same point of measurement. The comparisons indicate scatter in [CO<sub>2</sub>] because samples were sequential, not synchronous. The mean standard error was  $< 0.05$  ppm. The wind comparisons were made using a 3D sonic as the standard for the 2D sonic anemometers, resulting in a mean standard error of about  $0.005 \text{ ms}^{-1}$ . Ambient subcanopy wind speed was on the order of a few  $\text{cm s}^{-1}$  and can be reliably measured in the subcanopy space by the system. After intercomparison, the sonic anemometers and the CO<sub>2</sub> inlet tubes were moved from the small tower center point and deployed about 2 meters above ground as indicated in Figure 2.

We examined to what extent the subcanopy sensor geometry of CO<sub>2</sub> allows the system to function as a “*network*”, where each point of the measurements are correlated and the space

between them is on the order of the relevant scales of transport or smaller. We test whether the network can be used to capture the relevant gradients and transport processes in very low wind conditions [Staebler and Fitzjarrald, 2004]. Figure 3 (left panel) shows the 3-min data autocorrelation of CO<sub>2</sub> and wind fields determined from continuous measurements.

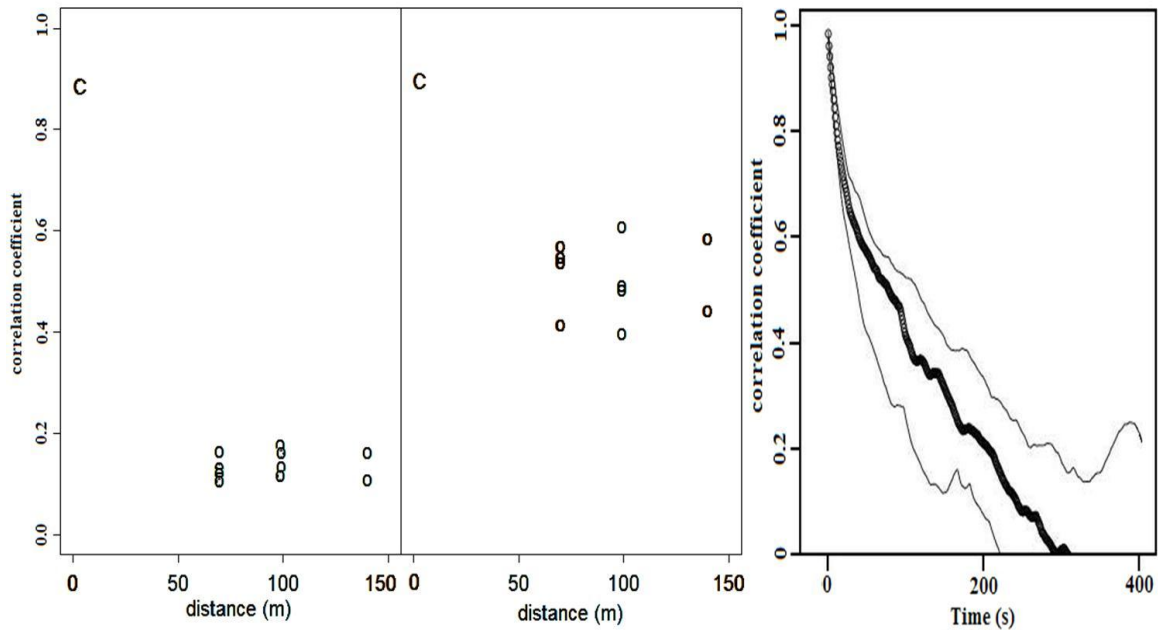


**Figure 3.** The autocorrelation coefficient for total wind speed (left panel) and CO<sub>2</sub> concentration (center panel) as a function of distance between sampling points 1.8m above ground in the subcanopy. (3-minute averages data from “Draino” Phase 1 (DOY 198-238/2003). “C” represents the calibration period. The right panel shows the temporal autocorrelation for wind, the solid line represents the median, and the thinner lines the upper and lower quartiles. Mean wind speed in the subcanopy was  $0.13 \text{ m}\cdot\text{s}^{-1}$ .

The relevant spatial scale  $X$  is approximately 70-150 m. We assessed our choice of network size by examining observed spatial and temporal autocorrelations of the wind measurements. The spatial autocorrelation of horizontal wind speed (Figure 3 - center panel) drops rapidly to 0.2 in 60 m, but fluctuations in CO<sub>2</sub> (Figure 3 - left panel) exhibit a larger integral scale 100-200 m, while the temporal integral is approximately 100-300s (Figure 3, right panel). This is consistent with results obtained by Staebler and Fitzjarrald [2004] in a very different forest, except that the characteristic horizontal CO<sub>2</sub> scale is larger than that at

Harvard Forest, consistent with the thicker canopy at the Tapajós National Forest. We do not understand why the spatial correlations do not decrease with increasing distance, as was observed in *Staebler and Fitzjarrald* [2004]. This could be a consequence of the temporal scale variations being larger than are the spatial ones.

## 2.4. CO<sub>2</sub> conservation equations

The net ecosystem exchange (NEE) for a horizontal plane at height  $h$ , which represents the exchange rate between forest and atmosphere, is given by,

$$NEE_h = F_0 + \int_0^h \bar{s} dz \quad (1),$$

where  $F_0$  is the soil flux entering (or leaving) the control volume at the bottom and the  $\bar{s}$  integral describes the sum of all sources and sinks in the canopy space. The Reynolds average conservation equation of a scalar “ $c$ ”, ignoring molecular diffusion process, can be expressed by,

$$\frac{\partial \bar{c}}{\partial t} + \bar{u}_i \frac{\partial \bar{c}}{\partial x_i} + \bar{c} \frac{\partial \bar{u}_i}{\partial x_i} + \frac{\partial \overline{u_i'c'}}{\partial x_i} = \bar{s} \quad (2),$$

with  $\bar{u}_i = (u, v, w)$ . Considering using equations 1 and 2, and considering incompressibility, after integrating vertically, it can be written in the form,

$$\int_0^h \frac{\partial \bar{c}}{\partial t} dz + \int_0^h \bar{u} \frac{\partial \bar{c}}{\partial x} dz + \int_0^h \bar{v} \frac{\partial \bar{c}}{\partial y} dz + \int_0^h \bar{w} \frac{\partial \bar{c}}{\partial z} dz + \int_0^h \frac{\partial \overline{u'c'}}{\partial z} dz + \int_0^h \frac{\partial \overline{v'c'}}{\partial z} dz + \left( \overline{w'c'} \right)_h = \int_0^h \bar{s} dz \quad (3),$$

$$[1] \quad [2] \quad [3] \quad [4] \quad [5] \quad [6] \quad [7] \quad [8]$$

where  $u$ ,  $v$ , and  $w$ , are wind components and “ $c$ ” a scalar, such as CO<sub>2</sub>. The term [4] is the vertical advection term and term [8] the sum of all sinks and sources between  $z=0$  and  $z=h$ , including everything crossing the lower boundary at  $z=0$ .

In the case of horizontal homogeneity, terms [1], storage in the canopy space, and [7], vertical eddy flux at  $z=h$  (57.8 m for the site studied), are obtained from standard EC and profile sensors at the flux site. Terms [5] and [6] are the horizontal turbulent flux divergence and negligible when compared with other terms [Yi *et al.*, 2000; Turnipseed *et al.*, 2003]. The terms [2], [3] and [4] respectively are horizontal and vertical advection. The vertical mean advection was integrated using the method of Lee [1998]:

$$[\overline{w\bar{c}}]_0^h - \frac{\overline{w}_h}{h} \int_0^h \bar{c}(z) dz = \overline{w}_h \left( \bar{c}(h) - \frac{1}{h} \int_0^h \bar{c}(z) dz \right) \quad (4),$$

where  $\overline{w}_h$  and  $\bar{c}(h)$  are the residual vertical velocity and the mean concentration at the top of the layer (57 m), respectively [see in Staebler and Fitzjarrald, 2004]. Staebler and Fitzjarrald [2004] argued that Lee's approach is an overestimate, noting that the assumption of a linear increase of  $\overline{w}_h$  with height is often violated. Comparisons of the divergence measurements at 1.8 m height with measured vertical velocities at 46 m and 57.8 m were made for a few days of wind data and the results show no correlation indicating that Lee's approach is also violated for the site studied here. However, Lee's formulation will be used to provide an upper estimate of the vertical advection term in order to compare its potential significance relative to the other terms. The calculation of mean vertical advection was made only during phase 2 (DOY 250-366/2004 and 01-32/2005) when sufficient data for the calculation was available. We recognize that obtaining credible mean vertical velocity from sonic anemometers is still a challenge (e.g., Vickers and Mahrt, [2006]). However, the difficulties in assessing one term in the continuity equation should not preclude efforts to obtain the others.

## 2.5. Vertical integration of the horizontal advection terms

To perform a complete three-dimensional forest CO<sub>2</sub> box budget it is necessary to obtain vertical profiles of the horizontal gradient measurements for the entire control volume, and this is generally not feasible. We lacked resources to install a network of towers to measure the CO<sub>2</sub> profile at a number of locations in the canopy. Noting, as in *Staebler and Fitzjarrald* [2004], that the product  $uc$  is largest near the forest floor, we relied on subcanopy measurements made 1.8 m above the ground. To compensate for the missing network of vertical profiles, we approximate the vertical integration through the canopy of the horizontal advective terms [2] and [3] following methods developed by *Staebler and Fitzjarrald* [2004]. One hypothesizes spatial similarity between vertical CO<sub>2</sub> and wind profiles and their product (horizontal transport)  $uc$ , where  $\underline{u}$  is the average wind and  $\underline{c}$  the average CO<sub>2</sub> concentration. In this assumption, the shapes of the profiles throughout the canopy space are considered similar to the central point where the profiles are measured (Figure 2).

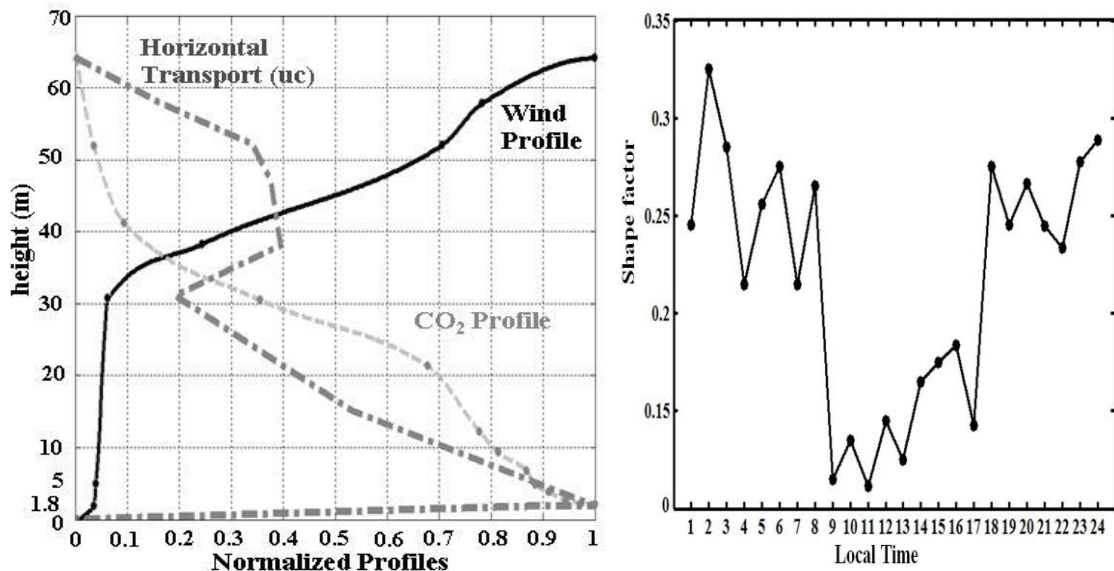


**Figure 4.** Typical nighttime normalized median profiles of CO<sub>2</sub>, wind speed and their product ( $uc$ ) horizontal transport (left panel); and the diurnal cycle of the shape factor for horizontal advection (right panel).

Figure 4 presents a typical feature of the shape factor profiles of CO<sub>2</sub> concentration, wind and horizontal transport. The horizontal subcanopy measurement height (1.8 m) is a height where the advection term is expected to be significant, providing confidence for single level height measurements to determine the integrated layer advection.

The procedure of integrating vertically is formalized through,

$$c^*(x, z) = f(z) c^*(x, z_1) \quad , \quad (5)$$

where  $f(z)$  is the (assumed constant) shape of the CO<sub>2</sub> profile relative to height  $z_1 = 1.8\text{m}$  (horizontal plane). The difference between the actual CO<sub>2</sub> concentration and nocturnal CO<sub>2</sub> concentration above the canopy (baseline value) is defined as  $c^*(z) = c(z) - c_0$ . The  $c^*$  was used instead of  $c$  because there is a practical lowest limit of CO<sub>2</sub> =  $c_0$ , indicative of the atmospheric base state, since it has no effect on the budget. Then, the vertical integration gives:

$$\int_0^h \frac{\partial c^*(x, z)}{\partial x} dz = \frac{\partial c^*(x, z_1)}{\partial x} \int_0^h f(z) dz = \frac{\partial c^*(x, z_1)}{\partial x} h S_c \quad (6),$$

where  $S_c$  is the shape factor for the CO<sub>2</sub> concentration profile. Applying the same procedure to describe the wind speed profile yields the advection estimates:

$$\begin{aligned} \int_0^h u(x, z) \frac{\partial c^*(x, z)}{\partial x} dz &= \int_0^h g(z) u(x, z_1) f(z) \frac{\partial c^*(x, z_1)}{\partial x} dz = \left( u(x, z_1) \frac{\partial c^*(x, z_1)}{\partial x} \right) \int_0^h f(z) g(z) dz \\ &= \left( u(x, z_1) \frac{\partial c^*(x, z_1)}{\partial x} \right) \cdot (hS) \end{aligned} \quad (7),$$

where  $S$  is the shape factor for horizontal advection of CO<sub>2</sub>. The nocturnal time shape factor values for both studied periods averaged 0.28, while the daytime value was typically 0.14 (Figure 4). This is consistent with results obtained by *Staebler and Fitzjarrald* [2004], possibly due to similar shape factors for CO<sub>2</sub> and wind speed profiles at both sites.



### 3 – Results and Discussion

#### 3.1. CO<sub>2</sub> concentration field

The average composite of horizontal concentration of CO<sub>2</sub> measured at 2-m height in nocturnal conditions for Phase 1 and Phase 2 (Figure 5) shows that the horizontal CO<sub>2</sub> field varied significantly at night during both observation phases. During Phase 1, the CO<sub>2</sub> concentrations at night were higher than during Phase 2. This may be associated with vegetation response to drier, cooler conditions and lighter wind during this phase, according to Figure 6.

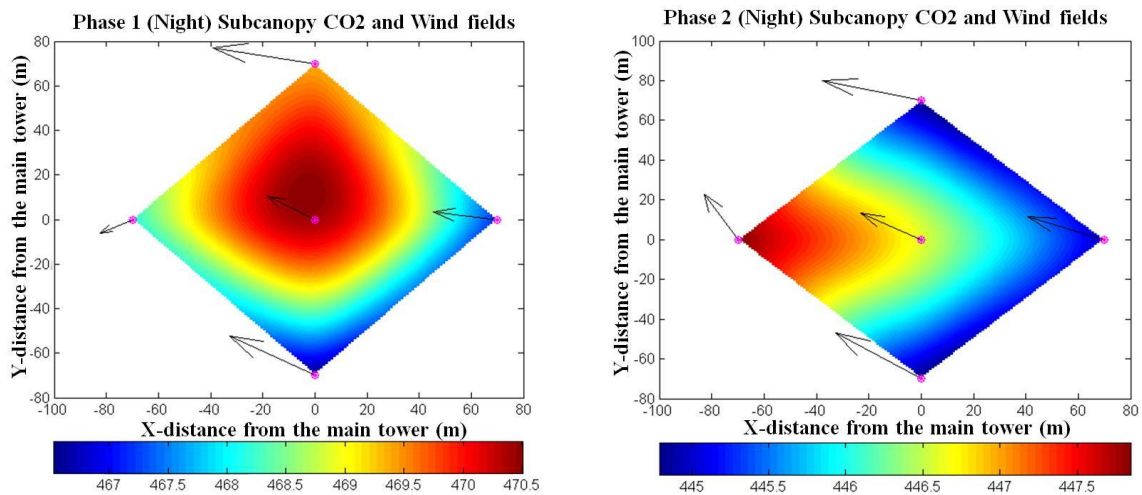


**Figure 5.** Night time composite of averaged subcanopy CO<sub>2</sub> concentration field and wind vectors for Phase 1 and Phase 2 campaigns. The units are in ppm and ms<sup>-1</sup>, respectively. (Largest arrow is 0.15 m s<sup>-1</sup>)

The typical values of average horizontal CO<sub>2</sub> gradients were about  $-0.026 \left( \frac{\partial \bar{c}}{\partial x} \right)$ , East-West) and  $0.023 \left( \frac{\partial \bar{c}}{\partial y} \right)$ , North-South) ppm m<sup>-1</sup> for all nights considered (7390 and 18366 average 3-minute data values, Phase 1 and Phase 2, respectively). These results are

comparable to the range of horizontal CO<sub>2</sub> gradients that have been reported in the literature, 0.025 to 0.079 ppm m<sup>-1</sup> [Feigenwinter et al., 2004; Staebler and Fitzjarrald, 2004; Aubinet et al., 2005]. One expects CO<sub>2</sub> concentrations and gradients near the ground to be site-specific under calm night wind speed conditions, due to varying soil respiration rates that depend on soil and litter layer composition, temperature and moisture.

Vertical profiles of temperature, water vapor concentration, CO<sub>2</sub> concentration and wind speed characterize the microclimate observed during each phase (Figure 6). The drier Phase 1 presents daytime and night patterns that contrast with the wetter Phase 2 conditions.

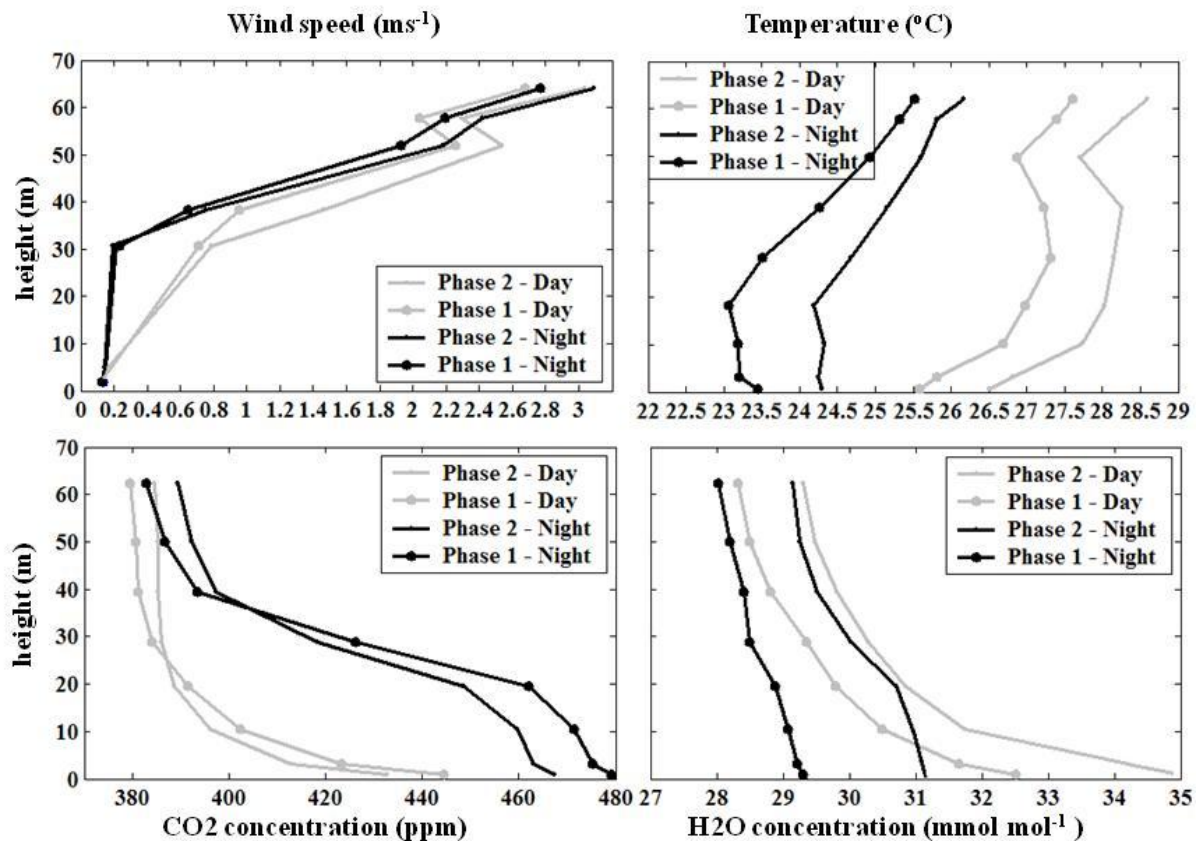


**Figure 6.** Vertical profiles of concentration of CO<sub>2</sub>, wind speed, temperature, and water vapor, for both Phases (dry and wet).

The wind speed profile had a similar shape during both phases, but above the canopy the magnitude of wind speed was greater in Phase 2 compared with Phase 1 period. This

suggests a reduction on turbulence level or vertical mixing during the nighttime, as shown in Figure 7. The temperature profiles show the same pattern for the two phases, however, the dry phase was about 2°C warmer. During the daytime, for both dry and wet periods, a maximum air temperature was observed at 30 m associate with the absorption of sunlight by vegetation, generating a light unstable condition between 30 and 50 m, and stable condition below 30 m.

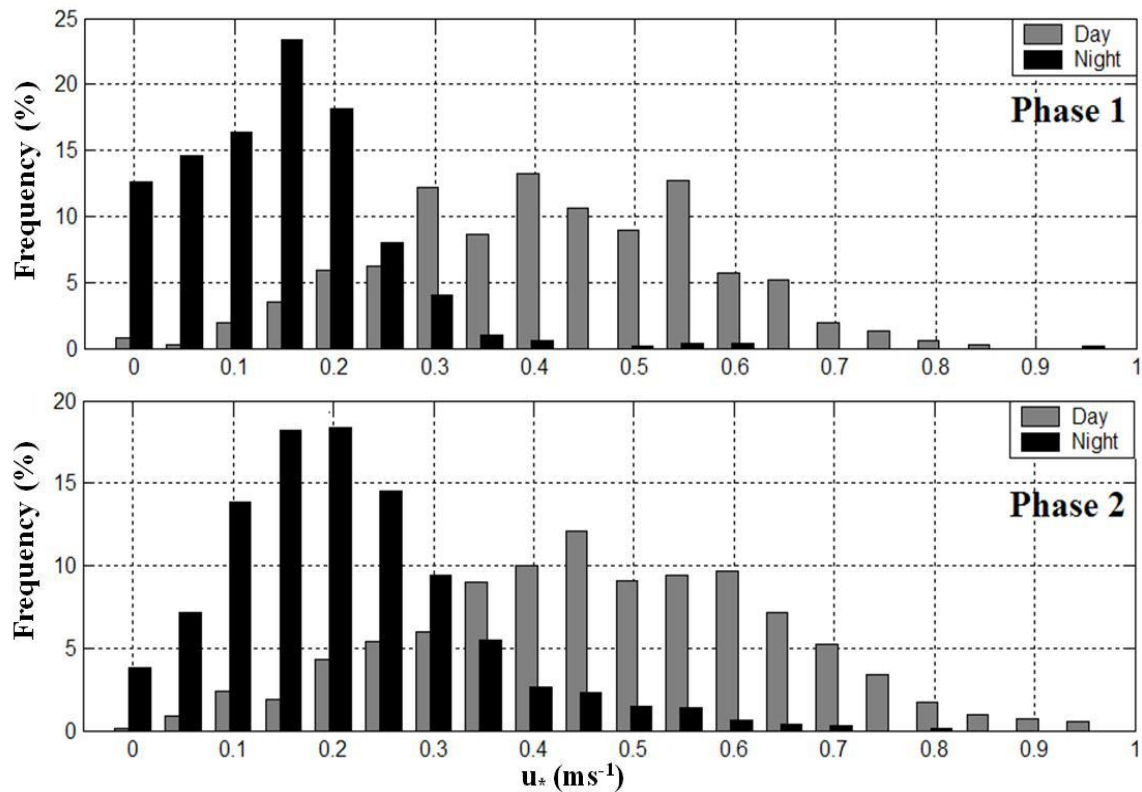


**Figure 7.** Frequency distribution histogram of friction velocity ( $u_*$ ) at 57.8 m, for Phase 1 and Phase 2 measurements, separate day and night periods.

During the nighttime the net loss of thermal radiation cooled the vegetation relative to the air adjacent, generating local stability and affecting above-canopy momentum transport. However, from the observed temperature profiles, in the layer below 20 m, trunk space layer, just below the upper canopy; the subcanopy temperature profile was dry and cold relative to the underlying air ( $\approx -0.25^\circ\text{C m}^{-1}$ ). This combination of the cooling above 20 m and warming

below generates instability associated with negative buoyancy [see also *Fitzjarrald et al.*, 1990; *Fitzjarrald and Moore*, 1990]. This process may be contributing or creating horizontal flow gravitationally such as suggested by *Lee* [1998]. Similar temperature profiles were reported by *Goulden et al.*, [2006] for km83 LBA site 16 km away to the south.

As expected, the vertical concentration of CO<sub>2</sub> reflects both atmospheric transport and forest physiological processes, in which during the daytime photosynthesis removes CO<sub>2</sub> from the air depleting concentration levels, and during the nighttime the concentration builds up due to respiration, the reduction of turbulence, and absence of photosynthesis.

The frequency distribution of the friction velocity above the canopy for the both dry (Phase 1) and wet (Phase 2) periods (Figure 7) shows very small values at nighttime. Nocturnal values of friction velocity smaller than 0.2 ms<sup>-1</sup> accounted for more than 85% and 65% for dry and wet periods, respectively. Therefore, we define deficit nights, using the procedure outlined by *Staebler and Fitzjarrald* [2004], when NEE (CO<sub>2</sub> eddy flux plus storage term) was less than total ecosystem respiration (see *Saleska et al.* [2003] and *Hutyra et al.* [2007], for details of these datasets). About 130 selected nights in each period, Phase 1 and Phase 2 match these criteria and were considered calm nighttime conditions.

Recently, *Saleska et al.* [2003] and *Miller et al.* [2004] have used a cutoff value of 0.3 ms<sup>-1</sup> for  $u_*$  correction to NEE estimates for the site studied. As show in Figure 7, much of the observed data must be discarded using this criterion, possibly altering the results. As reported by *Miller et al.* [2004], the tropical forest in Amazonia becomes a source than sink of atmospheric CO<sub>2</sub> depending of the cutoff value  $u_*$  used.

### 3.2. Subcanopy horizontal wind field

To calculate horizontal advection (terms [3] and [4] Equation 3), we estimated the horizontal wind field on the subcanopy space using the measurement subcanopy network described above. Though the site was considered flat in earlier reports [*Saleska et al.*, 2003; *Miller et al.*, 2004], a high resolution image shows that the forest floor gently slopes in a west-northwest direction from the main tower, according to Figure 2. *Goulden et al.* [2006] inferred the presence of drainage flows toward the SE at the km83 site to the south of the present study site, but they did not demonstrate subcanopy motion forced by density anomalies. Figure 8 shows statistics of the subcanopy wind field at night. There is a persistent wind direction that follows the local topographic gradient (see also Figure 1).

These nocturnal horizontal wind directions are in accord with nocturnal wind directions observed at the Jamaraguá station (Figure 1) close to the river Tapajós [*Fitzjarrald et al.*, 2004]. The statistics indicate that the nocturnal horizontal wind magnitude, varies among the subcanopy measurement points, probably due to the large heterogeneity of vegetation structure obstructions [see also *Staebler and Fitzjarrald*, 2004]. The average magnitude of the horizontal wind field in the subcanopy varied from 0.1 to 0.45 m s<sup>-1</sup>.

The observed subcanopy wind direction was prevailing from the southeast, with an interesting shift compared to the top of the main tower (57.8 m) wind direction, indicating a clearly uncoupled situation (Figure 8). Apparently, it seems that the subcanopy flow responds primarily to the local terrain gradients. *Goulden et al.* [2006] have reported a similar shift of the wind direction following the terrain gradient, even at 20 m when compared against the 64 m wind direction (see Figure 6, pg. 8 there in). *Sun et al.*, [2007] have also indicated that this shift happen at large spatial scales using short term datasets.

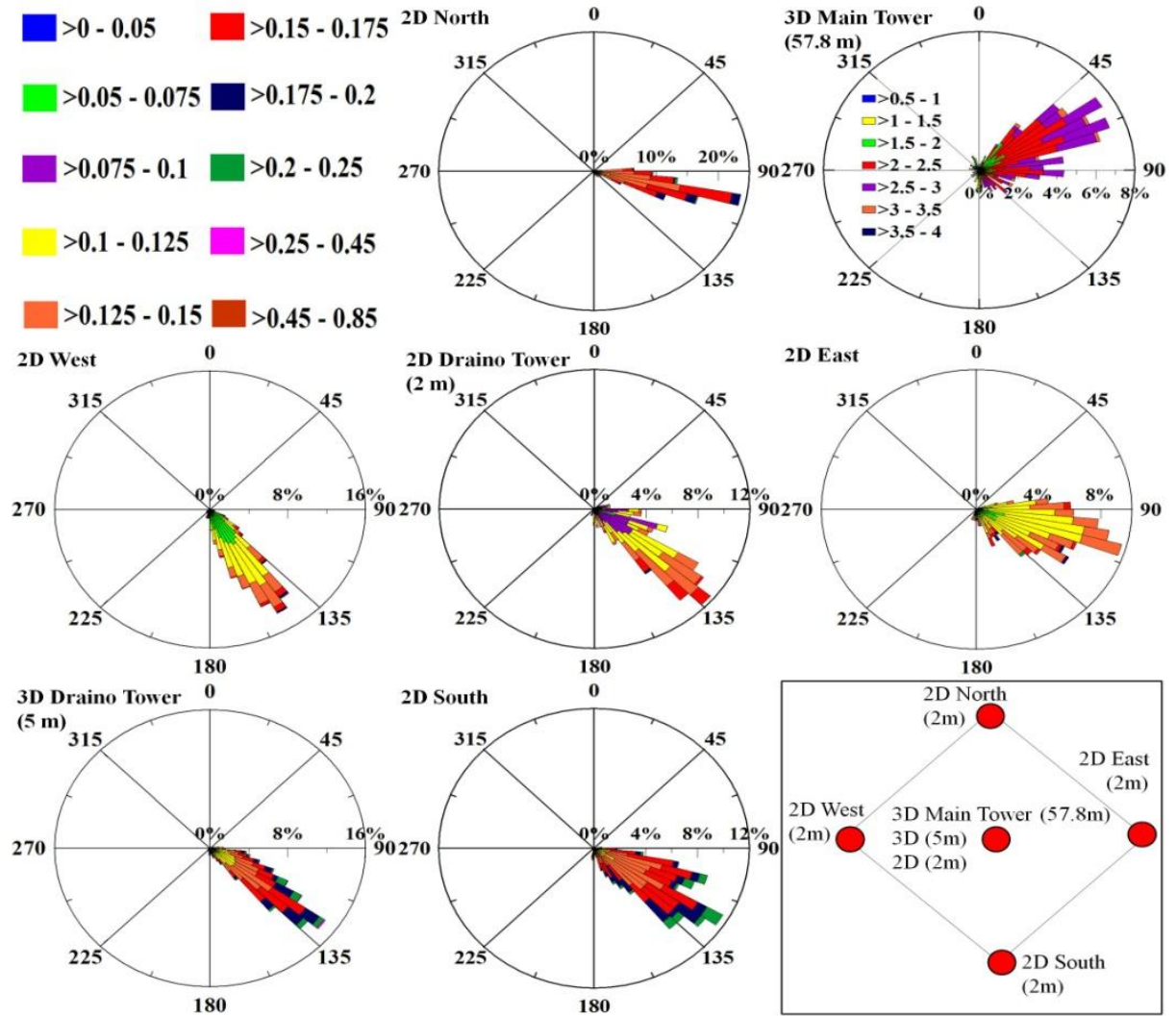


**Figure 8.** Nighttime distribution of the wind rose and its magnitude ( $\text{m s}^{-1}$ ) for the Draino sonic anemometer network and at top of main tower (57.8 m), including its localization (see Figure 2).

### 3.3. Subcanopy flow forcing terms

We follow the analysis presented by *Staebler and Fitzjarrald* [2004]. Subcanopy flows are generated by the balance of three driving forces; the pressure gradient perturbations, the buoyancy and the stress divergence, according to the momentum equation. The

momentum equation is given by,  $\frac{\partial u}{\partial t} + u \frac{\partial u}{\partial x} + w \frac{\partial u}{\partial z} = -\frac{1}{\rho} \frac{\partial p'}{\partial x} - g \frac{\theta'_v}{\theta_v} \frac{\partial h}{\partial x} - \frac{\partial \tau}{\partial z}$ , where  $\rho$  is the

density,  $p'$  the pressure perturbation,  $\theta_v$  the virtual temperature,  $\theta_v'$  the local departure of  $\theta_v$  from the mean,  $\frac{\partial h}{\partial x}$  the topographic slope, and  $\tau$  is the vertical stress, and drag effects are ignored. We do not believe that the terrain at the site studied is not so steep as to produce pressure perturbations strong enough to affect subcanopy flow locally, and it is ignored in the subsequent analysis. Thereby, the relative importance of buoyancy ( $b_{term} = \left| g \frac{\theta_v'}{\theta_v} \frac{\partial h}{\partial x} \right|$ ) and stress divergence ( $t_{term} = \left| \frac{\partial \tau}{\partial z} \right|$ ) terms will be considered. Observed fractions of the buoyancy term ( $b_{term}/(b_{term}+t_{term})$ ) and stress divergence term ( $t_{term}/(t_{term}+b_{term})$ ) indicate that the buoyancy term was more important during the nighttime than was the stress divergence term (Figure 9). The stress divergence term was more significant during the daytime associated with a higher degree of turbulent mixing as expected (Figure 9).

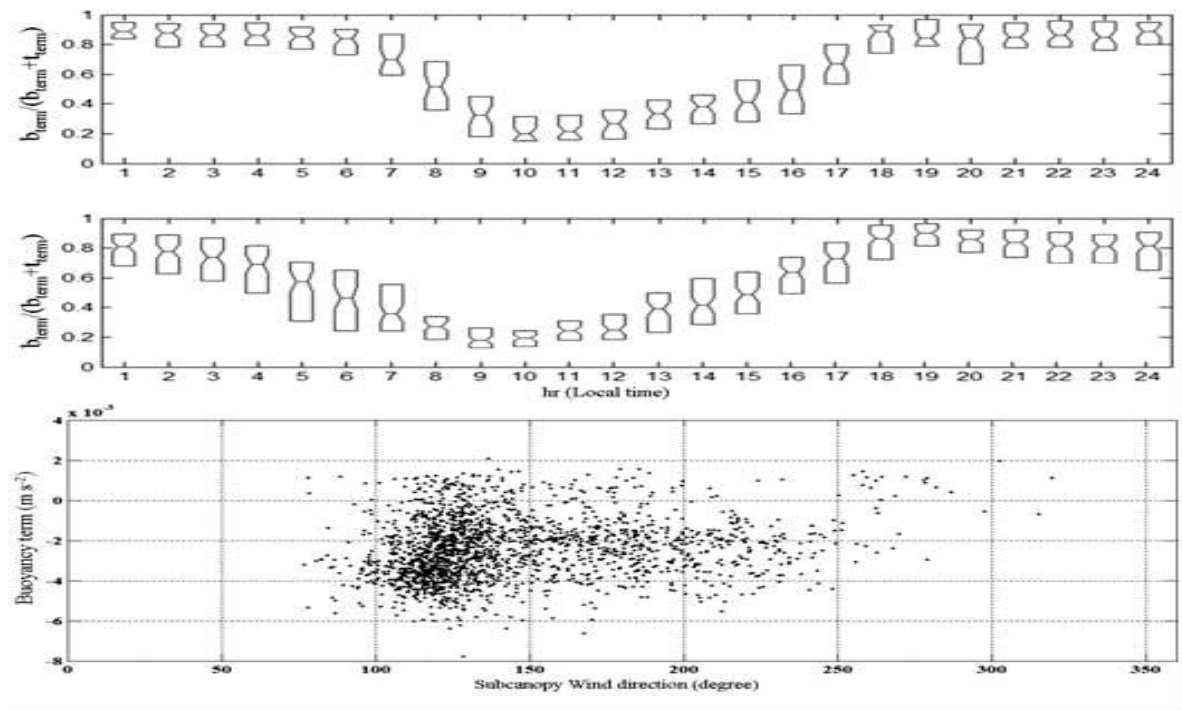


**Figure 9.** Diurnal cycle of buoyancy term forcing fractions relative to stress divergence term for Phase 1 (top panel) and Phase 2 (middle panel) observations, and (bottom panel) the buoyancy forcing term vs. subcanopy wind direction for both Phases.

Flows generated by the buoyancy term force the flow down the dominant terrain slope. Nocturnal wind directions were predominantly from the southeast toward northwest, as would be expected given the local topographic gradient (Figure 1). Our observations strongly indicate that the negative buoyancy term is the physical mechanism that explains the nocturnal drainage flow at this relatively flat study site.

### 3.4. Estimates of Advection Terms

The horizontal advection terms ([2] and [3] in Equation 3) were estimated using subcanopy wind speed components and CO<sub>2</sub> observation datasets from Phase 1 and Phase 2 (14350 and 36459 3-min valid observations, respectively). The horizontal CO<sub>2</sub> gradients were calculated using a linear least-square planar fit (Figure 5). (Note that the interpolated fields shown in Figure 5 were not used in the calculation).

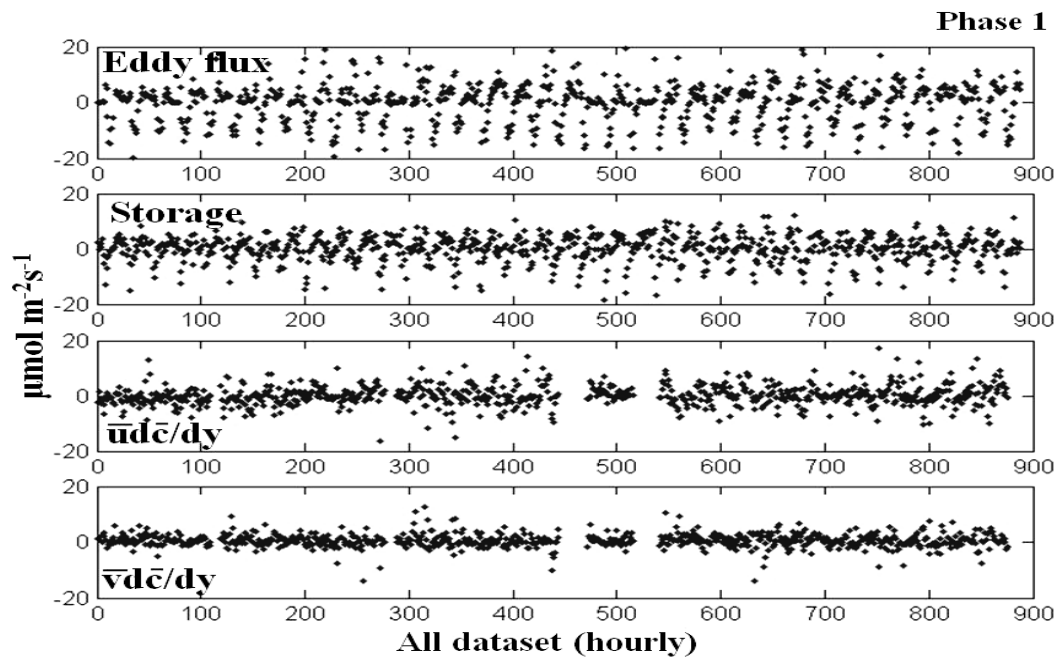


**Figure 10a.** Hourly-averaged summary of results for the Phase 1 and all the terms except eddy flux are average values for 0 to 57.8 m control volume. Top panel: vertical eddy flux at 57.8 m; 2<sup>nd</sup> panel: storage; 3<sup>th</sup> panel: east-west advection; and 4<sup>th</sup> panel: south-north advection, terms.



The hourly time series of average measurement flux terms for the CO<sub>2</sub> budget (Figure 10a and 10b) illustrate that the advective terms and eddy flux are of comparable magnitude, in accordance with recent published results at other sites [Staebler and Fitzjarrald, 2004; Aubinet et al., 2005; Marcolla et al., 2005; Sun et al., 2007; Feigenwinter et al., 2008]. Although the advective terms exhibit large scatter, their magnitude is comparable to the other flux terms. When averaged over all periods (for wet and dry phases) we obtained values significantly different from zero. For both phases (dry and wet) at the site studied, indicate a positive contribution to the total flux (i.e. transporting CO<sub>2</sub> out of the control volume around the tower).

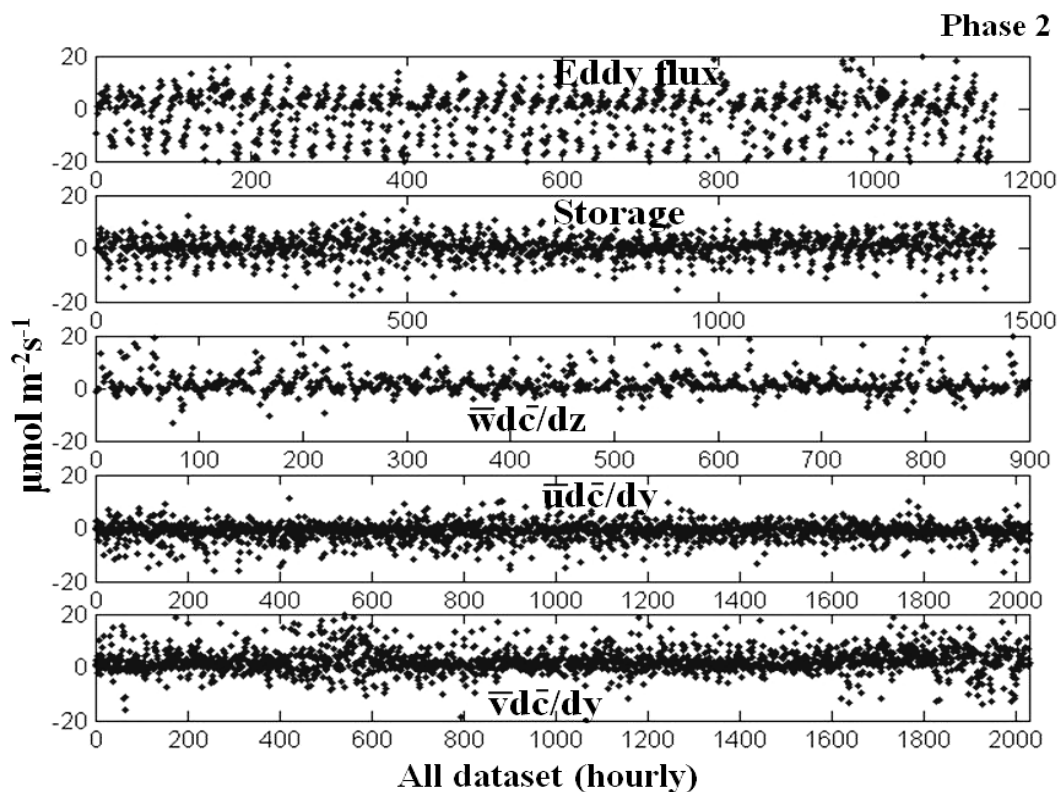


**Figure 10b.** Hourly-averaged summary of results for the Phase 2 and all the terms except eddy flux are average values for 0 to 57.8 m control volume. Top panel: vertical eddy flux at 57.8 m; 2<sup>nd</sup> panel: storage; 3<sup>rd</sup> panel: vertical advection; 4<sup>th</sup> panel: east-west advection; and 5<sup>th</sup> panel: and south-north advection, terms.

The average diurnal cycle of the flux terms for both dry (Phase 1) and wet (Phase 2) periods (Figure 11a and 11b) show the expected diurnal eddy flux pattern, negative during the day and positive at night. The vertical advection term plays no important contribution on average, but has a positive sign, since the mean vertical velocity and vertical CO<sub>2</sub> gradients were negative. The observed storage term is positive during the night, corresponding to CO<sub>2</sub> build-up in the canopy during stable conditions, and negative in the morning, owing to the release of the accumulated CO<sub>2</sub> due to mixing and onset of photosynthesis.

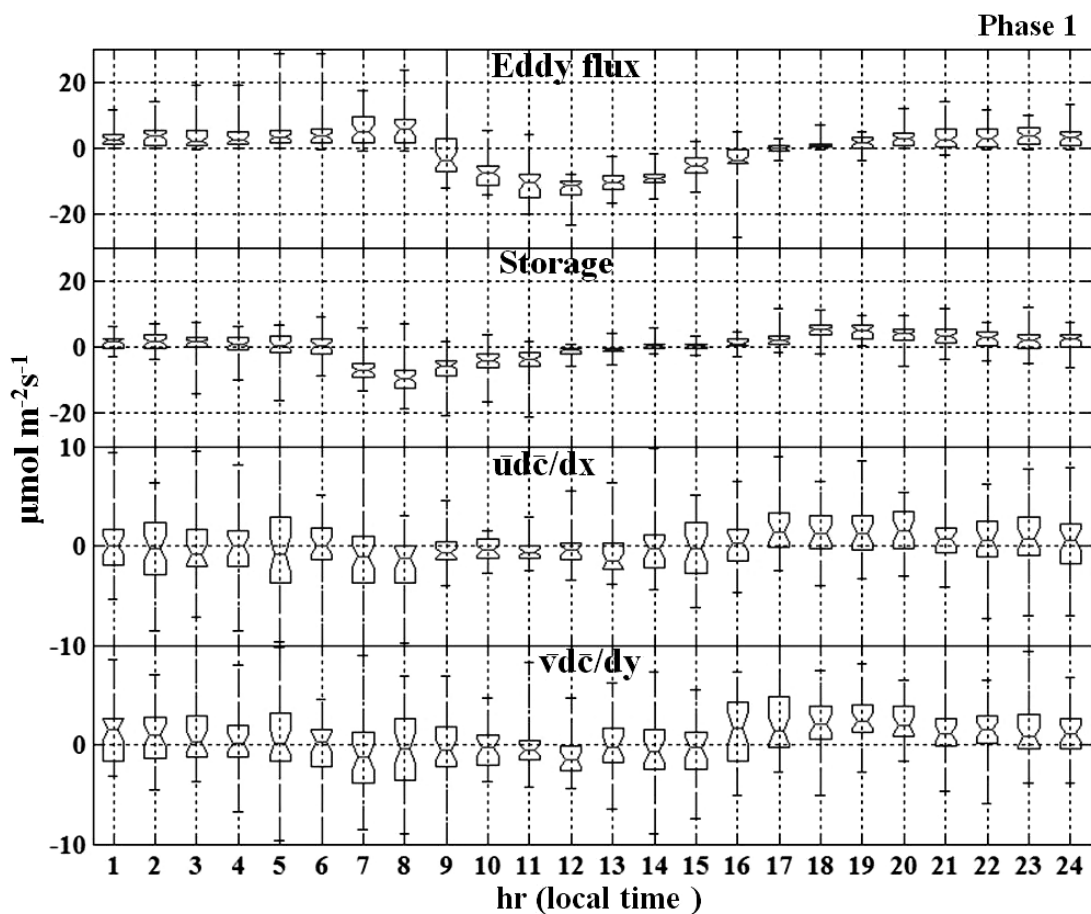


**Figure 11a.** Top panel: Hourly-averaged vertical eddy flux at 57.8 m; 2<sup>nd</sup> panel: storage term; 3<sup>rd</sup> panel: east-west advection term; and 4<sup>th</sup> panel: and south-north advection, terms. Note the change in vertical scale between the phases.

A notable feature in Figure 11a and 11b is that CO<sub>2</sub> storage during the second part of the night (between 01 - 06 LT) was 2 to 3 times smaller than the CO<sub>2</sub> storage in first part

(between 17 - 22 LT). This variability might be explained partially by differing CO<sub>2</sub> respiration source intensity from soil, canopy air space stability and canopy structure, but also could have resulted from the drainage flows. Similar patterns were observed by *Yang et al.*, [1999] in a Boreal Aspen Forest (USA), see Figure 3 there in. *Aubinet et al.* [2005] made this hypothesis, but did not demonstrate it observationally. It appears that between 1 and 6 LT our observations are consistent with significant positive horizontal advection, transport out of the control volume. The 17-22 LT observations also show positive horizontal advection. However, the high ecosystem respiration rate maintains a large storage term, and this partially offsets this horizontal advection in the CO<sub>2</sub> budget.

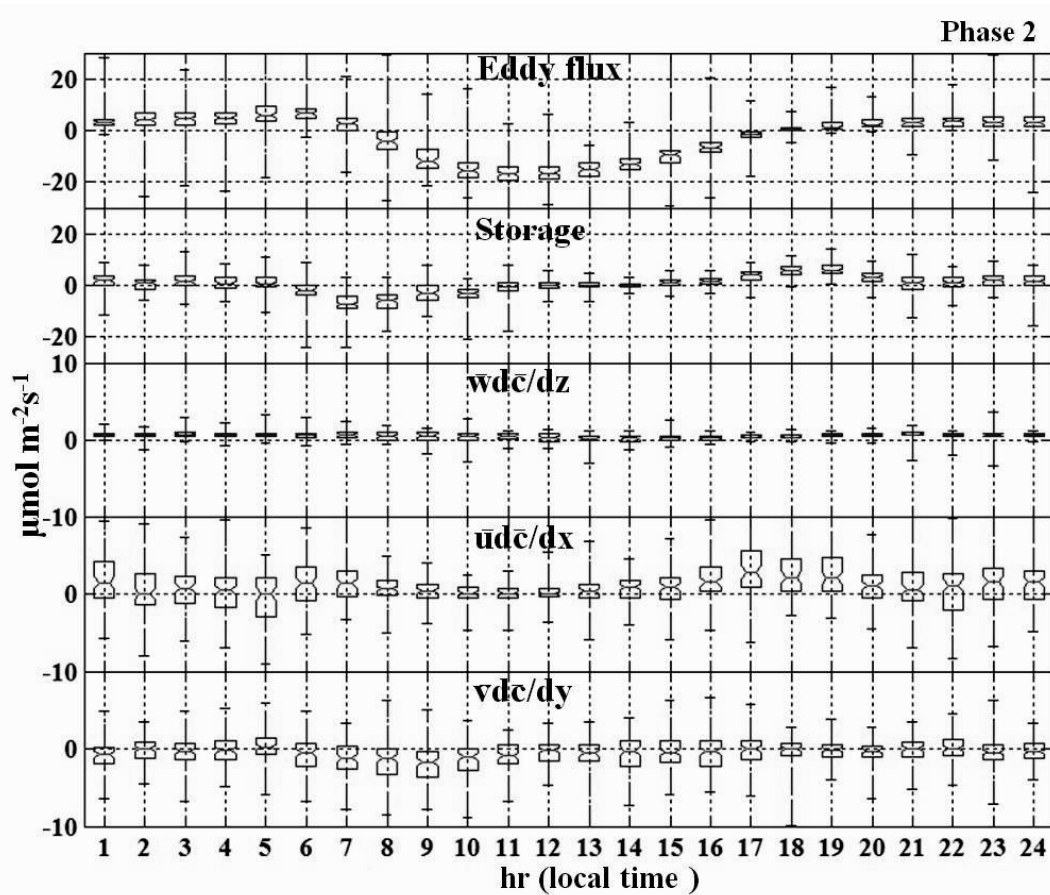


**Figure 11b.** Top panel: Hourly-averaged vertical eddy flux at 57.8 m; 2<sup>nd</sup> panel: storage term; 3<sup>rd</sup> panel: vertical advection term; 4<sup>th</sup> panel: east-west advection term; and 5<sup>th</sup> panel: and south-north advection terms. Note the change in vertical scale between the phases.

### 3.5. CO<sub>2</sub> budget

To determine the relative contribution of the nocturnal advection terms to the CO<sub>2</sub> budget, we compare the mean nocturnal variation of NEE (eddy flux + storage) with and without considering the observed advection terms and ecosystem respiration during dry (Phase 1) and wet (Phase 2) periods of observation (Figure 12a and 12b).

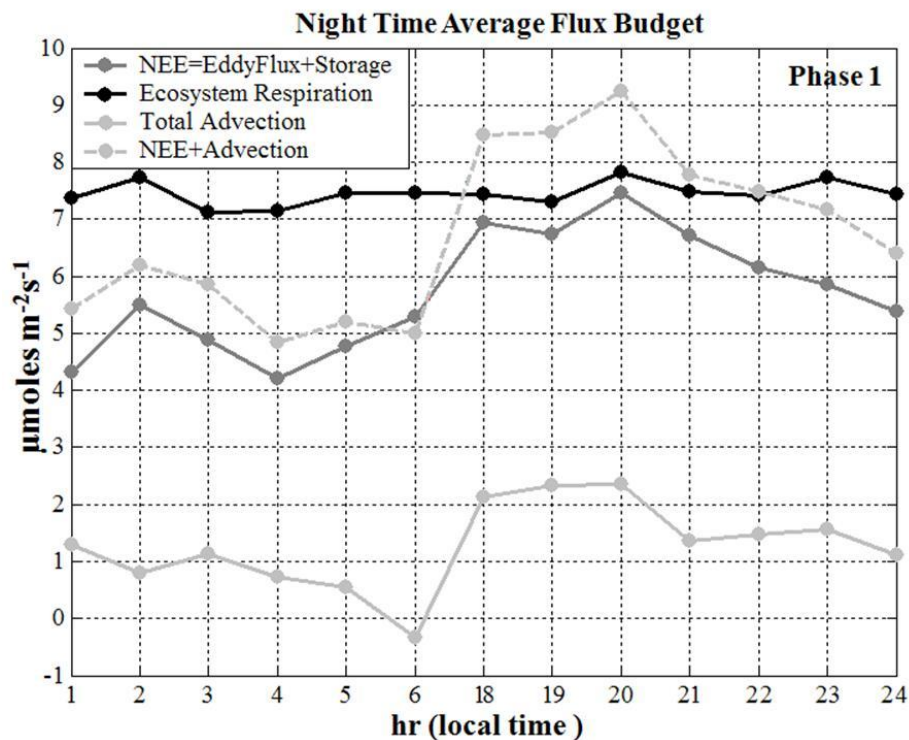


**Figure 12a.** Mean nocturnal variation of the NEE (Eddy covariance flux + storage), ecosystem respiration, horizontal advection and NEE plus advection, for Phase 1 (Dry period).

The ecosystem respiration, EC flux, and storage were measured by the CD-10 group [Saleska *et al.*, 2003; Hutryra *et al.*, 2007]. Results show that the differences between NEE and ecosystem respiration are improved when the advection term is accounted for (Table 2 and Figure 12a and 12b). The advection term accounts for  $1.27 \mu\text{mol m}^{-2}\text{s}^{-1}$  and  $0.91 \mu\text{mol m}^{-2}\text{s}^{-1}$ , for Phase 1 and Phase 2 respectively, representing 71% and 73% of the observational ‘deficit’ between ecosystem respiration and NEE.

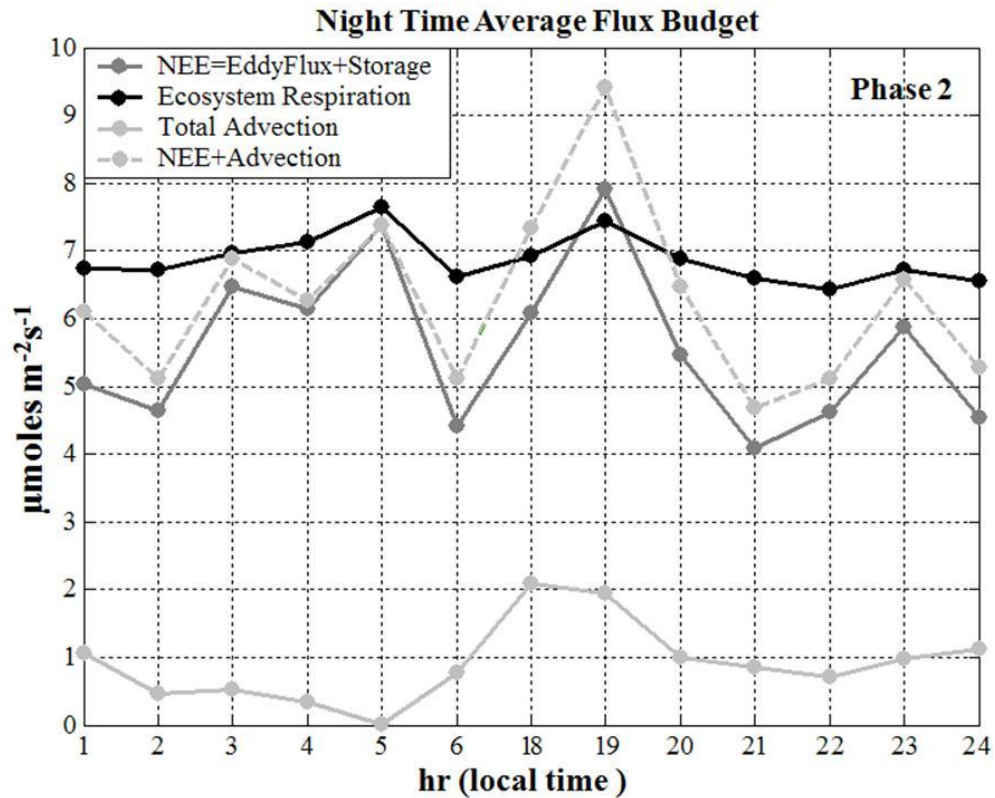


**Figure 12b.** Same Figure 12a, for Phase 2 (Wet period).

**Table 2.** Summary of mean nocturnal CO<sub>2</sub> budget for Phase 1 and Phase 2

Flux components (µmol m <sup>-2</sup> s <sup>-1</sup> )	Phase 1	Phase 2
NEE	5.71	5.58
Respiration	7.45	6.87
Deficit	1.74	1.29
Advection	1.27	0.91
NEE + Advection	6.98	6.49

### 3.6. Correlation between advection components and friction velocity

For the site studied here, the threshold value for friction velocity [e.g., *Falge et al.*, 2001; *Gu et al.*, 2005] was reported by *Saleska et al.* [2003] and *Miller et al.* [2004] to be between 0.2 and 0.3 m s<sup>-1</sup>. Is the assumption that advection is only significant below this

threshold valid? Our results show a clear dependence of the advection term on friction velocity for both observation periods (Figure 13). There is a significant positive advection contribution to the CO<sub>2</sub> budget that should be included in the NEE calculation, even when the friction velocity is higher than the threshold values commonly used. Our results in the Tapajós forest indicate that this interval lies between 0.3 and 0.6 m s<sup>-1</sup>.

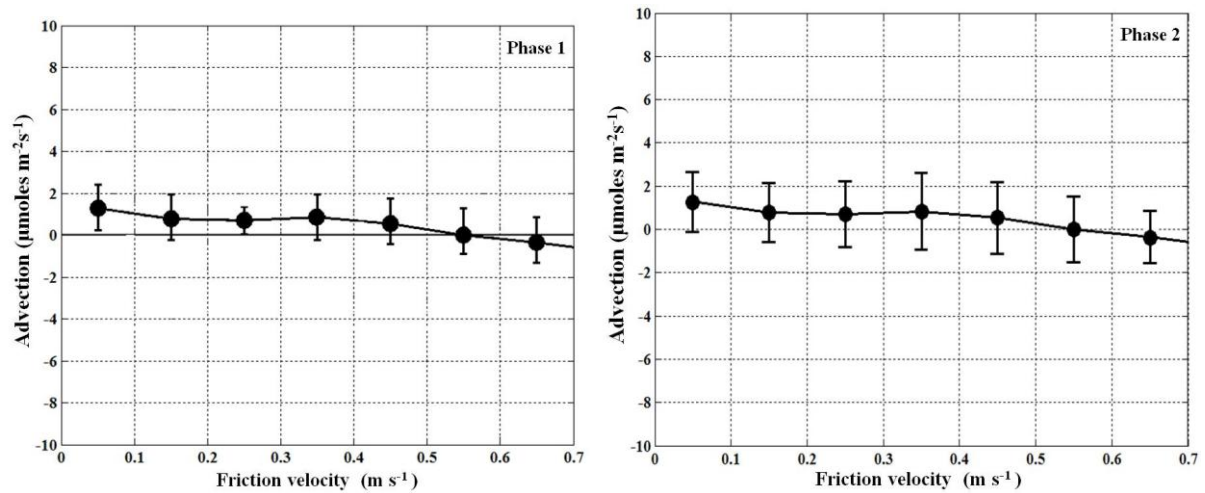


**Figure 13.** Mean nocturnal variation of the advection term as a function of the friction velocity rank, for Phase 1 (left panel) and Phase 2 (right panel) datasets. Solid line with dots indicates binned average values (0.1 intervals). Error-bar also is plot with standard deviation, respectively.

#### 4. Summary and Conclusions

We present results of the first effort to determine observationally the importance of the nocturnal advection processes on the CO<sub>2</sub> budget in the Amazon tropical rain forest. We tested the hypothesis that persistent nocturnal subcanopy horizontal advection exists and transports an important amount of CO<sub>2</sub> out of the control volume at one old-growth tropical

rain forest site. We determined the magnitude of the horizontal subcanopy gradients of CO<sub>2</sub> and of the wind field and found sufficient net horizontal advection to affect the CO<sub>2</sub> budget.

The methodology established by *Staebler and Fitzjarrald* [2004, 2005] was applied and tested to measure the subcanopy scalar gradients and wind field. These data were complemented by eddy flux and mean profile observations made at the same site on a 65-m tower (section 2). The measurements were performed in the dry season (DOY 198-238 2003 - Phase 1) and in the wet season (DOY 278-366 2004 and 1-32 2005 - Phase 2). The horizontal gradient of the CO<sub>2</sub> concentration and average wind speed, were on the order of 0.02 ppm m<sup>-1</sup> and 0.12 m s<sup>-1</sup>, respectively (section 3.1).

Prevailing subcanopy wind directions were from the southeast and were well correlated with gentle undulations of the landscape near the tower. The tropical forest subcanopy near the forest floor was stable at all times of day, but it was more pronounced during all 130 selected nights analyzed (section 3.2). That there was little coupling with the flow aloft indicates that there is potential for lateral export of subcanopy CO<sub>2</sub> even during the daytime, when this effect is often ignored. The negative buoyancy term was the principal physical mechanism responsible for generating the nocturnal subcanopy flow. During the daytime the stress divergence term was dominant, suppressing the dominance of the buoyancy effect (Section 3.3).

The results from direct measurements of the horizontal gradients of CO<sub>2</sub> and wind speed components measured in the subcanopy indicated that their magnitudes were sufficiently significant to produce a net nocturnal horizontal advection average between 0.91 and 1.27 μmol m<sup>-2</sup> s<sup>-1</sup> for dry and wet observation periods, respectively. Nocturnal horizontal advection was of the same order as the vertical EC and storage flux components. Depletion of the storage component was due in large part to net positive horizontal advection, primarily during the second part of the night (01 – 06 LT; section 3.4).

Comparison of the nocturnal deficit from ecosystem respiration and NEE measured on the eddy flux tower demonstrated the important contribution of the mean nocturnal horizontal advection on the atmospheric CO<sub>2</sub> budget. The mean nocturnal advection component represented 73% and 71% of this deficit for dry and wet periods analyzed (130 nights), respectively.

This suggests an important role of the nocturnal advection for the total CO<sub>2</sub> budget at this site. It was also verified that for nighttime intervals, with friction velocity between 0.3 and 0.6 m s<sup>-1</sup> (commonly accepted as sufficient to provide correct nighttime eddy fluxes), there was a positive net horizontal transport of CO<sub>2</sub> by the advection component. Therefore, even under considerable high turbulence levels at night, horizontal advection transport in the total CO<sub>2</sub> budget is significant.

These results confirm that few sites are flat enough that horizontal advective effects can be ignored *a priori*. In future work the validity of the CO<sub>2</sub> profile similarity hypothesis we invoked to introduce *shape factors* in (4) should be linked explicitly to the observed mean vegetation profile. Observational estimates of the effect of mean vertical velocity on scalar budgets may be the major source of uncertainty in the budget. Continuous, long-term observations with redundant instrumentation are needed to clarify this issue.



## **Capítulo II - Amazon rain forest subcanopy flow and the carbon budget: Manaus LBA Site - a complex terrain condition <sup>2</sup>**

### **Abstract**

On the moderately complex terrain covered by dense tropical Amazon rainforest (Reserva Biologica do Cuieiras – ZF2 - 02°36'17.1"S, 60°12'24.5"W) subcanopy horizontal and vertical gradients of the air temperature, CO<sub>2</sub> concentration and wind field were measured for dry and wet periods in 2006. We tested the hypothesis that horizontal drainage flow over this study area is significant and can affect the interpretation of the high carbon uptake rates reported by previous works. A similar experimental design as the one by *Tóta et al.* [2008] was used with a network of wind, air temperature and CO<sub>2</sub> sensors above and below the forest canopy. A persistent and systematic subcanopy nighttime upslope (positive buoyancy) and daytime downslope (negative buoyancy) flow pattern on a moderately inclined slope (12%) was observed. The micro-circulations observed above the canopy (38 m) over the sloping area during nighttime presents a downward motion indicating vertical convergence and correspondent horizontal divergence toward the valley area. During the daytime an inverse pattern was observed. The micro-circulations above the canopy were driven mainly by buoyancy balancing the pressure gradient forces. In the subcanopy space the micro-circulations were also driven by the same physical mechanisms but probably with the stress forcing contribution. The results also indicated that the horizontal and vertical scalar gradients (e.g., CO<sub>2</sub>) were modulated by these micro-circulations above and below canopy, then suggesting that estimates of advection using previous experimental approaches are not appropriate due to the tri-dimensional nature of the vertical and horizontal transport locally.

**Key words:** Amazon Rainforest; Advection, Drainage Flow, Eddy Covariance, Subcanopy.

---

<sup>2</sup> Tóta, J., Fitzjarrald, D.R., Parker, G., Sakai, R.K., Silva Dias, M.A.F., Manzi, A.O., 2009. Amazon rain forest subcanopy flow and the carbon budget: Manaus LBA Site - a complex terrain condition (to be submitted).

## 1. Introduction

The terrestrial biosphere is an important component of the global carbon system. The uncertainty level of its long term exchanges estimates is a challenge and has resulted in ongoing debate [*Baldocchi et al.*, 2008; *Aubinet et al.*, 2008]. For monitoring long-term net ecosystem exchange (NEE) of carbon dioxide, energy and water in terrestrial ecosystems, tower-based eddy-covariance (EC) techniques have been established worldwide [*Baldocchi et al.*, 2008].

It is now recognized that the EC technique has serious restrictions for application over complex terrain and under calm and stable nighttime conditions with low turbulence or limited turbulent mixing of air [e.g., *Goulden et al.*, 1996; *Black et al.*, 1996; *Baldocchi et al.*, 2001; *Massman and Lee*, 2002; *Loescher et al.*, 2006; *Aubinet et al.*, 2008]. To overcome this problem, the friction velocity ( $u_*$ )-filtering approach has been formalized by the FLUXNET committee for the estimation of annual carbon balances [*Baldocchi et al.*, 2001; *Gu et al.*, 2005]. This approach simply discarded calm nights flux data (often an appreciable fraction of all nights) and replaced them with ecosystem respiration rates found on windy nights [*Miller et al.*, 2004]. *Papale et al.*, [2006] pointed out that this approach itself must be applied with caution and the friction velocity ( $u_*$ ) corrections threshold is subject to considerable concerns and is very site specific. *Miller et al.*, [2004] reported that depending of the  $u_*$  threshold value used to correct the flux tower data at Santarem LBA site the area can change from carbon sink to neutral or carbon source to the atmosphere.

The transport of CO<sub>2</sub> by advection process has been suggested by several studies as the principle reason for the “missing” CO<sub>2</sub> at night [*Lee*, 1998; *Finnigan*, 1999; *Paw U et al.*, 2000; *Aubinet et al.*, 2003; *Feigenwinter et al.*, 2004; *Staebler and Fitzjarrald*, 2004]. The search for this missing CO<sub>2</sub> has spurred a great deal of research with the goal of explicitly estimating advective fluxes in field experiments during the last decade, in order to correct the NEE bias over single tower eddy covariance measurements (*Aubinet et al.*, 2003, 2005;

*Staebler and Fitzjarrald*, 2004, 2005; *Feigenwinter et al.*, 2004; *Marcolla et al.*, 2005; *Wang et al.*, 2005; *Sun et al.*, 2007; *Heinesch et al.*, 2008; *Leuning et al.*, 2008; *Tóta et al.*, 2008; *Yi et al.*, 2008; *Feigenwinter et al.*, 2009a, b).

The complexity of topography and the presence of the valley close to the eddy flux tower have increased the importance to investigating if subcanopy drainage flow account for the underestimation of CO<sub>2</sub> as past studies have asserted [*Froelich and Schmid*, 2006]. The Manaus LBA site is an example of moderately complex terrain covered by dense tropical forest. The NEE bias is reported by previous works [*Kruijt et al.*, 2004; *de Araújo et al.*, 2008; *de Araújo*, 2009; and references there in], and a possible explanation for this is that advection process is happening in that site. This work examines subcanopy flow dynamics and local micro-circulations features and how they relate to CO<sub>2</sub> spatial and temporal distribution on the Manaus LBA site in contrast with previous work done during the Santarem LBA Site experiment [see, *Tóta et al.*, 2008].

## **2. Material and Methods**

### **2.1. Site description**

The study site (54° 58'W, 2° 51'S) is located in the Cuieiras Biological Reserve, controlled by National Institute for Amazon Research (INPA), about 100 km northeast from Manaus city. At this site, named K34, was implemented a flux tower with 65m height to monitoring long term microclimate, energy, water and carbon exchanges (*Araújo et al.*, 2002), and various studies that have been conducted in its vicinity. The measurements are part of the Large-Scale Biosphere-Atmosphere experiment in Amazonia (LBA). Figure 1 presents the study site location including the topographical patterns where the maximum elevation is 120m and the total area (upper panel) is 97.26 km<sup>2</sup>, with distribution of the 31% of plateau, 26% of slope and 43% of valley [*Rennó et al.*, 2008]. The site area is formed by a topographical feature with moderately complex terrain including a landscape with mosaics of plateau, valley and slopes, with elevation differences about 50m (Figure 1), and with distinct vegetation

cover (Figure 2). The eddy flux tower at Manaus K34 site has footprints that encompass this plateau-valley mosaic.

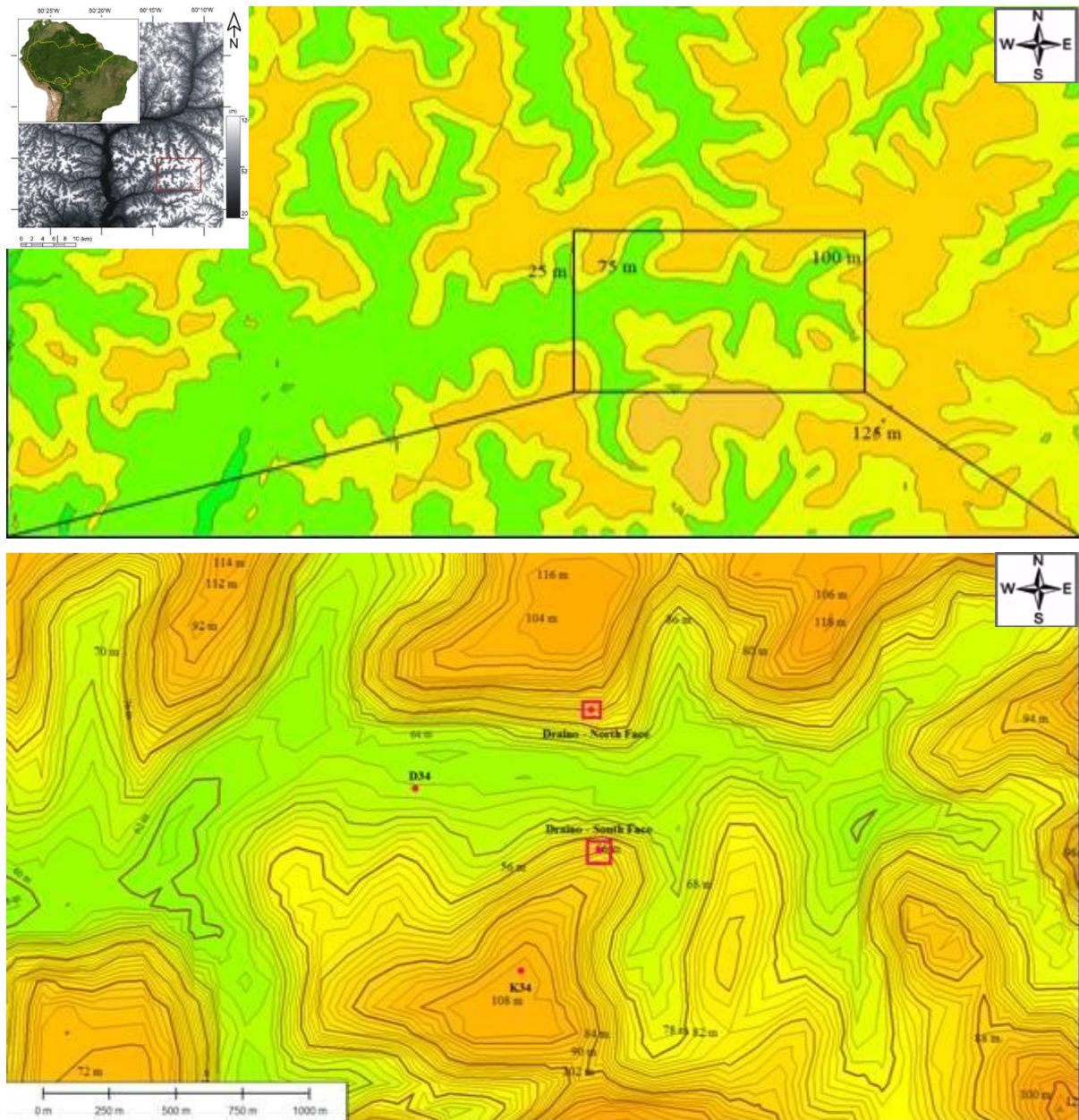


Figure 1: Detailed measurements towers's view in the ZF-2 Açu catchment (East-West valley orientation) from SRTM-DEM datasets. The large view in the above panel and below panel the points of measurements (B34 – Valley, K34 – Plateau, and subcanopy Draino system measurements over slopes in south and north faces (red square)).

The vegetation cover on the plateau and slope areas is composed by tall and dense terra firme (non-flood) tropical forest with height varying 30 to 40m, maximum surface area density of the  $0.35 \text{ m}^2\text{m}^{-3}$  (Figure 2b, see also *Parker et al.*, [2004]), and average biomass of

the 215 to 492 ton.ha<sup>-1</sup> [Laurance *et al.*, 1999; Castilho, 2004]. On the valley area the vegetation is open and smaller with heights from 15 to 25 m, but with significant surface area density more than the 0.35 m<sup>2</sup>m<sup>-3</sup> (Figure 2b). The soil type on the plateau and slopes area is mainly formed by Oxisols (USDA taxonomy) or clay-rich ferrasols ultisols (FAO soil taxonomy), while on the valley area, waterlogged podzols (FAO)/spodosols (USDA) with sand soil low drained predominates. Also, in the valley area the presence of small patchy of *Campinarana* typical open vegetation with low biomass is also common [Luizão *et al.*, 2004].

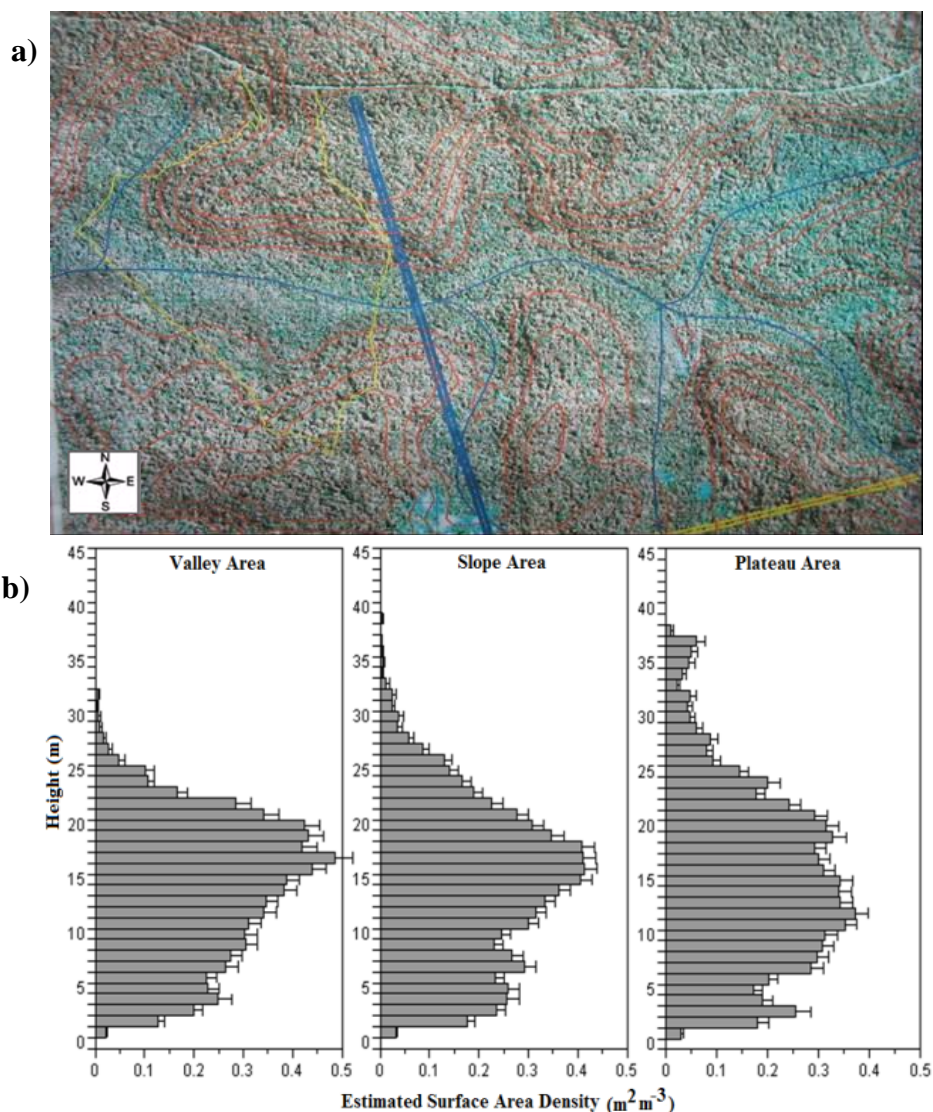


Figure 2: (a) IKONOS's image of the site at Açú Cachment with level terrain cotes and vegetation cover and (b) vegetation structure measured from LIDAR sensor over yellow transect in (a). From (a) the valley vegetation (blue color) and vegetation transition to plateau areas (red colors).



The precipitation regime on the site show wet (December to April) and dry (June to September – less than 100 mm.month<sup>-1</sup>) periods. The total annual rainfall is about 2400 mm and the average daily temperature is from 26 (April) to 28°C (September). For more detailed information about the meteorology and hydrology of this site see *Waterloo et al.* [2006], *Cuartas et al.* [2007], *Hodnett et al.* [2008], *Tomasella et al.* [2008], *Malhi et al.* [2008] and *de Araújo* [2009].

## 2.2. Measurements and instrumentation

The datasets used in this study include a measurement system to monitor airflow above and below the forest, horizontal gradients of CO<sub>2</sub>, and the thermal structure of the air below the canopy, named “DRAINNO System” [see, *Tóta et al.*, 2008]. The data used in this study were collected during the wet season (DOY 1-151) and the dry season (DOY 152-250) of the year 2006. Complementary information was used from flux tower K34 (LBA tower) on the plateau, and sonic anemometer data collected in the valley flux tower (B34, see *de Araújo* [2009] for details).

The flux tower K34 includes turbulent EC flux and meteorological observations of the vertical profiles of the air temperature, humidity and CO<sub>2</sub>/H<sub>2</sub>O concentrations, and vertical profile of wind speed, as well as radiation measurements. The fast response eddy flux data were sampled at 10 Hz and slow response (air temperature and wind profiles) at 30 min average [see *Araújo et al.*, [2002] for details information].

- *DRAINNO measurement System – Manaus LBA ZF2 site*

The Draino measurement system used in Manaus LBA Site was similar to that developed by State University of New York, under supervision of Dr. David Fitzjarrald), and applied at Santarem LBA Site, including the same methodological procedures and sampling rates [see, *Tóta et al.*, 2008]. However, due to the terrain complexity, it was modified for Manaus forest conditions including a long distance power line and duplication of CO<sub>2</sub> observations for different slopes areas (Figure 4). The Draino measurement system used in Manaus LBA Site was mounted in an open, naturally ventilated wooden house (Figure 3).



Figure 3: Draino measurement system used in Manaus LBA (South Face, see also Figure 4).

The system and sensors were deployed (Figure 4) with measurements of air temperature and humidity (red points), CO<sub>2</sub> concentration (green points), and wind speed and direction (blue points), for both south and north faces. The observations of the 3-D sonic anemometer were sampled at 10 Hz and all the other parameters (T, RH, and CO<sub>2</sub>) were sampled at 1 Hz (Figure 4).

The acquisition system developed at ASRC was employed (Staebler and Fitzjarrald, 2005). It consists of a PC operating with Linux, an outboard Cyclades multiple serial port (CYCLOM-16YeP/DB25) collecting and merging serial data streams from all instruments in real time, the data being archived into 12-hour ASCII files. At Manaus LBA Site two systems in the both south and north valley slope faces were mounted (Figure 3 and 4).

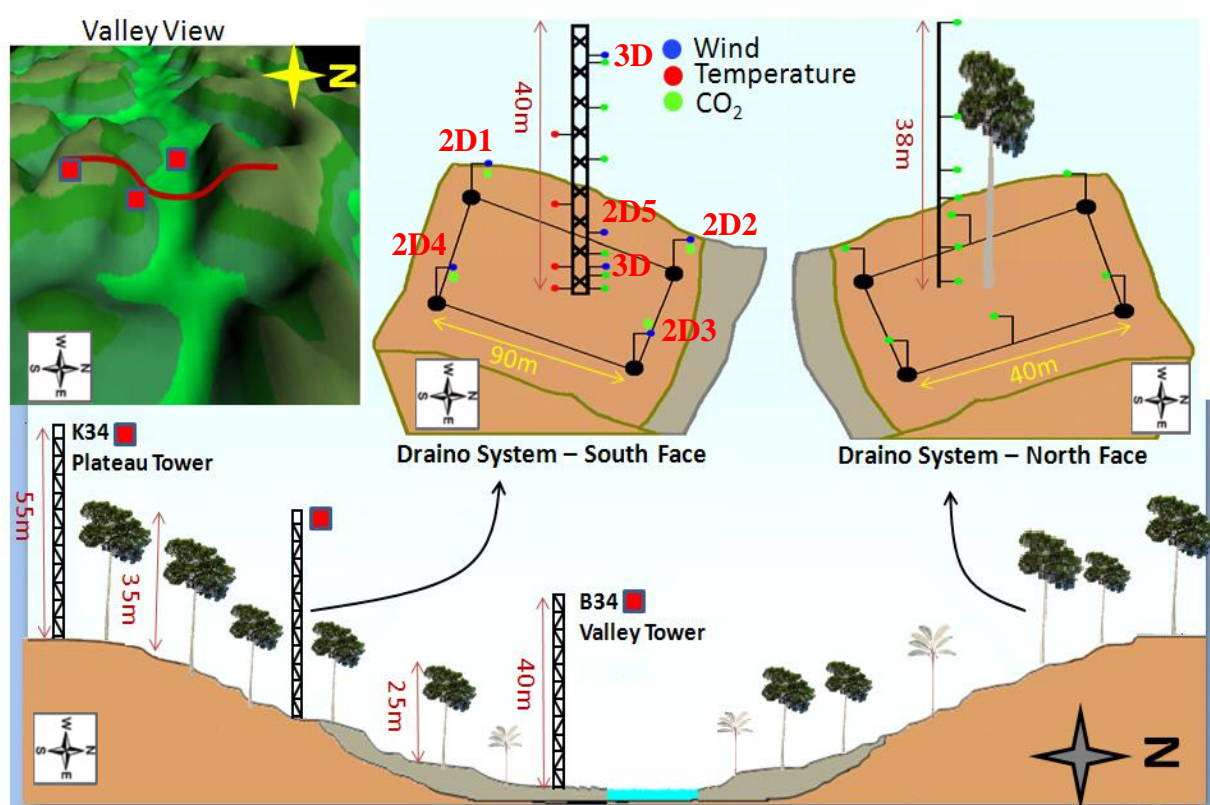


Figure 4: Draino measurement system (South and North Slope face) implemented at Manaus LBA Site, including topographic view and instrumentation deployed.

For each slope face, a single LI-7000 Infrared Gas Analyzer (LI-COR inc., Lincoln, Nebraska, USA) was used. A multi-position valve (Vici Valco Instrument Co., Inc.) controlled by a CR23x Micrologger (Campbell Scientific, Inc., Logan, Utah, USA), which also monitored flow rates was also used. This procedure minimizes the potential for systematic concentration errors to obtain the horizontal and vertical profiles. Following *Staebler and Fitzjarrald* [2004] and *Tóta et al.* [2008] a similar field calibration was



performed during the observations at Manaus LBA Site, including initial instrument intercomparison. The result was similar that obtained by *Tóta et al.* [2008], with CO<sub>2</sub> mean standard error was < 0.05 ppm and mean standard error of about 0.005 ms<sup>-1</sup> for wind speed measurements. After intercomparison, the sonic anemometers and the CO<sub>2</sub> inlet tubes were deployed as shown in Figure 4.

On the south face, the instrument network array (Figure 4 and Table 1) consisted of 6 subcanopy sonic anemometers, one 3-D ATI (Applied Technologies Inc., CO, USA) at 2m elevation in the center of the grid (named 3-D ATI), and 5 SPAS/2Y (Applied Technologies Inc., CO, USA), 2-component anemometers (1 sonic at 6m in the grid center and 4 sonic along the periphery at 2m, see Figure 4), with a resolution of 0.01 m s<sup>-1</sup>. Also, a Gill HS (Gill Instruments Ltd., Lymington, UK) 3-component sonic anemometer was installed above the canopy (38 m). The horizontal gradients of CO<sub>2</sub>/H<sub>2</sub>O were measured in the array at 2 m above ground, by sampling sequentially from 4 horizontal points surrounding the main tower location at distances of 70-90m, and from points at 6 levels on the main Draino south face tower, performing a 3 minute cycle. On the north face, similar CO<sub>2</sub> measurements were mounted including a 6 level vertical profile and 6 points in the array at 2 m above ground, performing a 3 minute cycle.

On both slope faces the air was pumped continuously through 0.9 mm Dekoron tube (Synflex 1300, Saint-Gobain Performance Plastics, Wayne, NJ, USA) tubes from meshed inlets to a manifold in a centralized box. A baseline air flow of 4 LPM from the inlets to a central manifold was maintained in all lines at all times to ensure relatively “fresh” air was being sampled. The air was pumped for 20 seconds from each inlet, across filters to limit moisture effects. The delay time for sampling was five seconds and the first ten seconds of data were discarded. At the manifold, one line at a time was then sampled using an infrared gas analyzer (LI-7000, Licor, Inc.). To minimize instrument problems, only one LI-7000 gas analyzer sensor, for each slope face, was used to perform vertical and horizontal gradients of the CO<sub>2</sub>.

**Table 1. DRAINNO system Sensors at ZF2 LBA Manaus Site**

Level (m)	Parameter	Instrument
38	$u' v' w' T'$	Gill 3D sonic anemometers
2	$u' v' w' T'$	ATI 3D sonic anemometer
6,2	$u' v' w' T'$	CATI/2 2D sonic anemometers
2	CO <sub>2</sub> Concentration (horizontal array)	LI-7000 CO <sub>2</sub> /H <sub>2</sub> O analyzer
38,26,15,3,2,1	CO <sub>2</sub> , H <sub>2</sub> O Profile (South face)	LI-7000 CO <sub>2</sub> /H <sub>2</sub> O analyzer
35,20,15,11,6,1	CO <sub>2</sub> , H <sub>2</sub> O Profile (North face)	LI-7000 CO <sub>2</sub> /H <sub>2</sub> O analyzer
18,10,2,1	Air Temperature and Humidity	Aspirated thermocouples

### 3 – Results and Discussion

The datasets analyzed in this study were obtained during the periods defined by dry (DOY 1-150 January to June) and wet (DOY 152-250 July to October) of the 2006. Figure 5 presents an example of the datasets cover, with 10 days composite statistic, for CO<sub>2</sub> concentration and air temperature at south face area of the DRAINNO system and the total precipitation on the plateau K34 tower measurements.

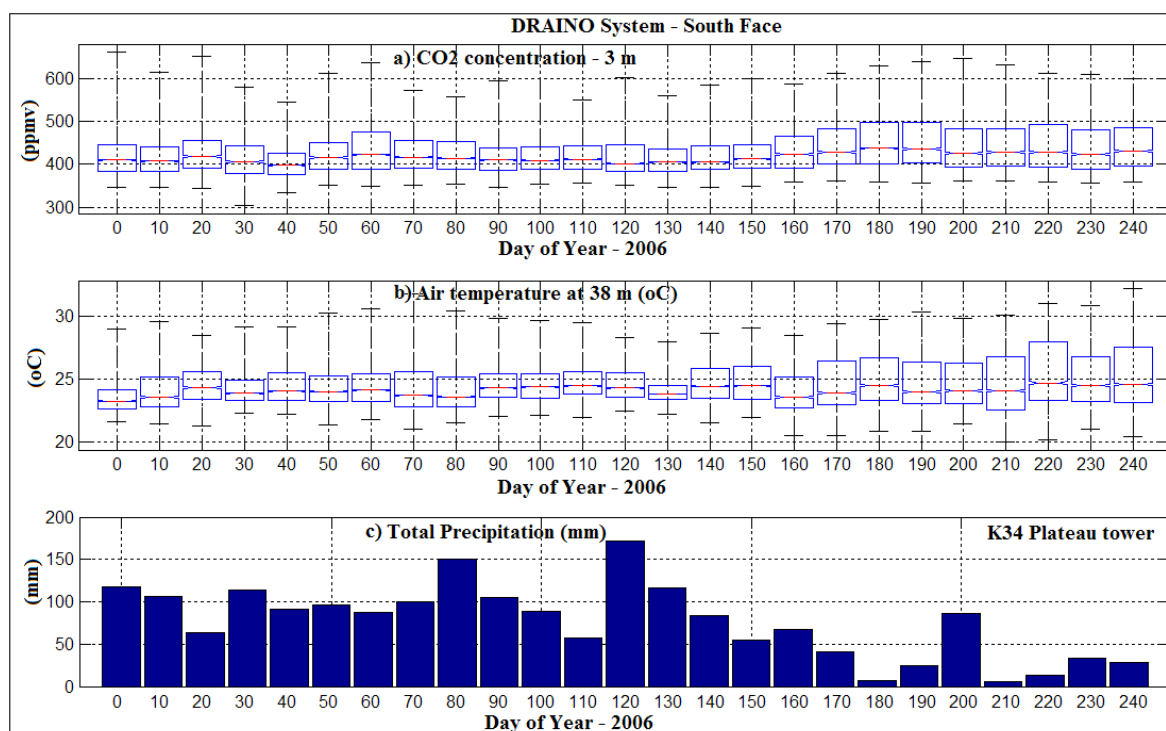


Figure 5: 10 days time series of the CO<sub>2</sub> concentration (a), air temperature (b) (DRAINNO System) and total precipitation (c) (plateau tower).

The measurements covered almost the entire year of 2006, including dry, wet and the transition from wet to dry season. The air temperature amplitude above canopy on the slope area of the DRAINO System was higher, as expected, in the dry season. A good relationship is observed between CO<sub>2</sub> concentration and air temperature with much large amplitudes in the dry season than in the wet season. It is probably associated with less vertical mixing during dry than wet season producing much higher subcanopy CO<sub>2</sub> concentration and vertical gradient along the forest.

### ***3.1. Air Temperature field***

#### *3.1.1 - Plateau K34 tower*

The vertical profiles of air temperature from plateau K34 tower show a very different pattern from that on the slope area, probably due to canopy structure differences (Figure 2b, *Parker et al.*, [2004]). The canopy structure is important for characterizing its thermal regime as it can be seen in Figure 6. The mean canopy layer stores large quantity of heat during the daytime and distributes it downward and upward throughout the nighttime (Figure 6, 7).

Above canopy layer, over plateau area, the neutral or unstable conditions were predominant during the daytime for both seasons (Figure 6a, c). While during the nighttime stable conditions are present for the dry period (Figure 6b) and neutral to stable conditions for the wet period (Figure 6d). Similar pattern has been reported elsewhere for plateau forests in the Amazonia (*Fitzjarrald et al.*, [1990]; *Fitzjarrald and Moore*, [1990]; *Kruijt et al.*, [2000]; *Goulden et al.*, [2006]).

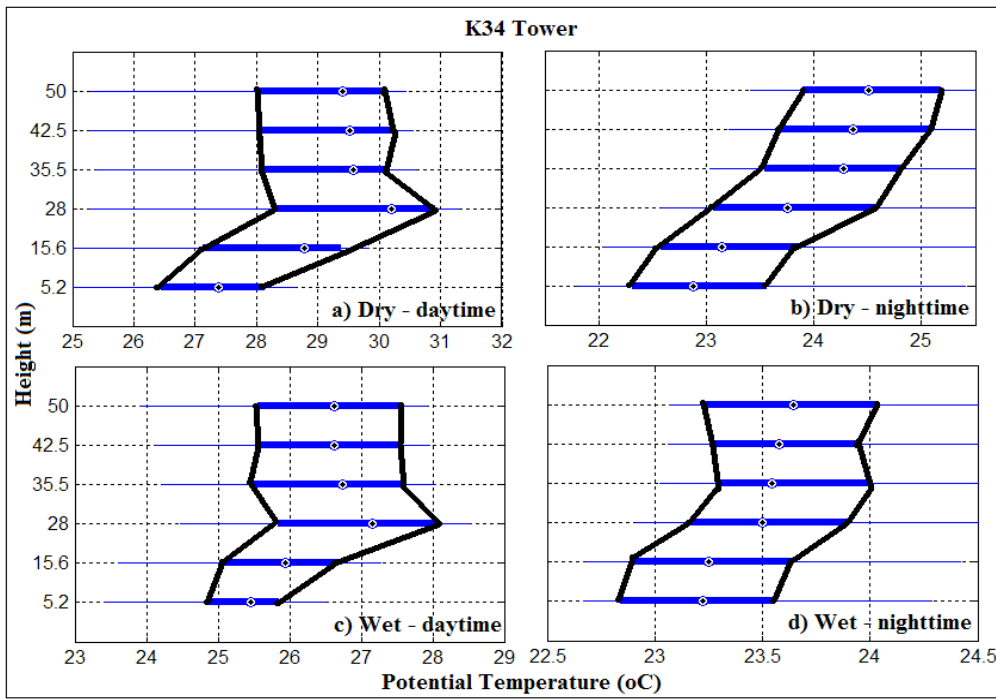


Figure 6: Boxplot of the virtual potential temperature vertical profile for dry (a, b) and wet periods (c, d) of the 2006 during night (b, d) and daytime (a, c), on the plateau K34 tower.

The below-canopy layer ambient air on the plateau area was stable at all times (Figure 6a, b, c, d), indicating that this layer is stable where the cold air concentrated in the lower part of the canopy air space as shown in Figure 7.

Figure 7 presents daily course of the vertical deviation of the virtual potential temperature, e.g.,  $([\theta'_v = \theta_v(z) - \overline{\theta_v(z)}_{5.2}^{55}])$ , the temperature differences from each level in relation to the vertical average profile. The subcanopy air space was relatively colder during both dry and wet season, showing a similar feature of strong inversion. The same pattern was reported by *Kruijt et al.* [2000] measured over a tower located 11 km northeast of our site with a similar forest composition.

Note that a very interesting length scale can be extracted from the observation when the deviation is about zero. That vertical length scale has mean value of about 30 m during nighttime and 20 m during daytime (yellow color in the Figure 7a, b). Those values are comparable with above canopy hydrodynamic instability length scale used in most averaged

wind profile models [Raupach *et al.*, [1996]; Pachêco, [2001]; Sá e Pachêco, [2006]; Harman and Finnigan, [2007]].

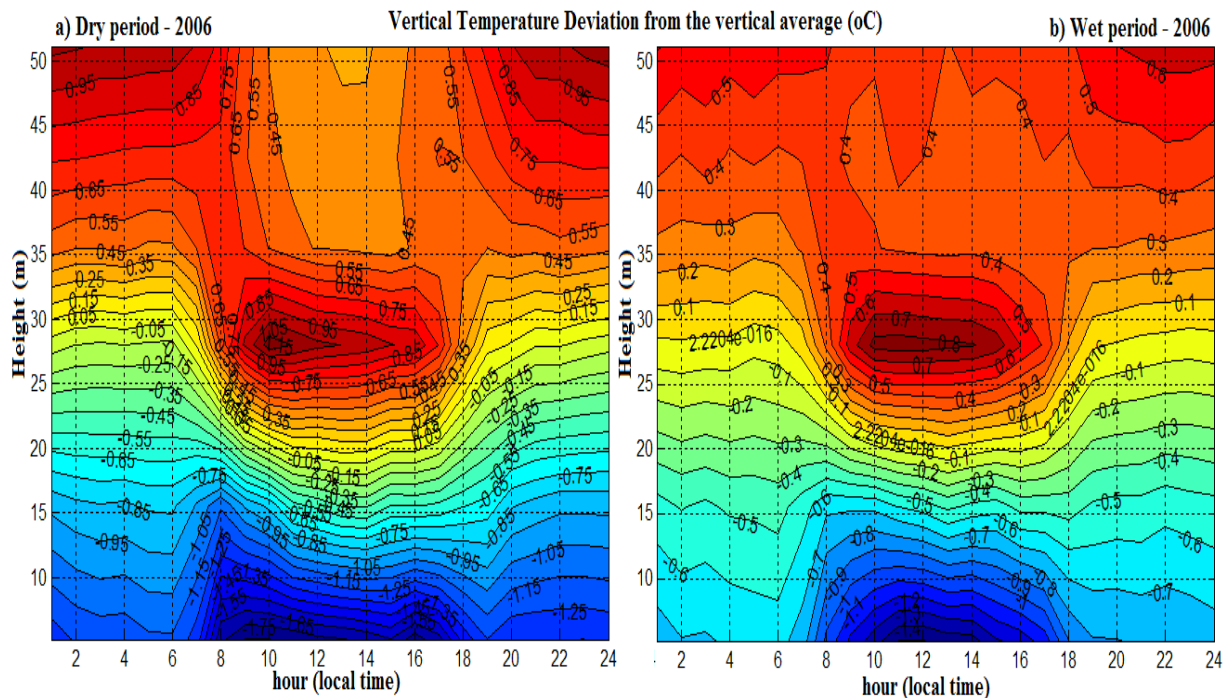


Figure 7: Daily course of the vertical deviation of the virtual potential temperature ( $[\theta'_v = \theta_v(\mathbf{z}) - \overline{\theta_v(\mathbf{z})}]$ ), during dry (a) and wet (b) periods of the 2006, over plateau K34 tower.

### 3.1.2 – DRAINOS System Slope tower

On the slope area south face (see Figure 2) air temperature at 5 levels underneath the canopy (heights 17, 10, 3, 2, and 1 m) was measured. The observations of the air temperature profile inside canopy are used to monitor the possible cold or warm air layer that generates drainage flow on the slope area. Figure 8 presents observations of the virtual potential temperature vertical profile for both dry and wet periods, during both day and nighttime. The pattern on the slope area is clearly very different when compared with that on the plateau K34 area (Figure 6), except in dry period during daytime when the air was stable inside the canopy.

During nighttime (wet and dry periods) a very stable layer predominates with inversion at about 9 m. These can likely be interpreted as a stable layer between two convective layers is associated with cold air (Figure 8). Yi [2008] hypothesized about a similar “*super stable layer*” developing during the night in sloping terrain at the Niwot Ridge AmeriFlux site. This hypothesis suggests that above this layer, vertical exchange is most important (vertical exchange zone) and below it horizontal air flow predominates (longitudinal exchange zone). The relationship between subcanopy thermal structure and the dynamic of the airflow on the slope area will be discussed in next section.

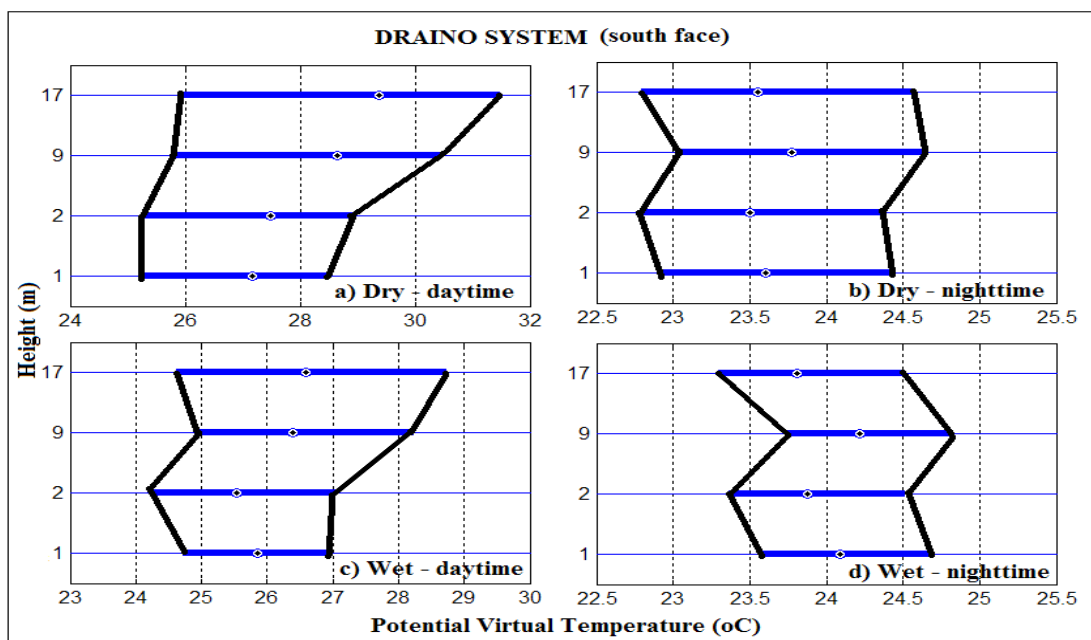


Figure 8: Boxplot of the virtual potential temperature vertical profile for dry (a, b) and wet periods (c, d) of the 2006 during night (b, d) and daytime (a, c), on the slope area DRAINNO System tower (south face, see Figure 2).

Figure 9 presents a daily cycle composite of the virtual potential temperature deviation from the vertical average ( $[\theta_v(z) - \overline{\theta}_v(z)]_1^{18}$ ). There is persistent cold air entering during nighttime for both dry and wet periods, a characteristic pattern observed on the slope area. It is a very different vertical thermal structure from that of the plateau area. The cold air in the subcanopy upper layer is probably associated with top canopy radiative cooling, while the

cold air just above floor layer is associated with upslope wind from the valley area (as discussed later in the next section).

The average of the vertical gradient virtual potential temperature was negative during nighttime and positive during daytime for both periods dry and wet (Figure 9). This observation shows that during the daytime a relative cooler subcanopy air layer predominates creating a inversion conditions. In contrast, a relative hotter subcanopy air layer generates a lapse conditions during nighttime. In general that is not a classical thermal condition find on the sloping open areas without dense vegetation. A similar pattern was reported by *Froelich and Schmid* [2006] during “leaf on” season.

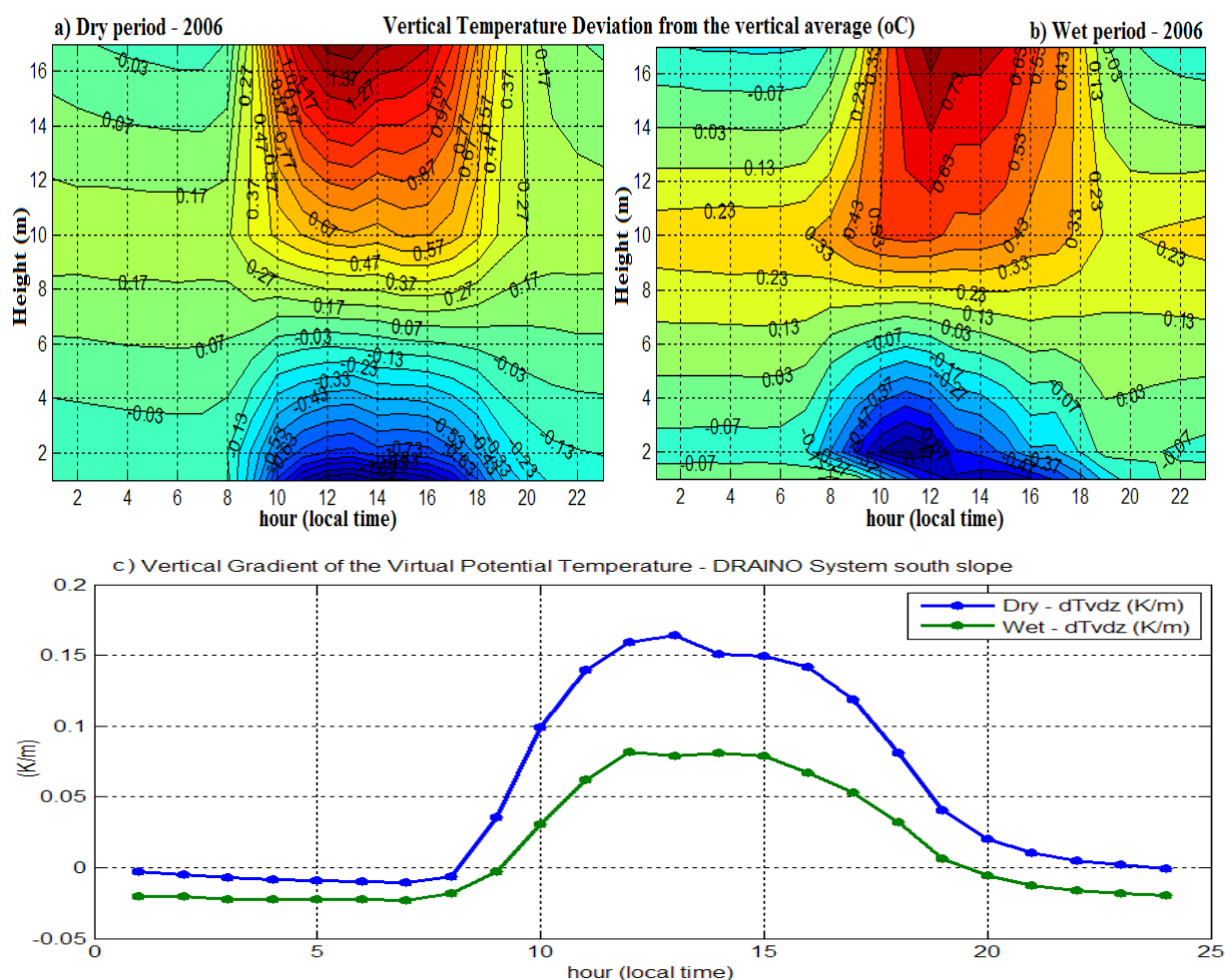


Figure 9: Daily course of the vertical deviation of the virtual potential temperature for dry (a) and wet (b) periods of the 2006, and the virtual potential temperature vertical gradient (c), over slope area DRAINNO System tower.

### 3.2. Wind field

The LBA Manaus Site has moderately complex terrain when compared with the Santarem LBA Site (Figure 1, 2). This complexity generates a wind airflow regime much complex to be captured by standard measurement system like a single tower. At the Manaus LBA site, we implemented a complementary measurement system on the slope area to support the plateau K34 tower and better understand how the airflow above and below the canopy interact and also to describe how the valley flow influences the slope airflow regimes. Note that the valley in the microbasin is oriented from East to West (Figure 2, 4).

#### 3.2.1 – Horizontal wind regime - *above canopy*

##### 3.2.1.1 - Plateau K34 tower

Above the canopy (55m above ground level – a.g.l.) on the plateau area K34 tower, the wind regime was strongest (most above 2 m.s<sup>-1</sup>) during daytime for both dry and wet periods of 2006, with direction varying mostly from southeast and northeast for dry and wet period, respectively (Figure 10).

During nighttime, the wind regime was slower (most below 3 m.s<sup>-1</sup>) and with same direction variation from northeast to southeast (Figure 10). As reported by *de Araújo* [2009], the above canopy valley area wind speed and direction was different from that of the plateau area, suggesting a decoupling mainly during nighttime. A clear channeling effect on the valley wind regime was observed; which was oriented by microbasin topography during both day and nighttime, with direction of the flow in the valley area determined by the valley orientation [as also reported by *de Araújo*, 2009].



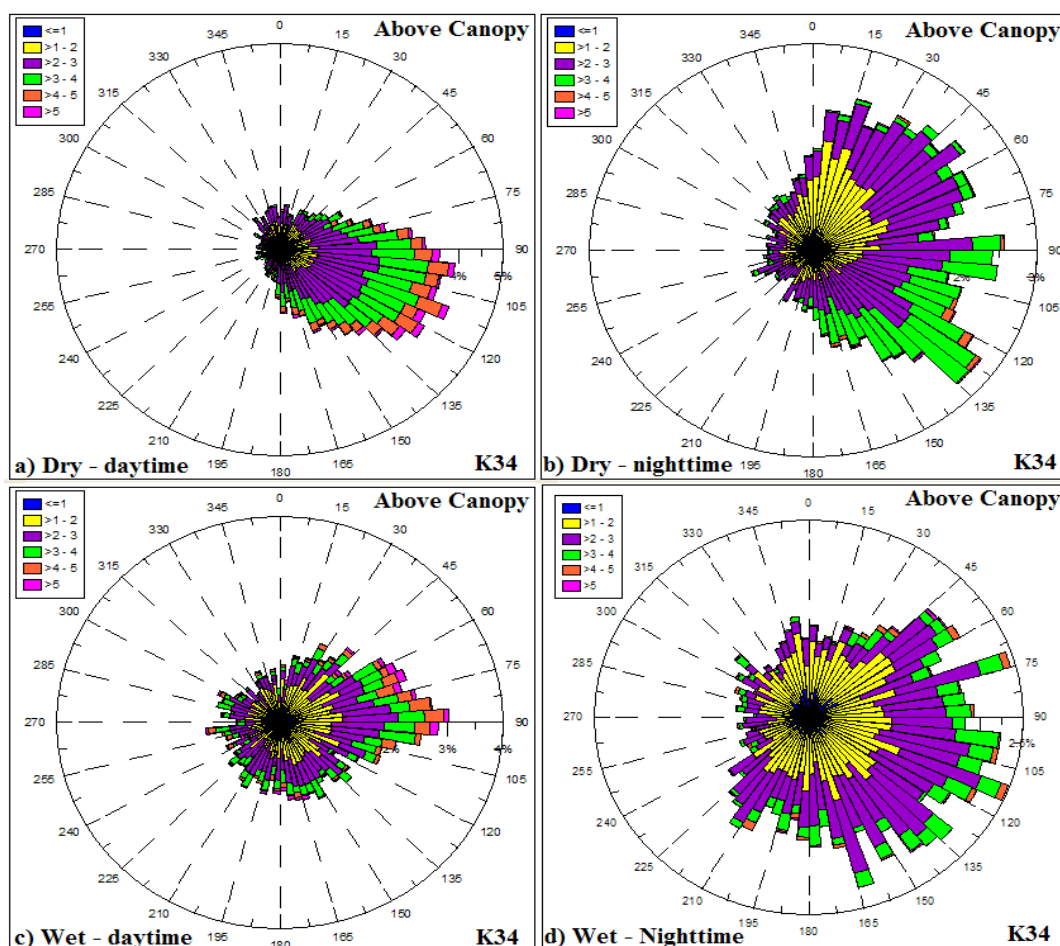


Figure 10: Frequency distribution of the wind speed and direction. For dry (a, b) and wet (c, d) periods from 2006 during day (a, c) and nighttime (b, d), on the plateau K34 tower.

### 3.2.1.2 -DRAIN0 System slope tower

The above canopy (38 m above ground level – a.g.l.) on the slope area DRAIN0 system south face (see Figure 4, 3D sonic), the wind regime was very persistent from East quadrant direction during day and nighttime in both dry and wet periods of the 2006 (Figure 11). The daytime wind speed during the dry season was between 1 to 3 m s<sup>-1</sup> and much stronger during the wet period with values up to 4 m s<sup>-1</sup>. During the nighttime the wind speed was slower than 2 m s<sup>-1</sup>, except from northeast during the wet period. The wind direction pattern was similar to that on the plateau K34 tower (Figure 10) prevailing from northeast to

southeast. This observation indicates that the airflow above the canopy on the slope area is related to how the synoptic flow enters in the eastern part of the microbasin (see Figure 2, 4).

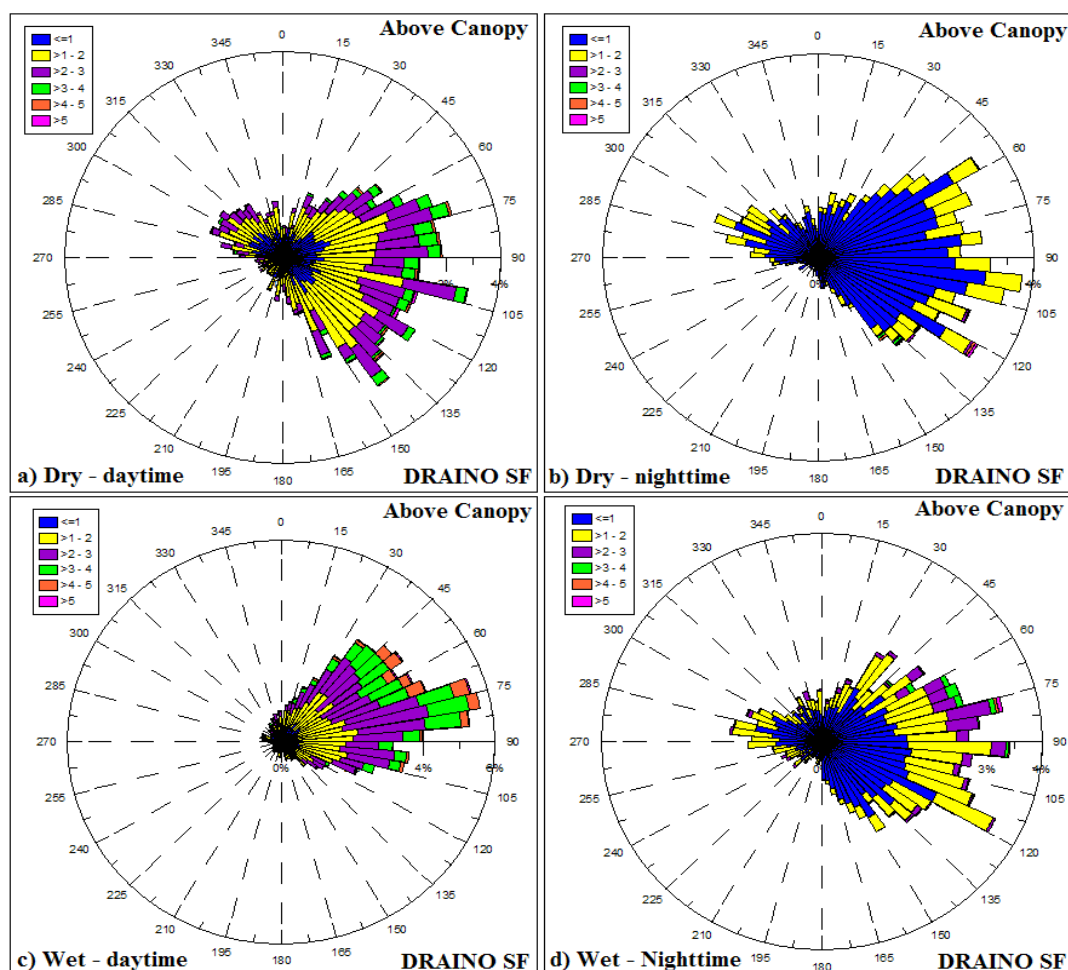


Figure 11: Frequency distribution of the wind speed and direction above canopy (38 m above ground level – a.g.l). For dry (a, b) and wet (c, d) periods from 2006 during day (a, c) and nighttime (b, d), on the slope area at DRAIN0 system tower.

### 3.2.2 – Horizontal wind regime – Subcanopy array measurements (2 m a.g.l)

In Figure 12 the subcanopy array frequency distribution of the wind speed and directions is shown for both dry and wet periods of the 2006, during both day and nighttime. The observations show that the airflow in the subcanopy is very persistent and with similar pattern during both dry and wet periods of 2006. Note that the south slope area in the DRAIN0 System (see Figure 4) is *downslope* from **south** and *upslope* from **north** quadrants.

### *Subcanopy daytime wind regime*

During daytime, in both dry (Figure 12a-c) and wet periods (Figure 12g-i), the wind direction prevailed from south-southeast (190-150 degrees) on the three southern slope regions [Figure 12, Top (a, d, g, j), Middle (b, e, h, k) and Low slope part (c, f, i, l)]. The airflow in the subcanopy was decoupled from the wind regime above the canopy (Figure 11) most of the time.

The wind direction in the subcanopy airflow was dominated by a daytime downslope regime during the majority of the period of study, suggesting a systematic daytime katabatic wind pattern. The wind speed in the subcanopy during the daytime was mostly from 0.1 to 0.4 m/s, and strongest at middle slope region (Figure 12b, e, h, k) about 0.3 to 0.5 m/s or above. A similar daytime katabatic wind regime was reported by *Froelich and Schmid* [2006] during “leaf on” season in Morgan-Monroe State Forest (MMSF), Indiana USA.

The daytime downslope wind was also supported by the subcanopy thermal structure (Figure 9), where the air was cooling along the day by inversion of the virtual potential temperature profile with a positive vertical gradient (Figure 9c). This results shows that subcanopy flows in a sloping dense tropical rainforest are opposite to the classical diurnal patterns of slope flows studied elsewhere in the literature [e.g.; *Manins and Sawford*, 1979; *Sturman* (1987); *Amanatidis et al.*, 1992; *Papadopoulos and Helmis*, 1999; *Kossmann and Fiedler*, 2000]. It is important to note that few studies have been done in forested terrain and it is unclear why similar reversed diurnal patterns have not been observed in studies at other forested sites [*Aubinet et al.*, 2003; *Staebler and Fitzjarrald*, 2004; *Yi et al.*, 2005], except by a single point subcanopy measurement observed by *Froelich and Schmid* [2006].

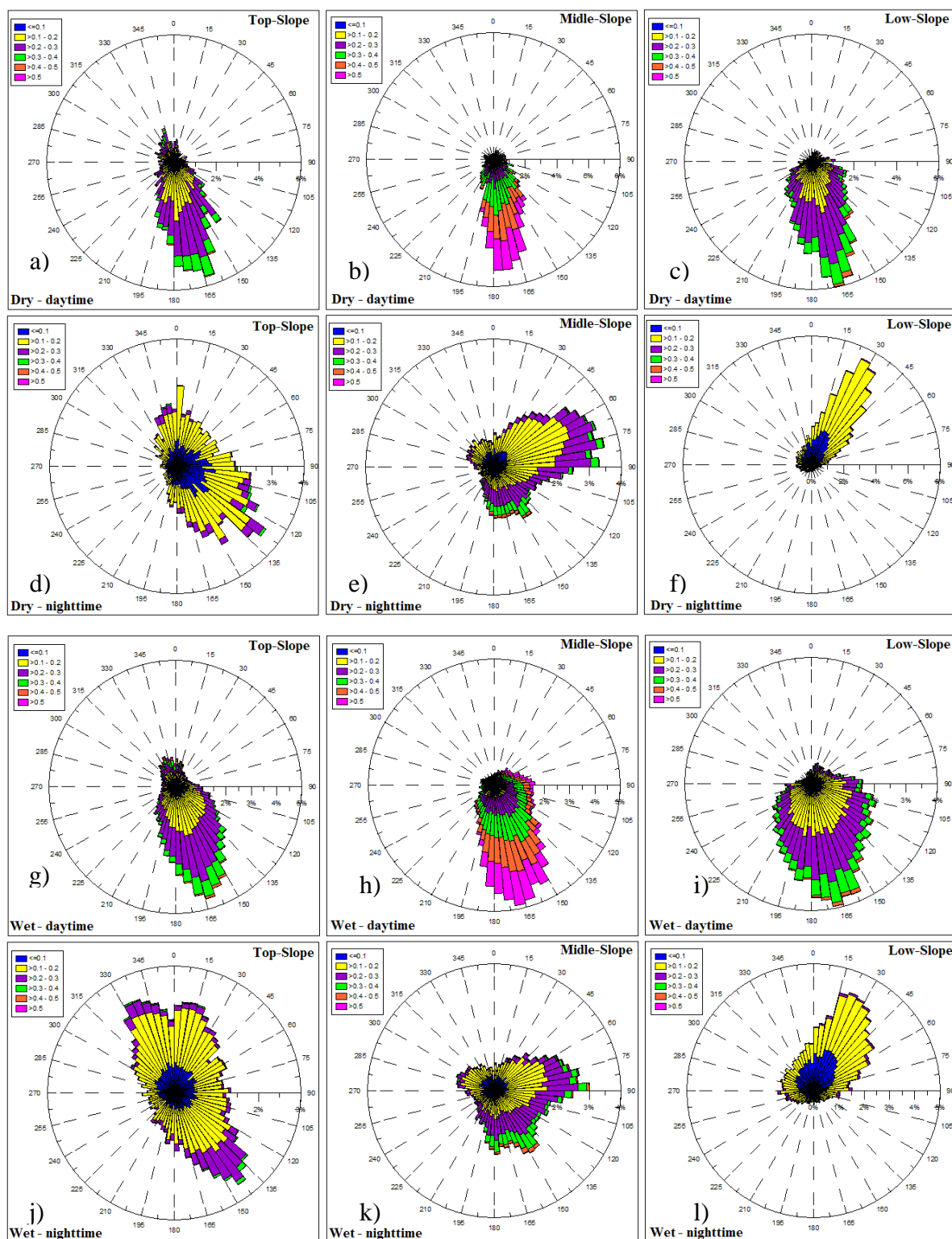


Figure 12: Frequency distribution of the wind speed and direction in the subcanopy array (2 m above ground level – a.g.l) on the microbasin south face slope area at DRAINO horizontal array system (see Figure 4). For dry (a-f) and wet (g-l) periods from 2006, during day (a, b, c, g, h, i) and nighttime (d, e, f, j, k, l).

### *Subcanopy nighttime wind regime*

The nighttime subcanopy wind regime on the slope area (see the terrain on Figure 4) was very complex and differentiates from that one above the canopy vegetation.

It was observed that, on the up-slope part, the nighttime airflow was southeast downsloping direction ( $130^{\circ}$ - $170^{\circ}$ ) and northeast-northwest ( $45^{\circ}$ - $340^{\circ}$ ) uphill direction (Figure 12d, j). In the middle-part of slope area, the wind moved uphill (from northeast;  $30^{\circ}$ - $90^{\circ}$ ) and also downsloping wind direction from southeast (Figure 12e, k), and with lightly higher wind speed. And finally, on the lower-part of the slope area (Figure 12f, l) the wind direction prevailed from the northeast ( $10^{\circ}$ - $70^{\circ}$ ), indicating upsloping pattern (anabatic).

Is interesting to note that, on the up-slope area, the wind direction regime (northeast-northwest,  $45^{\circ}$ - $340^{\circ}$ ) suggest a reversal lee side airflow (re-circulation or separation zone) probably in response to the above canopy wind (see Figure 11b, d). It is has been suggest by *Staebler* [2003] and reported by simulations using fluid dynamic models [*Katul and Finnigan*, 2003; *Poggi et al.*, 2008].

Also, the upsloping subcanopy flows pattern, on the lower-part the slope area, is supported by subcanopy relative heat air layer along the slope during the night, as observed by lapse rate condition of the virtual potential temperature negative vertical gradient (Figure 9c). This observation does not follow the classical concept of nighttime slope flow pattern. *Froelich and Schmid* [2006], has reported similar feature where they found anabatic wind regime during nighttime in their seasonal forest study area.

Figure 13 presents the frequency distribution of the subcanopy wind direction on the south face slope area at DRAINO horizontal array system during upsloping (from north quadrant) and downsloping (from south quadrant) events.

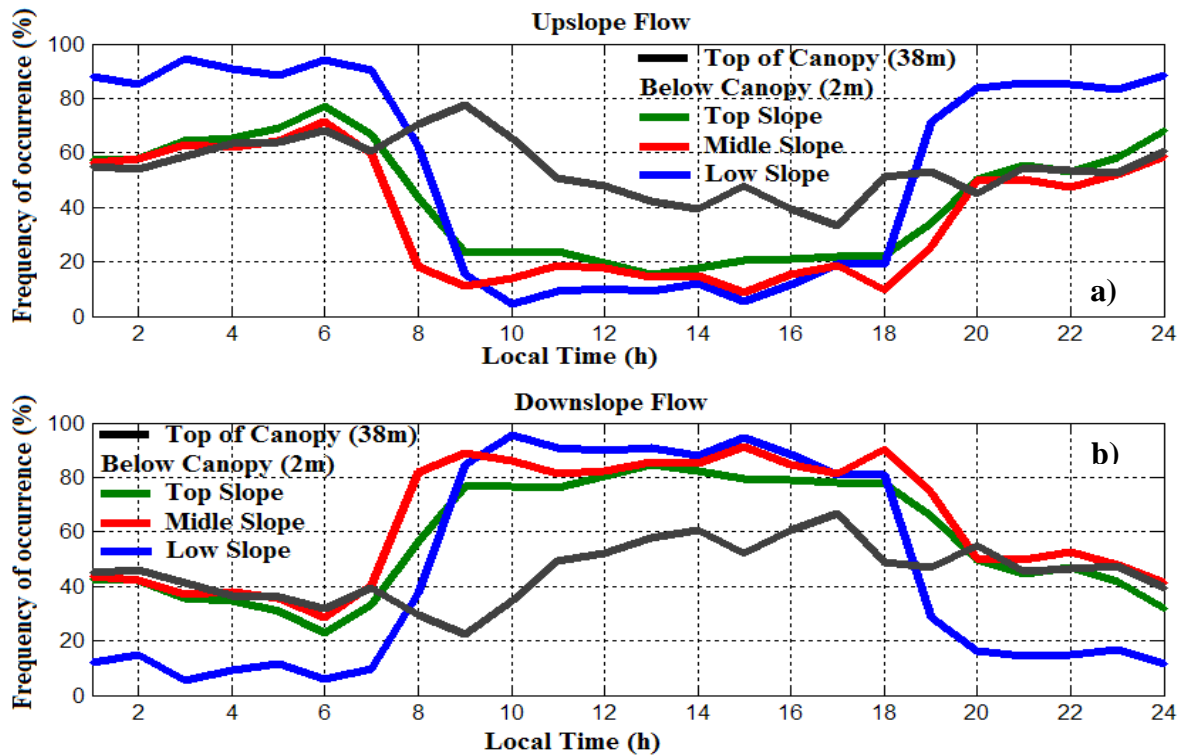


Figure 13: Frequency distribution of the subcanopy wind direction (a) **upsloping** (from north quadrant) and (b) **downsloping** (from south quadrant) on the south face slope area at DRAINNO horizontal array system (see Figure 4).

### 3.2.3 – Mean Vertical wind velocity – subcanopy and above canopy

Several correction methods have been proposed to calculate the mean vertical velocity, e.g. linear regression method [Lee, 1998], coordinate rotation [Finnigan *et al.*, 2003] and the planar fit method [Wilczak *et al.*, 2001]. We use the linear regression method by Lee [1998] to determine the “true” mean vertical velocity:  $\bar{w} = w - a(\alpha_i) - b(\alpha_i)u$ , where  $a$  and  $b$  are coefficients to be determined, for each  $\alpha_i$  ( $10^\circ$  azimuthal wind direction), by a linear regression of measured mean vertical velocity ( $w$ ) and horizontal velocity ( $u$ ) in the instrument coordinate system.

Figure 14a presents the original and the correction results by method application of the mean vertical velocity as function of wind direction. In Figure 14b, the results of the hourly mean vertical velocities for plateau K34, DRAINNO system (above and below canopy) and

valley B34 towers. As expected, low values were observed for all points of measurements, but non-zero values were also observed.

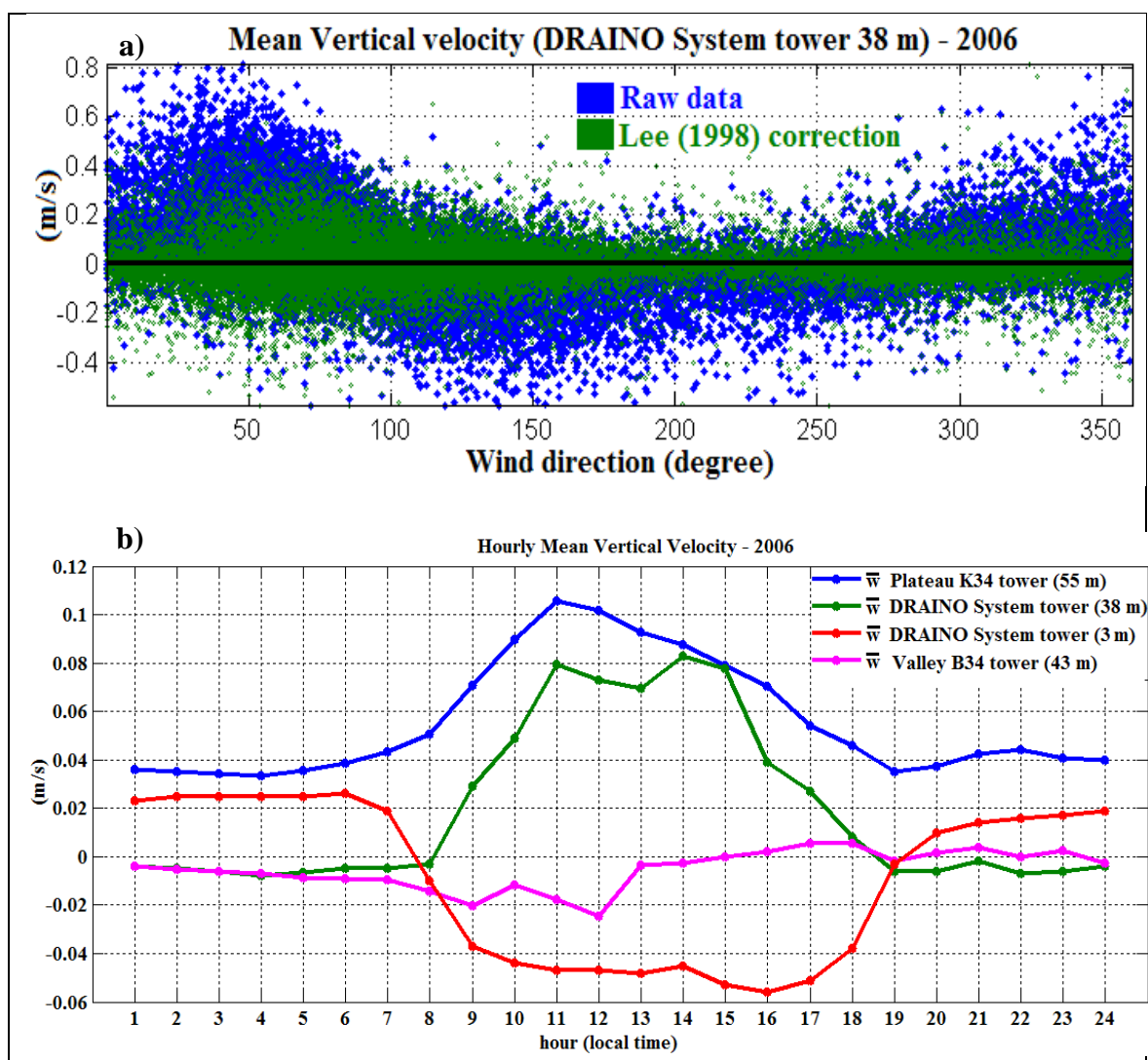


Figure 14: Mean vertical velocity raw and correct vertical velocity (a) for DRAINO system slope tower (38 m), and hourly mean vertical velocity (b) for: plateau K34 tower (55 m), DRAINO system slope tower (above canopy - 38 m and subcanopy - 3 m) and for valley B34 (43 m) towers (see Figure 4, for details).

On the plateau area, the mean vertical velocity was always positive indicating upward motion or vertical convergence at top of hill during night and daytime. In the valley area during nighttime, negative or zero values were observed, indicating a suppression of vertical motion (mixing) in the valley, as also reported by *de Araújo* [2009]. On the other hand, during the daytime a transition is observed, where beginning in the morning, downward motion is

observed, changing after mid-morning to upward motion (Figure 14b). This suggests that probably the cold air pooled during night moved downslope and started to warm, resulting in a breakdown the inversion over the valley (see *de Araújo* [2009], for detailed description and references there in for this process). The mechanism of the breakdown the inversion process over the valley is consistent with positive vertical velocity observed above canopy at slope area observed by the DRAINNO system tower during daytime (Figure 14b).

The subcanopy diurnal pattern of the mean vertical velocity observed shows positive values during nighttime and negative during daytime, consistent with observed up and downsloping flow regime, respectively (Figure 13 a, b). Also this is consistent with thermal vertical virtual potential temperature gradient on the slope (see Figure 9c), where during nighttime (daytime) an unstable (inversion) condition is associated with upward (downward) mean vertical velocity (see Figure 9c).



### 3.3. Phenomenology of the local circulations: Summary

The Figure 15 shows a schematic cartoon of local flow circulation from the previews sections observations.

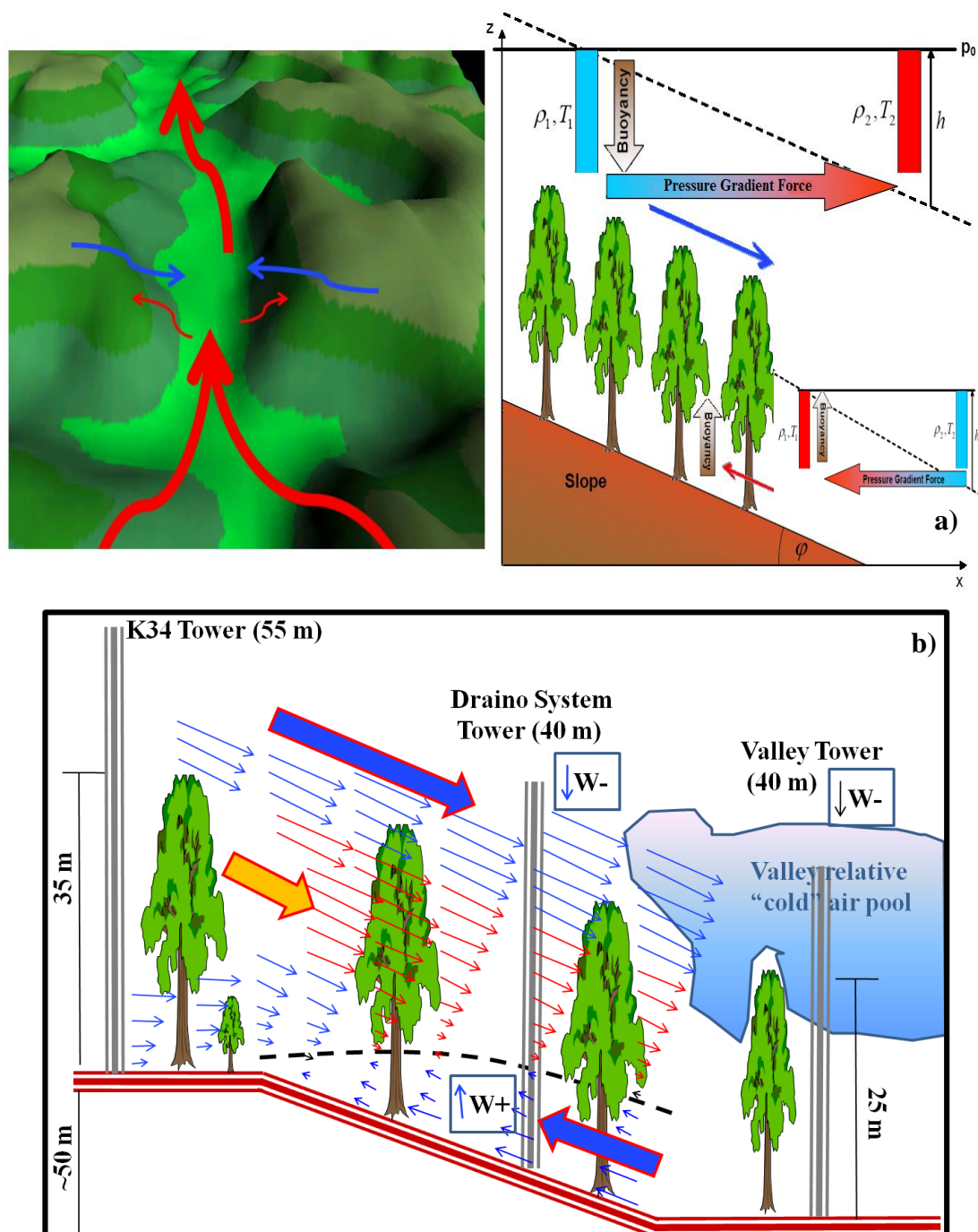


Figure 15: Schematic local circulations in the site studied, valley and slopes flow (a), 2D view from suggested below and above canopy airflow (b).

The above canopy airflow (red arrow Figure 15a) and forcing mechanisms associate. The observations result from previews sessions suggests that the balance of the buoyancy and

pressure gradient forces generates the airflow or microcirculations patterns in the site studied. During nighttime (Figure 15b), in the subcanopy there is an upslope flow reaching about 10 m height above ground, associate with positive mean vertical velocity (indicating upward movement). Also, above canopy there is a downslope flow associate with negative mean vertical velocity, downward convergence above the canopy. The microcirculation along the plateau-slope-valley is promotes by an feedback mechanism of accumulation of cold air drainage above canopy into the valley center (Figure 15b), creating the forcing need to sustain nighttime pattern. The air temperature structure above canopy in the valley (see Araújo, 2009) is a good indication of cold air pool in the center of the valley. Maybe, also, the local pressure gradient force due the cold air accumulation promoting the upward airflow in the both slopes of the valley. During daytime periods an inverse pattern is found (not show), indicating that this microcirculation is a systematic pattern in the site.

#### ***3.4. CO<sub>2</sub> concentration and subcanopy horizontal wind field***

The CO<sub>2</sub> concentration was measured by DRAINNO system on the south face slope area for dry and wet periods of the 2006, and on the north face slope during dry period (Figure 4). The Figure 16 presents an example, for midnight (local time), of the horizontal wind field and spatial CO<sub>2</sub> concentration over the DRAINNO System south face domain. The wind field was interpolated from the blue points onto a 10 m grid. Similar procedures have been reported in the literature (*Sun et al.*, 2007; *Feigenwinter et al.*, 2008). The horizontal wind regime plays important role in modulating the horizontal spatial distribution of CO<sub>2</sub> concentration (Figure 16).

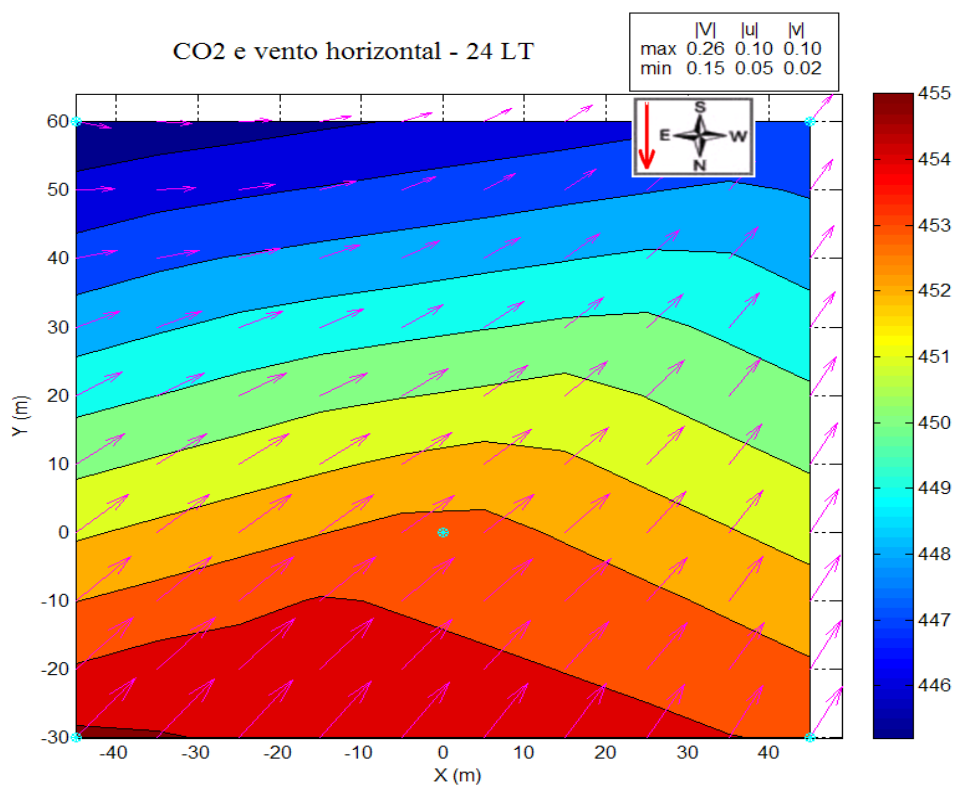


Figure 16: Example at midnight (local time) of the horizontal  $\text{CO}_2$  concentration over the DRAINNO System south face domain including an interpolated horizontal wind field (10 m grid), note the geographic orientation and the red arrow indicating slope inclination (see Figure 4).

In Figure 17 (a, b, c) the typical pattern observed is shown for both dry and wet periods of the 2006 measured by the DRAINNO system on the south-facing slope area. During the daytime (Figure 17c), the wind prevailed downslope inducing a strong horizontal gradient of  $\text{CO}_2$  in the slope area (about  $0.2 \text{ ppmv m}^{-1}$ ). In the evening, periods of changes of the horizontal wind pattern (as described in section 3.1) show an upsloping regime in the lower-part and downsloping in the upper-part of the slope areas (Figure 17b). The wind regimes produce direct responses in the spatial feature of the horizontal gradient of  $\text{CO}_2$  concentration. Later during the night, the upsloping regime is well established and also the horizontal gradient of  $\text{CO}_2$  is growing from lower part of slope to the top (Figure 17a). These observations suggest a subcanopy drainage flow and its influence on the scalar spatial distribution. Therefore, as discussed in the previews sections, the flow above the canopy indicates a reverse pattern of downward motion (negative mean vertical velocity, see section

3.2.3) that suggests vertical convergence and possible horizontally divergent flow during nighttime. The report by *Froelich and Schmid* [2006] and more recently *Feigenwinter et al.*, [2009a, b] describing similar features of the airflow interaction between above and below canopy.

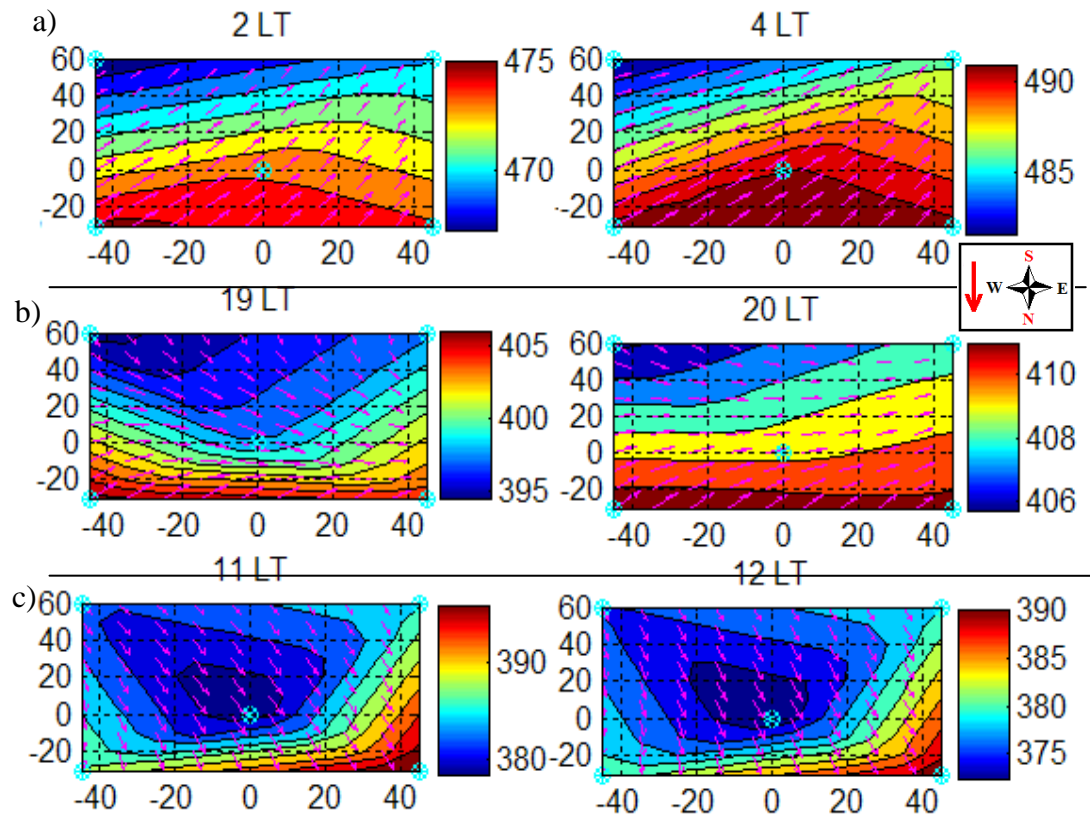


Figure 17: Hourly average of the subcanopy (2 m) CO<sub>2</sub> concentration and horizontal wind speed over DRAIN0 System south face area during dry period of the 2006, note the geographic orientation and the red arrow indicating slope inclination (see Figure 4). The axis represents distances from center of the main tower. Daytime (a), transition period - evening (b), established nighttime (c).

Along the north face, as shown in the Figure 18, the spatial distribution of the horizontal CO<sub>2</sub> concentration shows a similar pattern than the south face described previously. Despite, that there is no wind information in that area, if one assumes the same spatial correlation between horizontal wind and CO<sub>2</sub> concentration, is possible suggest that the wind should presents an inverse pattern from the south face. Its means that, during daytime the downslope wind direction should be from northeast (Figure 18c, from blue to red color).

During evening period (Figure 18b) should be indicating downslope (from northeast) in the upper part of the north face slope and upslope (from southeast) in the lower part of the slope, an inverse feature from Figure 17b. Finally, later in the night, on the north face slope, the wind pattern should present an upslope wind direction regime from southeast, an inverse regime that one from Figure 17a on the south face slope.

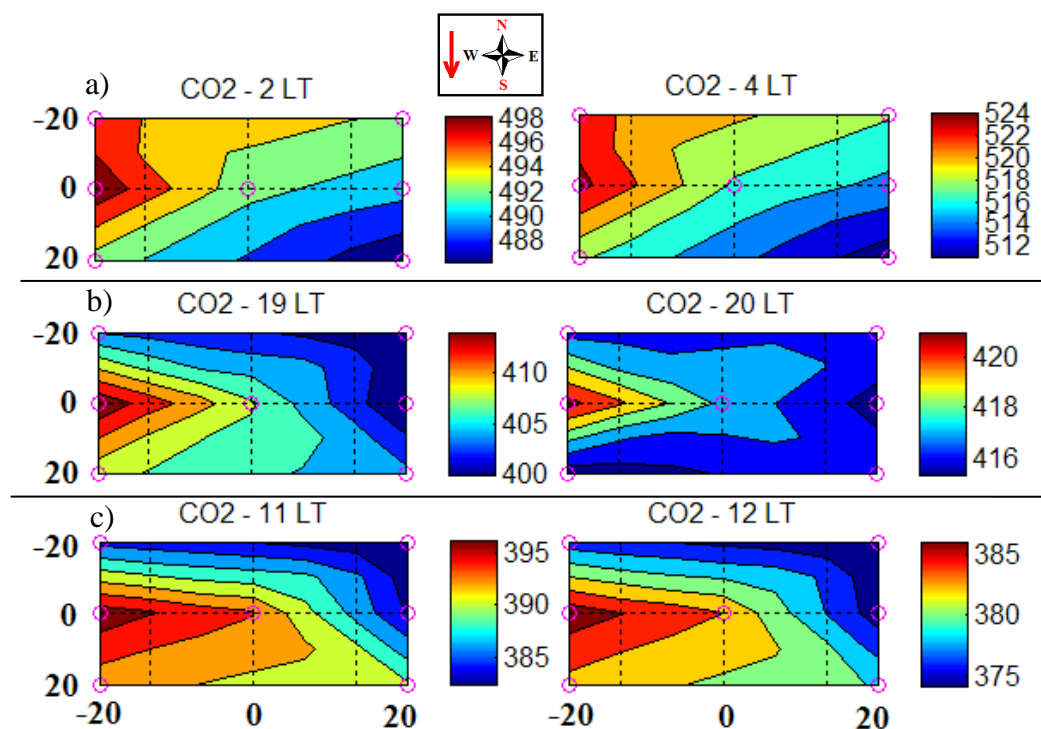


Figure 18: Hourly average of the subcanopy (2 m)  $\text{CO}_2$  concentration on the DRAINNO System north face area during dry period of the 2006, note the geographic orientation and the red arrow indicating slope inclination (see Figure 4). The axis represents distances from center of the main tower. Daytime (a), transition period - evening (b), established nighttime (c).

One possible explanation to this subcanopy slopes wind regime and spatial distribution of  $\text{CO}_2$  concentration, is the valley wind channeling effect and how it is meandering when enter in the valley topography [as described by Araújo, 2009]. This valley wind pattern, probably causes oscillations as those observed on the  $\text{CO}_2$  concentration along the day (Figures 17, 18), the known “Seiche phenomena” (Spigel and Imberger, 1980).

#### 4. Summary and Conclusions

The main objective of this study was to measure and understand the local circulation over a dense forest site in Manaus with moderately complex terrain and to verify the existence of the drainage flow regimes on slope and valley areas.

The main pattern of the airflow above and below the canopy in dense tropical forest in Amazonia was captured by a relative simple measure system, as also has been done by more sophisticated measurements system as those described recently by *Feigenwinter et al.*, [2009a, b].

As described and discuss in previews sections it was identified drainage flow in both day and nighttime periods in the site studied. Evidence of the drainage current above canopy was suggested by *Goulden et al.*, (2006) similar to that one observed here.

It was identified that the local micro-circulation was complicate and presented tri-dimensional nature where to estimate the advection flux at this site seems uncertain and not possible with the limited measurement system employed.

As reported recently by *Feigenwinter et al.*, [2009a, b], even using a more sophisticated measurement design, the level of uncertainties is still high and some processes are not yet known and need more exploration perhaps using a more complete spatial observation network or even applying model resources (*Foken*, 2008; *Aubinet*, 2008, *Belcher et al.*, 2008).

In summary, the drainage flow exists and is observed at K34 LBA site area and the high carbon uptake reported by previews work may be called into doubt and requires more research.

Also, the use of nighttime correction in order to save the urge necessity to estimate long term Net Ecosystem exchange is inappropriate by the using only turbulence information from above canopy, as has been pointed out here The interactions above and below canopy

breakdown the footprint principle and the representativeness of the eddy flux tower in most difficult conditions (complex terrain and calm nights).

In summary, the drainage flow exists and is observed at K34 LBA site. Very large carbon uptake estimates reported previously should be questioned [Kruijt *et al.*, 2004; Araújo *et al.*, 2002]. More research is needed. The use of nighttime  $u_*$  correction to avoid estimating canopy storage is inappropriate. One cannot get by using only above canopy turbulence information. The interactions between motions above and below canopy question the foundations of the footprint analysis [Schuepp *et al.*, 1990; Schmid, 2006]. The representativeness of the eddy flux tower is most in question for complex terrain, especially on calm nights).

## CONCLUSÃO GERAL

### **No Capítulo I foi apresentado que:**

- Foi realizado o primeiro esforço em determinar observacionalmente a importância dos processos de advecção noturna no balanço de CO<sub>2</sub> em uma densa floresta tropical na Amazônia.
- Foi testada a hipótese de que uma persistente advecção horizontal abaixo da floresta existe e transporta uma importante quantidade de CO<sub>2</sub> para fora do volume de controle representado pelas medidas da torre de fluxo do LBA em Santarém.
- Foi determinada a magnitude dos gradientes horizontais de CO<sub>2</sub> e do campo do vento abaixo da floresta e encontrado um saldo suficiente de advecção para afetar o balanço de CO<sub>2</sub>.
- A metodologia estabelecida foi aplicada e testada para medir os gradientes horizontais de CO<sub>2</sub> e do vento horizontal dentro da floresta. Esses dados foram complementados pelos fluxos turbulentos e observações dos perfis médios obtidos em uma torre de 65 metros de altura no mesmo sítio experimental (sessão 2). As medidas foram realizadas durante o período das estações seca (DOY 198-238 2003 – Fase 1) e úmida (DOY 278-366 2004 e 1-32 2005 – Fase 2).
- Os gradientes horizontais médio de CO<sub>2</sub> e do vento horizontal foram da ordem de 0.02 ppm m<sup>-1</sup> e 0.12 m s<sup>-1</sup>, respectivamente (seção 3.1).
- Abaixo da floresta a direção do vento horizontal foi bem correlacionada com a inclinação suave do terreno próxima a torre de medida dos fluxos. Foi observado que a direção do escoamento abaixo da floresta foi desacoplada do escoamento acima, o que sugere um potencial para transporte lateral de CO<sub>2</sub> mesmo durante o período diurno (sessão 3.2).
- O principal mecanismo físico responsável pela geração do escoamento noturno abaixo da floresta foi o termo de fluatibilidade negativa (seção 3.3).



- A comparação do déficit noturno entre a respiração total do ecossistema e NEE medida no sistema de fluxo da torre foi associado à advecção noturna média de CO<sub>2</sub>, a qual representou 73% e 71% do mesmo, para 130 noites analisados durante os períodos seco e chuvoso estudados. Isto indica um importante papel da advecção noturna no balanço total de CO<sub>2</sub>.
- Foi observado também que, durante períodos noturnos com níveis de turbulência significativos ( $u^*$  entre 0.3 a 0.6 m s<sup>-1</sup>, limiares considerados suficiente para fornecer corretas medidas pelos fluxos turbulentos), o transporte de CO<sub>2</sub> pela advecção horizontal foi significativo.
- Esses resultados confirmam que poucos sítios de medidas de fluxos são suficientemente planos e homogêneos para ignorar *a priori* os efeitos da advecção horizontal. Estimativa observacional do efeito da velocidade vertical média no balanço de escalares aparece como a maior fonte de incertezas, e medidas continua e de longo prazo com instrumentação mais adequada são necessárias para esclarecer este tema.

### **No Capítulo II foi apresentado que:**

- Seguindo a metodologia e design experimental desenvolvido no Capítulo I, foi possível ser aplicada também para um sítio experimental com topografia de maior complexidade.
- Foi observado que existem escoamentos de drenagem horizontal abaixo e acima da floresta, e que esses estão fortemente influenciados pela canalização do vento horizontal ao longo do vale da microbacia Asu próximo da torre de fluxo (K34) e das medidas nas encostas abaixo da floresta (Sistema DRAIN0).
- Especialmente no **sítio do LBA em Manaus**, não foi possível estimar quantitativamente a magnitude da advecção horizontal de CO<sub>2</sub>, em função da complexa heterogeneidade topográfica da área produzindo uma complicada natureza tridimensional do escoamento

abaixo e acima da floresta, que se interagem e criando uma barreira para medir em detalhe todas as informações com a metodologia e instrumentação disponível neste estudo.

- As sub-estimativas noturnas das taxas de respiração através de medidas aplicando a técnica de “Eddy Covariance” sobre vários tipos de ecossistemas e terrenos já é bem reconhecida pela comunidade científica mundialmente. Os estudos observacionais aqui apresentados suportam esta hipótese demonstrando a importância do transporte horizontal que ocorre abaixo do nível de medida das torres de fluxo de ambos **os sítios de medidas do LBA**. E finalmente adverte que correções dos fluxos turbulentos noturnos com base em condições acima da vegetação somente podem ser inapropriadas e com significativa incerteza.
- Como sugestões os estudos de modelagem do tipo LES, já que foi identificado um padrão de micro circulações locais de natureza tridimensional, seriam de fundamental importância para avaliar e ajudar a entender melhor as observações aqui obtidas.

## REFERÊNCIAS

- Acevedo, O. C. and Fitzjarrald, D.R. (2003), In the Core of the Night - Effects of Intermittent Mixing on a Horizontally Heterogeneous Surface. *Boundary-Layer Meteorology*, Dordrecht, v. 106, n. 1, p. 1-33.
- Antonia, R.A., Chambers, A.J., Frieh, C.A.E. and van Atta, C.W., (1979), Temperature ramps in the atmospheric surface layer. *J. Atmos. Sci.* 36, pp. 99–108.
- Araújo, A. C., et al., (2002), Comparative measurements of carbon dioxide fluxes from two nearby towers in a central Amazonian rainforest: The Manaus LBA site, *Journal of Geophysical Research*, 107(D20), 8090, doi:10.1029/2001JD000676.
- Araújo, A. C., et al., (2008), Interaction of micrometeorology and surface fluxes confounding the interpretation of CO<sub>2</sub> fluxes in Central Amazonia. *Submitted to Agricultural and Forest Meteorology*.
- Araújo, A. C., (2009), Spatial variaton of CO<sub>2</sub> fluxes and lateral transport in an area of terra firme forest in central Amazonia. PhD Thesis, Vrije Universiteit Amsterdam, VU, Holanda.
- Aubinet M, P. Berbigier, C. H. Bernhofer, A. Cescatti, C. Feigenwinter, A. Granier, T. H. Grunwald, K. Havrankova, B. Heinesch, B. Longdoz, B. Marcolla, L. Montagnani, P. Sedlak (2005), Comparing CO<sub>2</sub> storage and advection conditions at night at different Carboeuroflux sites. *Boundary Layer Meteorol.*, 116: 63-94.
- Aubinet, M., B. Heinesch, and M. Yernaux (2003), Horizontal and vertical CO<sub>2</sub> advection in a sloping forest, *Boundary Layer Meteorol.*, 108(3), 397–417.
- Aubinet, M., et al., (2000), Estimates of the annual net carbon and water exchange of forests: the EUROFLUX methodology. *Adv. Ecol. Res.*, 30, 113–175.
- Baker I. T., Prihodko, L., Denning, A.S., Goulden, M., Miller, S., da Rocha, H.R., (2008), Seasonal drought stress in the Amazon: Reconciling models and observations, *J. Geophys. Res.*, 113, G00B01, doi:10.1029/2007JG000644
- Baker, T.R. et al., (2004), Increasing biomass in Amazonian forest plots. *Philosophical Transactions of the Royal Society of London. Series B-Biological Sciences*, 359(1443): 353-365.
- Baldocchi, D. D., B. B. Hicks, and T. P. Meyers (1988), Measuring biosphere-atmosphere exchanges of biologically related gases with micrometeorological methods, *Ecology*, 69(5), 1331– 1340.
- Baldocchi, D., et al. (2001), FLUXNET: A new tool to study the temporal and spatial variability of ecosystem-scale carbon dioxide, water vapor, and energy flux densities, *Bull. Am. Meteorol. Soc.*, 82(11), 2415 – 2434.

- Baldocchi, D., J. Finnigan, K. Wilson, T. Paw U, and E. Falge (2000), On measuring net ecosystem carbon exchange over tall vegetation on complex terrain, *Boundary Layer Meteorol.*, 96(1–2), 257–291.
- Barr, S., (1971), A modeling study of several aspects of canopy flow. *Monthly Weather Review*, vol. 99, No. 6: 485-493.
- Baynton, H. W., Biggs, W. G., Hamilton, H. L., Jr., Sherr, P. E., and Worth, J. J. B., (1965), Wind Structure in and Above a Tropical Forest. *Journal of Applied Meteorology*, Vol. 4, No. 6: 670-675.
- Bergstrom, H., Hogstrom, U., (1989), Turbulent exchange above apine forest II. Organized structures. *Bound.-Layer Meteorol.*49: 231-263.
- Bitencourt, D.P. and Acevedo, O. C., (2008), Modelling the Interaction Between a River Surface and the Atmosphere at the Bottom of a Valley. *Boundary-Layer Meteorology*, v. 129, p. 309-321.
- Black, T. A., et al. (1996), Annual cycles of water vapour and carbon dioxide fluxes in and above a boreal aspen forest, *Global Change Biol.*, 2(3), 219–229.
- Bohrer, Gil, (2007), Large Eddy Simulations of Forest Canopies for Determination of Biological Dispersal by Wind. PhD Thesis. Department of Civil and Environmental Engineering, Duke University, 2007.
- Castilho, C., (2004), Variação espacial e temporal da biomassa arbórea viva em 64 km<sup>2</sup> de floresta de terra-firme na Amazônia Central. 87p. Doctoral Thesis, ecology, Instituto Nacional de Pesquisa da Amazônia, Manaus-AM.
- Chambers, J.Q. et al., (2004), Respiration from a tropical forest ecosystem: Partitioning of sources and low carbon use efficiency. *Ecological Applications*, 14(4): S72-S88.
- Cionco, R. M., 1965: A mathematical model for air flow in a vegetation canopy. *J. Appl. Meteor.*, 4, 517–522.
- Clark D. B. (1996), Abolishing virginity. *Journal of Tropical Ecology*, 12, 735–739.
- Cohen, J. C. P., Sá, L.D.A., Nogueira, D. S., Gandu, A.W., (2006), Jatos de baixos níveis acima da floresta amazônica em Caxiuana. *Revista Brasileira de Meteorologia*, São Paulo, v.21, n.3b, p. 271-282.
- Cuartas, L.A. et al., (2007), Interception water-partitioning dynamics for a pristine rainforest in Central Amazonia: Marked differences between normal and dry years. *Agricultural and Forest Meteorology*, 145(1-2): 69-83.
- da Rocha, H. R., M. L. Goulden, S. D. Miller, M. C. Menton, L. D. V. O. Pinto, H. C. de Freitas, and A. M. E. S. Figueira (2004), Seasonality of water and heat fluxes over a tropical forest in eastern Amazonia, *Ecol. Appl.*, 14(4), suppl. S, S22– S32.

- Denmead, O.T. and Bradley, E.F., (1985), Flux-gradient relationships in a forest canopy. *In: B.A. Hutchison and B.B. Hicks (Editors). The forest-atmosphere interaction*. D. Reidel Publishing Company, Dordrecht, Holland, pp. 421-442.
- Dias, M. A. F. S. and P. Regnier., (1996), Simulation of mesoscale circulations in a deforested area of Rondônia in the dry season. In *Amazonian deforestation and climate*, ed. J. H. C. Gash, C. A. Nobre, J. M. Roberts and R. L. Victoria:531-547. Chichester: J Wiley.
- Dixon, R.K., S.Brown, R.A. Houghton, A.M. Solomon, M.C. Trexler and J. Wisniewski, (1994), Carbon pools and flux of global forest ecosystems. *Science*, 263, 185-190.
- Falge, E., et al. (2001), Gap filling strategies for defensible annual sums of net ecosystem exchange. *Agric. For. Meteorol.* 107, 43-69.
- Fan, S.M., Wofsy, S.C., Bakwin, P.S., Jacob, D.J. and Fitzjarrald, D.R., (1990), Atmosphere-biosphere exchange of CO<sub>2</sub> and O<sub>3</sub> in the Central-Amazon-forest. *Journal of Geophysical Research-Atmospheres*, 95(D10): 16851-16864.
- Feigenwinter, C., C. Bernhofer, and R. Vogt, (2004), The influence of advection on the short term CO<sub>2</sub>-budget in and above a forest canopy, *Boundary Layer Meteorol.*, 113(2), 201–224.
- Feigenwinter, C., C. et al., (2008), Comparison of horizontal and vertical advective CO<sub>2</sub> fluxes at three forest sites, *Agric. Forest. Meteorol.*, 145,1–21.
- Feigenwinter, C., et al. (2009a), Spatiotemporal evolution of CO<sub>2</sub> concentration, temperature, and wind field during stable nights at the Norunda forest site. *Agric. Forest Meteorol.*, doi:10.1016/j.agrformet.2009.08.005
- Feigenwinter, C., Montagnani, L., Aubinet, M. (2009b), Plot-scale vertical and horizontal transport of CO<sub>2</sub> modified by a persistent slope wind system in and above an alpine forest. *Agric. Forest Meteorol.*, doi:10.1016/j.agrformet. 2009.05.009.
- Ferraz, J., Ohta, S. and Sales, S., 1988. Distribuição dos solos ao longo de dois transectos em floresta primária ao norte de Manaus. In: *N. Higuchi, M.A.A. Campos, P.T.B. Sampaio and J. dos Santos (Editors), Análise estrutural da floresta primária da bacia do rio Cuieiras, ZF-2, Manaus-AM, Brasil. MCT/INPA/JICA*, Manaus, pp. 109-144.
- Finnigan, J.J., R. Clement, Y. Malhi, R. Leuning and H.A. Cleugh, (2003), A reevaluation of long-term flux measurement techniques. Part I: Averaging and coordinate rotation. *Bound.-Layer Meteorol.*, 107, 1-48.
- Fitzjarrald, D. R., and K. E. Moore, (1990), Mechanisms of nocturnal exchange between the rain-forest and the atmosphere, *Journal of Geophysical Research*, 95(D10), 16,839–16,850.
- Fitzjarrald, D. R., K. E. Moore, O. M. R. Cabral, J. Scola, A. O. Manzi, and L. D. D. Sa (1990), Daytime turbulent exchange between the Amazon Forest and the atmosphere, *Journal of Geophysical Research*, 95(D10), 16,825 – 16,838.

- Fitzjarrald, D. R., R. K. Sakai, O. L. L. Moraes, M. J. Czikowsky, O. C. Acevedo, R. C. Oliveira, (2004), Mesoclimate of the LBA-ECO Santarém Study Area, paper presented at III LBA Scientific Conference, Braz. Minist. of Sci. and Technol., Brasilia, Brazil, July.
- Fitzjarrald, D. R., Stormwind, B.L., Fisch, G., Cabral, O. M. R. (1988), Turbulent Transport Observed Just Above the Amazon Forest, *Journal of Geophysical Research*, 93(D2), 1,551–1,563.
- Fitzjarrald, D.R., and K.M. Moore, (1995), Physical mechanisms of heat and mass exchange between forests and the atmosphere. In: M. Lowman and N. Nadkarni, eds., *Forest Canopies: A Review of Research on This Biological Frontier*, Academic Press, 45–72.
- Foken, T. (2008), The energy balance closure problem: An overview. *Ecological Applications*: Vol. 18, No. 6, pp. 1351-1367.
- Freitas, S. R., Longo, K.M., Silva Dias, M.A. F., Silva Dias, P.L., Chatfield, R., Prins, E., Artaxo, P., Grell, G., Recuero, F.S., (2005), Monitoring the transport of biomass burning emissions in South America, *Environ. Fluid Mech.*, 5(1–2), doi:10.1007/s10652-0050243-7.
- Freitas, S. R., M. A. F. Silva Dias, P. L. Siva Dias, K. M. Longo, P. Artaxo, M. O. Andreae, and H. Fischer (2000), A convective kinematic trajectory technique for low-resolution atmospheric models, *J. Geophys. Res.*, 105(D19), 24,375–24,386.
- Froelich, N.J. and Schmid, H.P., (2006), Flow divergence and density flows above and below a deciduous forest Part II. Below-canopy thermotopographic flows. *Agricultural and Forest Meteorology*, Volume 138, Issues 1-4.
- Gandu, A. W., Cohen, J.C.P., Souza, J. R. S., (2004), Simulation of deforestation in eastern Amazonia using a high-resolution model. *Theoretical and Applied Climatology*, Austria, v. 78, n. 1-3, p. 123-135.
- Gao, W., Shaw, R.H., Paw U, K.T., (1989), Observation of organized structure in turbulent flow within and above a forest canopy. *Bound.-Layer Meteorol.* 47: 349-377.
- Garratt, J. R., (1980), Surface Influence upon Vertical Profiles in the Atmospheric near-surface layer. *Quart. J. Roy. Meteorol. Soc.*, v.106, n.450, p. 803-819.
- Goulden, M. L., J. W. Munger, S. M. Fan, B. C. Daube, and S. C. Wofsy (1996), Measurements of carbon sequestration by long-term eddy covariance: Methods and a critical evaluation of accuracy, *Global Change Biol.*, 2(3), 169– 182.
- Goulden, M. L., S. D. Miller, H. R. da Rocha, M. C. Menton, H. C. de Freitas, A. M. E. S. Figueira, and C. A. D. de Sousa (2004), Diel and seasonal patterns of tropical forest CO<sub>2</sub> exchange, *Ecol. Appl.*, 14(4), suppl. S, S42–S54.
- Goulden, M.L., Miller, S.D. and da Rocha, H.R., (2006), Nocturnal cold air drainage and pooling in a tropical forest. *Journal of Geophysical Research-Atmospheres*, 111(D8), 10.1029/2005JD006037.

- Grace, J. et al., (1995a), Carbon-Dioxide Uptake by an Undisturbed Tropical Rain-Forest in Southwest Amazonia, 1992 to 1993. *Science*, 270(5237): 778-780.
- Grace, J., et al. (1995b), Carbon dioxide uptake by an undisturbed tropical rain forest in southwest Amazonia, *Science*, 270, 778–780.
- Grace, J., Y. Malhi, J. Lloyd, J. McIntyre, A. C. Miranda, P. Meir, and H. S. Miranda (1996), The use of eddy covariance to infer the net carbon dioxide uptake of Brazilian rain forest, *Global Change Biol.*, 2, 208– 217.
- Gu L., E. Falge, T. Boden, D. D. Baldocchi, T. A. Black, S. R. Saleska, T. Suni, T. Vesala, S. Wofsy, L. Xu (2005), Observing threshold determination for nighttime eddy flux filtering, *Agric. For. Meteorol.*, 128:179–197.
- Harman, I.N. and Finnigan, J.J., (2007), A simple unified theory for flow in the canopy and roughness sublayer. *Boundary-Layer Meteorology*, 123, 339-363.
- Hodnett, M.G., Tomasella, J., Cuartas, L.A., Waterloo, M.J., and Nobre, A.D., (2007), Subsurface hydrological flow paths in a Ferralsol (Oxisol) landscape in central Amazonia. *Hydrological Sciences Journal* (in press).
- Hutyra, L. R., J. W. Munger, S. R. Saleska, E. Gottlieb, B. C. Daube, A. L. Dunn, D. F. Amaral, P. B. de Camargo, and S. C. Wofsy (2007), Seasonal controls on the exchange of carbon and water in an Amazonian rain forest, *Journal of Geophysical Research*, 112, G03008, doi:10.1029/2006JG000365.
- Inoue, E., (1963), On the turbulent structure of air flow within crop canopies. *J. Meteor. Soc. Japan*, 41, 317–326.
- IPCC 2007. Climate Change 2007: The physical science basis. Contribution of Working Group I to the Fourth Assessment Report of the *Intergovernmental Panel on Climate Change*. WMO/UNEP, 18 pp.
- Iwata, H., Y. Malhi, and C. Von Randow, (2005), Gap-filling measurements of carbon dioxide storage in tropical rainforest canopy airspace. *Agricultural and Forest Meteorology*. 132, 3-4: 305–314.
- Kanda, M., R. Moriwaki, and F. Kasamatsu., (2004), Large-eddy simulation of turbulent organized structures within and above explicitly resolved cube arrays. *Boundary-Layer Meteorology* 112: 343-368.
- Katul, G.G., J.J. Finnigan and R. Leuning, (2003), The influence of hilly terrain on canopy-atmosphere carbon dioxide exchange. *Boundary Layer Meteorology*.
- Keller, M., et al. (2004), Ecological research in the large-scale biosphere atmosphere experiment in Amazonia: Early results, *Ecol. Appl.*, 14(4), suppl. S, S3– S16.
- Kruijt, B. et al., (2000), Turbulence statistics above and within two Amazon rain forest canopies. *Boundary-Layer Meteorology*, 94(2): 297-331.

- Kruijt, B. J., A. Elbers, C. von Randow, A. C. Arau'jo, P. J. Oliveira, A. Culf, A. O. Manzi, A. D. Nobre, P. Kabat, and E. J. Moors (2004), The robustness of eddy correlation fluxes for Amazon rain forest conditions, *Ecol. Appl.*, 14, suppl. S, S101–S113.
- Kruijt, B., et al., (2000), Turbulence Statistics Above and Within Two Amazon Rain Forest Canopies. *Boundary-Layer Meteorology*, v. 94, n. 2, p. 297-331.
- Laurance, et al., (1999), Relationship between soils and Amazon Forest biomass: a landscape-scale study. *Forest Ecology Management*, 118:127-138.
- Lee, X. H. (1998), On micrometeorological observations of surface-air exchange over tall vegetation, *Agric. For. Meteorol.*, 91(1–2), 39–49.
- Lee, X. and Hu, X., (2002), Forest-air fluxes of carbon and energy over non-flat terrain, *Boundary-Layer Meteorology*, 103: 277-301.
- Lee, X., Neumann, H.H., den Hartog, G., Fuentes, J.D., Black, T.A., Mickle, R.E., Yang, P.C. and Blanken, P.D., (1992), Observation of gravity waves in a boreal forest. *Bound.-Layer Meteorol.* 84, pp. 383–398.
- Leuning, R., Zegelin, S. J., Jones, K., Keith, H., Hughes, D., (2008), Measurement of horizontal and vertical advection of CO<sub>2</sub> within a forest canopy. *Agricultural and Forest Meteorology*, Volume 148, Issue 11, Pages 1777-1797.
- Li, B. and R. Avissar. 1994. The impact of spatial variability of land-surface characteristics on land-surface heat fluxes. *Journal of Climate* 7: 527-537.
- Lu, C.-H., and D.R. Fitzjarrald, (1994), Seasonal and diurnal variations of coherent structures over a deciduous forest. *Boundary-Layer Met.*, 69, 43-69.
- Lu, L., Denning, A S.; Silva Dias, M.A.F., Ssilva Dias, P. L., Longo, M., Freitas, S. R., Saatchi, S., (2005), Mesoscale circulations and atmospheric CO<sub>2</sub> variations in the Tapajós region, Pará, Brazil. *Journal of Geophysical Research*, doi 10.1029/2004JD005757, v. 110, n. D21102.
- Luizão, R.C.C., Luizão, F.J., Paiva, R.Q., Monteiro, T.F., Sousa, L.S., Kruijt, B., (2004), Variation of carbon and nitrogen cycling processes along a topographic gradient in a central Amazonian forest. *Global Change Biology*, 10: 592-600.
- Mahrt, L., (1982), Momentum balance of gravity flows. *J. Atmos. Sc.*, 39, 2701-2711.
- Malhi, Y., A. D. Nobre, J. Grace, B. Kruijt, M. G. P. Pereira, A. Culf, and S. Scott, (1998), Carbon dioxide transfer over a central Amazonian rain forest. *Journal of Geophysical Research*, 103, 31,593–31,612.
- Malhi, Y., et. al. (2009), Comprehensive assessment of carbon productivity, allocation and storage in three Amazonian forests. *Global Change Biology*, Volume 15, Issue 5, 1255-1274.



- Marcolla, B, A. Cescatti, L. Montagnani, G. Manca, G. Kerschbaumer and S. Minerbi, (2005), Importance of advection in the atmospheric CO<sub>2</sub> exchanges of an alpine forest. *Agric. For. Meteorol.*, 130, 193-206.
- Melillo, J.M. et al.,(1993), Global climate change and terrestrial net primary production. *Nature* 363, 234-240.
- Meroney, Robert N., (1968), Characteristics of Wind and Turbulence in and Above Model Forests. *Journal of Applied Meteorology*, Vol. 7, NO. 5: 780-788.
- Miller, S. D., M. L. Goulden, M. C. Menton, H. R. da Rocha, H. C. de Freitas, A. M. E. S. Figueira, and C. A. D. de Sousa (2004), Biometric and micrometeorological measurements of tropical forest carbon balance, *Ecol. Appl.*, 14(4), suppl. S, S114– S126.
- Moncrieff, J. B., J. M. Massheder, H. deBruin, J. Elbers, T. Friborg, B. Heusinkveld, P. Kabat, S. Scott, H. Soegaard, and A. Verhoef. “A system to measure surface fluxes of momentum, sensible heat, water vapour and carbon dioxide.” *Journal of Hydrology* 189, 1-4: (1997) 589–611.
- Montgomery, R.B., (1948), Vertical flux of heat in the atmosphere. *Journal of Meteorology*, 5, 265–274.
- Nogueira, D. S., Sá, L.D.A., Cohen, J. C. P., (2006), Rajadas Noturnas e Trocas de CO<sub>2</sub> Acima da Floresta de Caxiuanã, PA, Durante a Estação Seca. *Revista Brasileira de Meteorologia*, São Paulo, v.21, n.3b, p. 212-223.
- Pachêco , V. B., (2001), Algumas Características do Acoplamento entre o Escoamento Acima e Abaixo da Copa da Floresta Amazônica em Rondônia. 2001 109f. Dissertação (*Mestrado em Meteorologia*) - Instituto Nacional de Pesquisas Espaciais, São José dos Campos.
- Parker, G., and D. R. Fitzjarrald (2004), Canopy structure and radiation environment metrics indicate forest developmental stage, disturbance, and certain ecosystem functions, paper presented at III LBA Scientific Conference, Braz. Minist. of Sci. and Technol., Brasilia, Brazil, July.
- Parotta J.A., J. K. Franci, R. R. de Almeida (1995), Trees of the Tapajos: a photographic field guide. General Technical Report IITF-1. United States Department of Agriculture, Rio Piedras, Puerto Rico, 371 pp.
- Patton, E. G., (1997), Large-eddy simulation of turbulent flow above and within a plant canopy. Ph.D. Thesis, University of California Davis.
- Patton, Edward (2008), Large-eddy simulation (LES); Momentum and scalar transport in canopy-covered terrain. *ADVEX Workshop*.
- Paw U. K. T., D. D. Baldocchi, T. P. Meyers, and K. B. Wilson (2000), Correction of eddy covariance measurements incorporating both advective effects and density fluxes. *Boundary Layer Meteorol.*, 97, 487-511.

- Phillips, O.L. et al., (1998), Changes in the carbon balance of tropical forests: Evidence from long-term plots. *Science*, 282(5388): 439-442.
- Poggi, D., Katul, G., Finnigan, J. J., Belcher, S. E., (2008) Analytical models for the mean flow inside dense canopies on gentle hilly terrain. *Q. J. R. Meteorol. Soc.* 134: 1095–1112 (2008).
- Prandtl, L., (1925), Über die ausgebildete turbulenz. *Z. Angew. Math. Mech.*, 5, 136–139.
- Ramos da Silva, R., Avissar, R., (2000), A Large Eddy Simulation (LES) of the Boundary Layer Evolution Over a Deforested Region of Rondonia (Brazil). In: American Geophysical Union - Fall Meeting, 2002, San Francisco. EOS Trans., San Francisco: American Geophysical Union, 2002. v. 83.
- Raupach, M. R., and J. J. Finnigan., (1997), The influence of topography on meteorological variables and surface-atmosphere interactions. *Journal of Hydrology* 190, 3-4: 182–213.
- Raupach, M. R., J. J. Finnigan, and Y. Brunet., (1996), Coherent eddies and turbulence in vegetation canopies: The mixing-layer analogy. *Boundary-Layer Meteorology* 78: 351-382.
- Raupach, M. R., Thom, A. S., (1981), Turbulence in and above Plant Canopies. *Annual Review of Fluid Mechanics*, v. 13, p. 97-129.
- Raupach, M.R., Finnigan, J.J. and Brunet, Y., (1996), Coherent eddies and turbulence in vegetation canopies: The mixing layer analogy. *Boundary-Layer Meteorology*, 78, 351-382.
- Rennó, C. D., et al., (2008), HAND, a new terrain descriptor using SRTM-DEM: Mapping terra-firme rainforest environments in Amazonia. *Remote Sensing of Environment*, doi:10.1016/j.rse.2008.03.018
- Sá, L. D. A., Pachêco, V. B., (2001), Relação de Similaridade para os Perfis de Velocidade do Vento dentro da Copa da Floresta Amazônica em Rondônia. *Revista Brasileira de Meteorologia*, v.16, n. 1, p. 81-89, 2001.
- Sá, L. D. A., Pachêco, V.B., (2006), Wind velocity above and inside Amazonian Rain Forest in Rondônia. *Revista Brasileira de Meteorologia*, v.21, n.3a, 50-58, 2006.
- Sakai, R., D. Fitzjarrald, and K. E. Moore., (2001), Importance of low-frequency contributions to eddy fluxes observed over rough surfaces. *Journal Applied Meteorology*, 40: 2178–2192.
- Saleska, S. R., et al. (2003), Carbon in Amazon forests: Unexpected seasonal fluxes and disturbance-induced losses, *Science*, 302(5650), 1554– 1557.
- Shaw, R. H., 1977: Secondary wind speed maxima inside plant canopies. *J. Appl. Meteor.*, 16, 514–521.
- Shuttleworth, W.J., (1989), Micrometeorology of temperate and tropical forest. *Philosophical Transactions of the Royal Society of London*, series B, 324, 1223: 299-334.

- Silva Dias, M.A.F. (2006), Meteorologia , desmatamento e queimadas na Amazônia: uma síntese de resultados do LBA. *Revista Brasileira de Meteorologia*, v.21, n.3a, 190-199, 2006.
- Silva Dias, M.A.F., Silva Dias, P. L., Longo, M., Fitzjarrald, D. R., Denning, A S., (2004), River breeze circulation in eastern Amazon: observations and modeling results. *Theoretical and Applied Climatology*, DOI 10.1007/s00704-004-0047-6, v. 78, n. 1-3, p. 111-121.
- Silver W. L., et al., (2000), Effects of soil texture on belowground carbon and nutrient storage in a lowland Amazonian forest ecosystem. *Ecosystems*, 3, 193–209.
- Sousa, A.M.L. (2005), Estudo Observacional de Jatós de Baixos Níveis no Litoral Norte e Nordeste do Pará Durante o Período Chuvoso e Seco. 140 f. *Dissertação Mestrado em Meteorologia*, UFPel, Pelotas, RS.
- Souza, J.S.D., (2004), Dinâmica espacial e temporal do fluxo de CO<sub>2</sub> do solo em floresta de terra firme na Amazônia central. *MSc Thesis, Universidade Federal do Amazonas, Manaus, Brazil*, 62 pp.
- Staebler R.M., and Fitzjarrald D.R. (2005), Measuring canopy structure and kinematics of subcanopy flows in two forests. *J. Appl. Meteor.*, 44, 1161-1179.
- Staebler, R. M., and D. R. Fitzjarrald (2004), Observing subcanopy CO<sub>2</sub> advection, *Agric. For. Meteorol.*, 122(3– 4), 139– 156.
- Staebler, R.M., 2003. Forest subcanopy flows and micro-scale advection of carbon dioxide. Ph.D. Dissertation, SUNY Albany.
- Sun J., S. P. Burns, A. C. Delany, S. P. Oncley, A. A. Turnipseed, B.B. Stephens, D. H. Lenschow, M. A. LeMone, R. K. Monson, D. E Anderson (2007), CO<sub>2</sub> transport over complex terrain. *Agric. Forest. Meteorol.*, 145,1–21.
- Swinbank, W.C., (1951), The measurements of vertical transfer of heat and water vapor by eddies in the lower atmosphere. *Journal of Meteorology*, 8, 135–145.
- Tomasella, J. et al., (2008), The water balance of an Amazonian micro-catchment: the effect of interannual variability of rainfall on hydrological behaviour. *Hydrological Processes*, 22(13): 2133-2147.
- Tóta J., Fitzjarrald, D.R., Staebler, R.M., Sakai, R.K., Moraes, O.M.M., Acevedo, O. C., Wofsy, S.C., Manzi, A.O., (2008), Amazon rain Forest subcanopy flow and the carbon budget: Santarém LBA-ECO site, *Journal Geophysical Research - Biogeosciences*, 113, G00B02, doi:10.1029/2007JG000597.
- Tóta, J., Santos, R., Fisch, G., Querino, C., Silva Dias, M.A.F., Artaxo, P., Guenther, A., Martin, S., Manzi, A.O., (2008b), Nocturnal Boundary Layer measurements during the Amazonian Aerosol Characterization Experiment - AMAZE. In: 2008 AGU Fall Meeting, A11C-0125, Dec-08, San Francisco-CA.

- Turnipseed A. A., D. E. Anderson, S. Burns, P. D. Blanken, and R. K. Monson (2004), Airflows and turbulent flux measurements in mountainous terrain. Part 2. Mesoscale effects. *Agricultural and Forest Meteorology*, 125, 187-205.
- Turnipseed, A. A., D. E. Anderson, P. D. Blanken, W. M. Baugh, and R. K. Monson., (2003), Airflows and turbulent flux measurements in mountainous terrain: Part 1 - Canopy and local effects. *Agricultural and Forest Meteorology*, 119:1–21.
- Urbanski, S., Barford, C., Wofsy, S., Kucharik, C., Pyle, E., Budney, J., McKain, K., Fitzjarrald, D.R., Czikowsky, M., Munger, J.W. (2007), Factors controlling CO<sub>2</sub> exchange on timescales from hourly to decadal at Harvard Forest, *Journal Geophysical Research - Biogeosciences*. 112.
- van Diepen, R., (2006), Spatial variability of soil respiration in a micro-scale rain forest catchment in Central Amazonia, Brazil. *MSc Thesis, Vrije Universiteit Amsterdam, Amsterdam, the Netherlands*, 68 pp.
- Vickers, D., L. Mahrt, (2006), Contrasting mean vertical motion from tilt correction methods and mass continuity, *Agric. For. Meteorol.*, 138, 93 –103.
- Von Randow, C., (2007), On turbulent exchange processes over Amazonian Forest. Tese de Doutorado em Ciências Ambientais. Wageningen University and Research Centre, WUR, Holanda.
- Waterloo, M.J. et al., (2006), Export of organic carbon in run-off from an Amazonian rainforest blackwater catchment. *Hydrological Processes*, 20(12): 2581-2597.
- Wilczak, J.M., S.P. Oncley, and S.A. Stage (2001), Sonic anemometer tilt correction algorithms. *Bound.-Layer Meteorol.*, 99, 127-150.
- Wilson, N. R., and R. H. Shaw, (1977), Higher-order closure model for canopy flow. *J. Appl. Meteor.*, 16, 1197–1205.
- Wofsy, S. C., Goulden, M.L., Munger, J.W., Fan, S.M., Bakwin, P.S., Daube, B.C., Bassow, S.L., Bazzaz, F.A., (1993), Net ecosystem exchange of CO<sub>2</sub> in a midlatitude forest, *Science* 260, pp. 1314–1317.
- Yang, P.C., T. A. Black, H. H. Neumann, M. D. Novak, and P. D. Blanken, (1999), Spatial and temporal variability of CO<sub>2</sub> concentration and flux in a boreal aspen forest. *Journal of Geophysical Research*, 104 (D22), 27653-27661.
- Yi C, K. J. Davis, P. S. Bakwin, B. W. Berger, and L. Marr (2000), The influence of advection on measurements of the net ecosystem-atmosphere exchange of CO<sub>2</sub> from a very tall tower. *Journal of Geophysical Research*, 105, 9991-9999.
- Yi, C., (2008), Momentum transfer within canopies. *Journal of Applied Meteorology and Climatology*, 47, 262-275, doi:10.1175/2007JAMC1667.1.

- Yi, C., R. K. Monson, Z. Zhai, D. E. Anderson, B. Lamb, G. Allwine, A. A. Turnipseed, and S. P. Burns (2005), Modeling and measuring the nocturnal drainage flow in a high-elevation, subalpine forest with complex terrain, *Journal of Geophysical Research*, 110, (D22)303, doi:10.1029/2005JD006282.
- Yoshino, M.M. (1984), Thermal belt and cold air drainage on the mountain slope and cold air lake in the basin at quiet, clear night. *GeoJournal*, 8 (3), 235–250.